Mechanistic Modelling and Validation of Constant Load C-ring Apex Stresses for Stress Corrosion Cracking Testing in Supercritical Water

by

Rogan Swift

BScE (Chemical), University of New Brunswick, 2013

A Thesis Submitted in Partial Fulfillment
of the Requirements for the Degree of

Masters of Science in Engineering

in the Graduate Academic Unit of Chemical Engineering

Supervisor: William Cook, PhD, Chemical Engineering

Examining Board: Guida Bendrich, PhD, Chemical Engineering, Chair
Felipe Chibante, PhD, Chemical Engineering
Andy Simoneau, PhD, Mechanical Engineering

This thesis is accepted by the
Dean of Graduate Studies

THE UNIVERSITY OF NEW BRUNSWICK

May, 2017

©Rogan Swift, 2017

ABSTRACT

Canada is contributing significant research towards the Supercritical Water-cooled Reactor, one of the next-generation nuclear reactor designs, including characterization of stress corrosion cracking (SCC) resistance of candidate alloys in supercritical water at the operating conditions of 625 ºC and 25 MPa.

To quantify SCC resistance, a modified constant-load C-ring technique was developed through modeling and validated in both the finite-element software Abaqus and Monte-Carlo simulations. The proposed modification achieves the target C-ring apex stress with precision through thermal expansion and model-calculated initial deflection.

From Monte-Carlo simulations, the apex stress is within 4.16 MPa of the target stress in 96.3% of experiments. Preliminary in-situ experimentation has found no SCC in 310 stainless steel samples after 500 hours at 600 ºC and 25 MPa over a wide range of apex stress. The modified technique is stress-limited for some alloys with a yield-strength anomaly; suitable alloys include 316 SS, 310 SS and A800.

ACKNOWLEDGEMENTS

First, I would like to thank my supervisor Dr. William Cook for access to his wealth of corrosion and research knowledge, Dr. Philip Garland for his experience with Abaqus and the use of his dedicated server, and Sylvia Demerson for helping me navigate my Masters student journey.

I would also like to thank Adon Briggs and Keith Rollins of UNB for their fantastic machining work and Graham Steeves for providing advice and friendship throughout my research.

Finally, special appreciation is owed to my dad, Douglas Swift, for regular encouragement, food and incredibly cost-efficient housing.

This work is sponsored by The Natural Sciences and Engineering Research Council of Canada (NSERC), Natural Resources Canada (NRCan), Atomic Energy Canada Limited (AECL), and the Generation IV International Forum.

Without these people and groups, this thesis would be a shadow of what it is today.

Table of Contents

ABSTRACT ii
ACKNOWLEDGEMENTS iii
Table of Contents iv
List of Tables vi
List of Figures vii
List of Symbols, Nomenclature or Abbreviations ix
1 Introduction 1
1.1 Generation IV International Forum 1
1.2 Canadian SCWR (CANDU-SCWR) 2
Overview of Plant Configuration 3
Design Challenges and Requirements 6
1.3 Objectives 8
2 Literature Survey 9
2.1 Stress Corrosion Cracking and Cracking Mechanics 9
2.2 Experimentation Techniques 10
2.3 Previous Modelling Work 13
3 Test Methods 19
3.1 Sample and Autoclave Setup 19
Loaded Sample Tree 19
Pre-processing 21
Post-processing 22
3.2 Modelling 24
Deflection Balance 24
Elastic Compression 25
Thermal Expansion 31
Material Properties 33
C-ring Stress 35
Assumptions 38

4 Results 41
4.1 Finite Element Analysis Validation – Abaqus 41
4.2 Model and Implementation 48
4.3 Autoclave Results 51
Optical Microscope Pictures 52
Scanning Electron Microscope (SEM) Pictures 53
4.4 Stress While Heating Up 56
4.5 Variation of Parameters Analysis 60
4.6 Ways to Reduce Stress Variation 64
5 Conclusions 68
6 Recommendations 69
6.1 Sample and Autoclave Setup 69
6.2 Modelling 70
6.3 Validation 70
6.4 Future Work 71
7 Bibliography 72
8 Appendices 75
8.1 Raw Data 75
8.2 Full VBA Code with Comments 82
8.3 Sample Calculations 96
Parameters 96
Deflection Balance and Newton Method 97
Deflection Balance Terms 99
Force to Stress 111
Variation of Parameters 113
Curriculum Vitae

List of Tables

Table 1: I625 Thermal Expansion Coefficient Calculation Table 34
Table 2: I625 Example Test Part Lengths Before Loading (mm) 48
Table 3: I625 Example Test Part Lengths Before Heating (mm) 49
Table 4: I625 Example Test Part Lengths After Heating (mm) 49
Table 5: Previous Work Samples Re-calculated 50
Table 6: Test Conditions 51
Table 7: Sensitivities of Measured Model Parameters 63
Table 8: Master List of Raw Data Sources 75
Table 9: Offset Springs Calculated Parameters 76
Table 10: Raw Numerical Results – C-ring (No Hole) 76
Table 11: Raw Numerical Results – C-ring (Hole) 76
Table 12: Raw Numerical Results – Washer 77
Table 13: Raw Numerical Results - Nut 77
Table 14: Raw Numerical Results – Disc Spring 77
Table 15: Raw Numerical Results - Tree Trunk Contact With Infinite Bar 78
Table 16: Raw Numerical Results - Tree Trunk Contact With Washer 78
Table 17: Raw Numerical Results - Disc Spring Offset Wide Side 79
Table 18: Raw Numerical Results - Disc Spring Offset Short Side 80
Table 19: I625 Apex Stress during Heating 81
Table 20: Newton Method Root Finding 98
Table 21: Disc Spring Dimensions 99
Table 22: C-ring Dimensions 106
Table 23: Backing Washer Dimensions 107
Table 24: Tightening Nut Dimensions 108
Table 25: Tree Trunk Dimensions 109
Table 26: Tree Branch Dimensions 109
Table 27: C-ring Dimensions 111

List of Figures

Figure 1: Supercritical-water-cooled Reactor Design 3
Figure 2: CANDU-SCWR Reactor Vessel 4
Figure 3: Pressure Tube 4
Figure 4: High Efficiency Fuel Channel Cross-section [5] 5
Figure 5: C-ring Constant Load (Red is Volume of Tensile Stress) 11
Figure 6: Constant Extension Rate Test (Red is Volume of Highest Tensile Stress) 13
Figure 7: Tree Loaded with Sample - Raoul 14
Figure 8: CANMET Validation Against Equation 6 18
Figure 9: C-ring Loaded on Sample-holding Branch 20
Figure 10: Combined Offset Disc Spring Force To Deflection Curve 30
Figure 11: C-ring Deflection Diagram 37
Figure 12: Symmetry Boundary Conditions 42
Figure 13: Complete Abaqus Part 42
Figure 14: Von Mises Stress, C-ring with Mounting Hole 43
Figure 15: Von Mises Stress, C-ring without Mounting Hole 43
Figure 16: C-ring Force to Deflection 44
Figure 17: C-ring Force to Stress 44
Figure 18: Washer Geometry 45
Figure 19: Washer and Tree Branch Abaqus Validation 45
Figure 20: Nut Geometry 45
Figure 21: Nut Abaqus Validation 45
Figure 22: Disc Spring Geometry 45
Figure 23: Disc Spring Abaqus Validation 45
Figure 24: Tree Trunk Validation with Infinite Bar (Low Force) 46
Figure 25: Tree Trunk Validation with Infinite Bar (High Force) 46
Figure 26: Tree Trunk Validation with Washer Geometry 47
Figure 27: Disc Spring Wide Side Offset – Force to Deflection 47
Figure 28: Disc Spring Short Side Offset – Force to Deflection 48
Figure 29: I1.SC Before (Left) and After (Right) Trial 52

Figure 30: I2.SC Before (Left) and After (Right) Trial 52
Figure 31: F11.SC Cross-section with Scanning Electron Microscope 54
Figure 32: F11.SC Void Near Crack Tip 55
Figure 33: F11.SC magnification of Void 55
Figure 34: F11.SC Base Metal 55
Figure 35: F11.SC Oxide Coating 55
Figure 36: F11.SC Epoxy 55
Figure 37: I625 Apex Stress during Heating 56
Figure 38: Setup Force to Deflection Curves with Operating Positions 58
Figure 39: I625 Apex Stress during Heating (Alternate) 60
Figure 40: Monte Carlo (All Parameters Varying) 62
Figure 41: Monte Carlo (All Parameters Except Yield Strength) 62

List of Symbols, Nomenclature or Abbreviations

Symbols

a	Coefficient, units depend on case
A	cross-sectional area, mm^2; $w * (r_{outer} - r_{inner})$
A_m	Bending moment area, mm; $\frac{A}{r_n}$
c	Tree trunk contact length, mm; $D_{Outer,washer} - D_{Inner,washer}$
d	Deflection, mm
D	Diameter, mm
E	Young's Modulus of Elasticity, MPa
F	Applied force, N
g	Shift in location of the neutral axis, mm; $R - r_n$
h	Unloaded disc spring height, mm;
L	Part length parallel to the tree branch, mm
m	A measurement of a setup parameter, units of that measurement
M	Bending moment, MPa*mm; $F * R$
p	Cardano method intermediate parameter, mm^3
P	Pressure, MPa
q	Cardano method intermediate parameter, mm^2
Q	Offset between adjacent disc springs, mm
r	Radius, mm
r_n	Neutral axis radius, mm; $\frac{r_{outer} - r_{inner}}{\ln\left(\frac{r_{outer}}{r_{inner}}\right)}$
R	Centroidal axis radius, mm; $\frac{r_{outer} + r_{inner}}{2}$
s	Cardano method intermediate parameter, mm
S	Von Mises stress at the apex of the C-ring, MPa
t	Thickness, mm
T	Temperature, ^{o}C
u	Cardano method intermediate parameter, mm

U	A calculation coefficient, MPa^{-1}; $\frac{1-\mu_1^2}{\pi * E_1} + \frac{1-\mu_2^2}{\pi * E_2}$
v	Variability of some measurement, units of that measurement
V	Volume, mm^3
w	Width, mm
z	Distance from the neutral axis to the radius of interest, mm; $r_n - r_{Outer}$

Greek Letters

α	Instantaneous coefficient of thermal expansion, 1/K
λ	Disc spring calculation intermediate parameter, N/mm; $\frac{4 * E * t^3}{(1-\mu^2) * K * D_{Outer}^2}$
μ	Poisson ratio
π	The ratio of the circumference of a circle to its diameter
ρ	density, kg/m^3
σ	Compressive stress at the apex of the C-ring, MPa

Non-Dimensional Numbers

#	Number of
e	Euler's number, approximately 2.718
K	A calculation coefficient; $\frac{1}{\pi} * \frac{\left(\frac{\frac{D_{out}}{D_{in}} - 1}{\frac{D_{out}}{D_{in}}}\right)^2}{\frac{\frac{D_{out}}{D_{in}} + 1}{\frac{D_{out}}{D_{in}} - 1} - \frac{2}{Log\left(\frac{D_{out}}{D_{in}}\right)}}$

Subscripts or Superscripts

1, 2, 3,…	Numbering to different coefficients, materials or states
average	Having been averaged over a temperature range
autoclave	Sample pressure vessel
branch	Tree branch
C-ring	C-ring
curved	Curved section of the offset spring force to deflection curve

discs	Ceramic washers, tightening nut, tree trunk, and/or backing washers
EC	Elastic compression
ET	Elastic tension
initial	At loading conditions, before heating and pressurizing
inner	Internal surface of the part
ISCC	Critical stress intensity
linear	Linear section of the offset spring force to deflection curve
m	Some measured parameter, units are units of the parameter
n	At the neutral axis of the C-ring, without tensile or compressive stress
OneSpring	A single disc spring
operating	At experimental operating temperature and pressure
outer	External surface of the part
part	For each part. Normally used in a summation
room	At room temperature and pressure
SampleTree	Sample-holding tree
springs	All disc springs
TE	Thermal expansion
transition	Point shared by the linear and curved sections of the offset spring force to deflection curve
trunk	Sample-holding tree trunk
untightened	Before the initial deflection has been applied
washers	Washers
water	Water
x	Parallel to the sample-holding tree branch

Acronyms and abbreviations used in text

AECL	Atomic Energy Canada Limited
ASTM	American Society for Testing and Materials
CAE	Complete Abaqus Environment
CANDU	Canada Deuterium Uranium, referring to the reactor design

CERT	Constant Extension Rate Test
EC	Elastic Compression, mm
ET	Elastic Tension, mm
GFR	Gas-cooled Fast Reactor
LFR	Lead-cooled Fast Reactor
MSR	Molten Salt Reactor
NRCan	Natural Resources Canada
NSERC	The Natural Sciences and Engineering Research Council of Canada
PWR	Pressurized Water Reactor
SCC	Stress Corrosion Cracking
SCW	Supercritical Water
SCWR	Supercritical-Water-cooled Reactor
SEM	Scanning Electron Microscope/Microscopy
SFR	Sodium-cooled Fast Reactor
SSRT	Slow Strain Rate Test
TE	Thermal Expansion, mm
UNB	The University of New Brunswick
VHTR	Very-High-Temperature Reactor

Alloy Abbreviations

316 SS	316 stainless steel (UNS S31600)
I625	Inconel 625 (UNS N06625)
310 SS	310 stainless steel (UNS S31008)
347 SS	347 stainless steel (UNS S34700)
A800HT	Alloy 800HT (UNS N08811)
H214	Haynes 214 (UNS N07214)
Hast-C	Hastalloy C (UNS N10002)
Hast-C276	Hastalloy C-276 (UNS N10276)
I718	Inconel 718 (UNS N07718)
410 SS	410 stainless steel (UNS S41000)

1 Introduction

1.1 Generation IV International Forum

The growing global consumption of electricity coupled with the limited global electricity-producing resources produces an impetus for global collaboration. To meet this need through collaborative research, the Generation IV International Forum was formed as an international membership looking to prepare the next generation of nuclear reactors. Canada, the People's Republic of China, Euratom, France, Japan, the Republic of Korea, the Russian Federation, the Republic of South Africa, Switzerland, and the United States are the ten active members who have signed or consented to the Framework Agreement, which acts as a charter for the Forum. [1]

The guide for the specific research interests of each country and where they overlay is laid out in the Technology Roadmap, which was written in 2002 [2] and updated in 2013. [3] The Technology Roadmap details the six most promising preliminary nuclear facility designs, the upcoming research and development requirements for those designs and the focus of each country as they relate to research and development.

Principal in every design are the four Generation IV goal categories: sustainability, economics, safety and reliability, and proliferation resistance and physical protection have been considered, rated and optimized. Sustainability has metrics for long-term availability, effective fuel utilization, minimization of waste, and a reduction of stewardship burden. Economics has metrics for life-cycle cost advantage and financial

risk. Safety and reliability has metrics for overall safety and reliability, likelihood/degree of reactor core damage, and minimization of required offsite emergency response. Proliferation resistance and physical protection has metrics related to terrorism resistance. [4]

Each reactor design achieves the above goals in a different way. The very-high-temperature reactor (VHTR) will use a single-phase, inert helium coolant in the thermal neutron spectrum and operate between 700 ^{o}C and 900 ^{o}C to produce heat, electricity and/or hydrogen. The gas-cooled fast reactor (GFR) will use a single-phase, inert helium coolant in the fast neutron spectrum to produce electricity. The sodium-cooled fast reactor (SFR) will use a liquid sodium coolant to take advantage of great thermal properties and low oxygen, limiting corrosion. The lead-cooled fast reactor (LFR) will use a single-phase, inert Pb or Pb-Bi-alloy coolant. The molten salt reactor (MSR) will operate with either fissile material dissolved in molten fluoride salt (case 1) or with the molten salt being a coolant (case 2). The supercritical-water-cooled reactor (SCWR) is an evolution of existing fossil-fired supercritical water plants using a coolant of single-phase light water past the critical point (374 ^{o}C, 22.1 MPa). [2]

1.2 Canadian SCWR (CANDU-SCWR)

Of the ten active members of the Generation IV International Forum, Canada is the only country to focus on a single reactor design, the supercritical-water-cooled reactor.

Overview of Plant Configuration

The big difference between other reactor designs and the SCWR is that the SCWR uses light water as a coolant and heavy water as a moderator. The advantage of water over other coolants and moderators is that the properties and behavior of water are well-known at high temperature. As well, technology can be carried over from Generation II and III light water reactors and supercritical-water-cooled fossil-fired power plants.

Considering the number of countries working on SCWR research and changes to the preliminary design over time, there are multiple SCWR layout designs. Shown below as Figure 1 is an overview of the Canadian SCWR design which shows the water flow and general equipment.

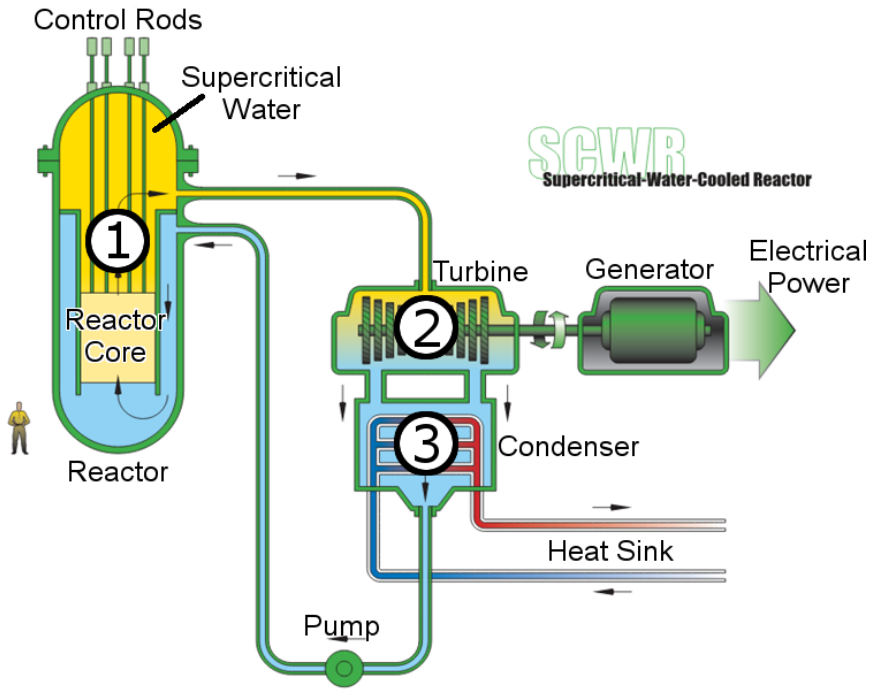

Figure 1: Supercritical-water-cooled Reactor Design

After [2]

Starting at the pressure-tube style reactor core, (Figure 1, label 1) the light water coolant is heated and pressurized past the critical point of water (374 ^{o}C, 22,1 MPa) to the core outlet temperature and pressure of 625 ^{o}C and 25 MPa, respectively. This supercritical water is sent to the high-pressure turbine, (Figure 1, label 2) where it expands and depressurizes below the critical pressure. The fluid is then cooled to below the critical temperature (Figure 1, label 3) and sent back to the reactor vessel. (Figure 1, label 1)

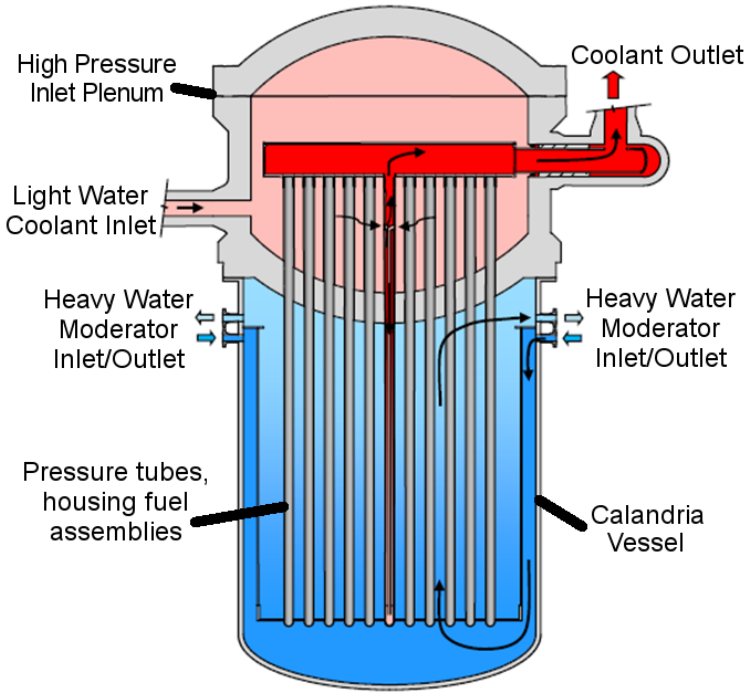

Figure 2: CANDU-SCWR Reactor Vessel
After [5]

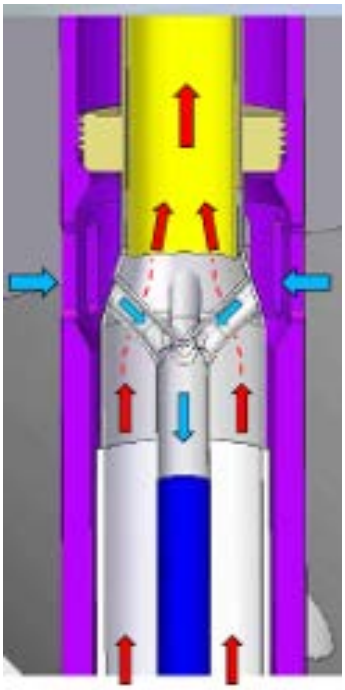

Figure 3: Pressure Tube
[5]

In the pressure-tube reactor vessel, light water coolant from the overall loop enters the high-pressure inlet plenum (Figure 2 above) and then the individual pressure tubes, which

house the fuel channels and assemblies. (Figure 3 above) These fuel channels are predicted through modeling to reach temperatures between 725 ºC and 800 °C. [6]

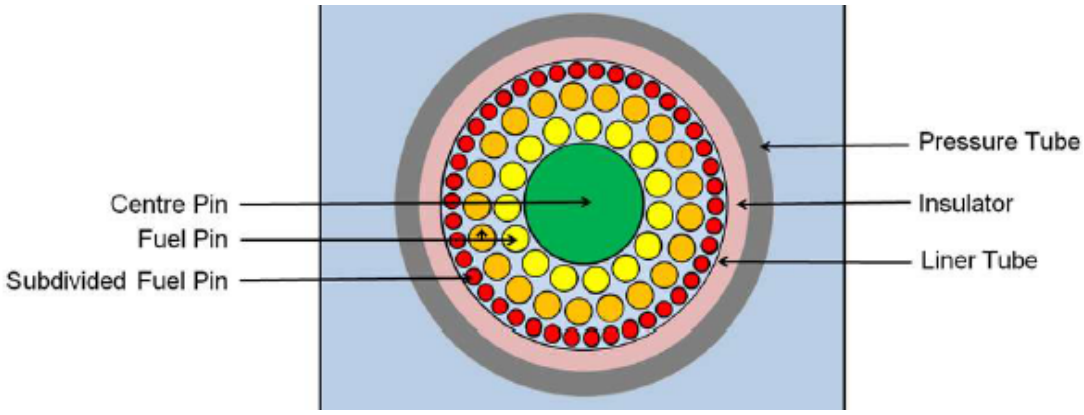

Figure 4: High Efficiency Fuel Channel Cross-section [5]

In each fuel channel, the coolant descends the center pin to the bottom of the fuel channel, then rises back up to the top in the liner tube against the fuel pins. (Figure 4 above) The CANDU-SCWR will operate in the thermal neutron spectrum using a fuel mixture of thorium oxide and plutonium oxide as a fissile starter to breed the thorium. [7] As thorium fuel requires a significant amount of research to reach usability, AECL has initiated a multi-year Thoria Roadmap Project. [8]

Surrounding most of the fuel assembly is the low-pressure calandria vessel, which houses the heavy water moderator. In addition to neutron moderation, the heavy water is passively circulated for long-term cooling. [3]

This design came about as an evolution of previous CANDU reactors and supercritical-water-cooled fossil-fired power plants, such as the John W. Turk Jr. ultra-supercritical power plant in Arkansas. [9] Supercritical water remains a single-phase fluid, so much of the equipment to manage liquid and vapor water in existing reactors can be omitted, such as steam generators, steam separators and dryers. As well, supercritical water has a higher enthalpy than superheated steam, which means a smaller turbine system is required, and the one-phase flow reduces the number of coolant pumps required. The result of these factors is that there are lower capital costs for a given electric power, increased thermal efficiency (44% for CANDU-SCWR from 34-36% for earlier plants) and better fuel utilization. [3]

Design Challenges and Requirements

A significant amount of required SCWR-related research was laid out in the 2002 Roadmap, including categories such as corrosion and SCC, materials, water chemistry, and alloy properties at high temperatures.

Regarding corrosion, the 2002 Roadmap requested corrosion rates, composition and structure as a function of temperature, dissolved gasses and irradiation effects. Specifically for SCC, the 2002 Roadmap requested general SCC information as a function of temperature and environment, as well as the effects of irradiation on SCC. [2]

This work was to be done using between two and four out-of-pile test loops for corrosion and SCC experiments with pre-irradiated, post-irradiated and unirradiated alloy samples over 6-10 years. Also requested were either three or four in-pile test loops for corrosion,

SCC and water chemistry control, split between fast and thermal spectrum electrons. The in-pile test setups were expected to start midway through the out-of-pile timeline and continue for either 10 years (thermal spectrum) or 15 years (fast spectrum). [2]

The 2014 Roadmap Update included a section of SCWR research that had been performed since the 2002 Roadmap, as well as the findings from that research and additional research to be done. Although many topics were covered, heat transfer models, qualification of cladding materials, and passive safety systems were mentioned in multiple places. With a focus on corrosion and SCC, the 2014 Roadmap Update stated the following: [3]

- Stainless steels with more than 20% chromium are promising up to 650 °C.
- Creep resistance can be improved by adding small amounts of elements such as zirconium to alloys.
- Oxide dispersion-strengthened steel alloys are an area of significant interest.
- Nickel-based alloys are less favorable due to high neutron absorption.

To manage these issues and complete the original 2002 Roadmap request, the 2014 Roadmap Update requested final qualification of candidate alloys for all key components within the next five years. This final qualification must consider irradiation, water radiolysis and corrosion product deposition at temperatures up to 850 °C. Additionally, research is required for the coolant conditions leading to SCC. [3]

Looking further ahead over the next ten years, the Roadmap Update includes a desire for a small-scale fuel assembly in a nuclear reactor at supercritical water conditions, as well as decisions for a full SCWR prototype. [3]

CANDU-SCWR researchers performed preliminary testing and determined a shortlist of candidate alloys. As discussed by Guzonas, Edwards and Zheng, "… five alloys, 347 SS, 310 SS, Alloy 800H, Alloy 625 and Alloy 214, were selected for a further, more detailed assessment using a combination of literature surveys and targeted testing to fill in major knowledge gaps." [10] All research for CANDU-SCWR materials must be applicable to these alloys.

1.3 Objectives

To remedy the issues of insufficient stress characterization and high-temperature loading difficulty, the following steps are objectives on the way to full determination of stress corrosion cracking resistance for the candidate materials:

1) Develop an accurate model of constant-load experimentation.
2) Develop a precise and cost-effective loading technique for use at high temperature and high pressure.
3) Validate the model and technique through known in-situ testing and computer simulation. If necessary, iterate development and validation.
4) Apply model and technique to new in-situ conditions and the candidate alloys.

2 Literature Survey

2.1 Stress Corrosion Cracking and Cracking Mechanics

Corrosion is a serious consideration for the next generation of nuclear reactors, as any sort of mechanical failure is catastrophic at the extreme operating conditions present in the CANDU-SCWR. General corrosion must be minimized with alloy selection and/or coatings so that heat exchange surfaces can be as thin as possible and other types of corrosion must be considered and carefully managed.

One concern is Stress Corrosion Cracking, (SCC) which cannot be mitigated with pipe and vessel wall thickness allowances. SCC is a combination of corrosion and tensile stress which can result in localized fracture long before failure would be expected by another means. For example, primary water SCC of an A600 vessel head penetration nozzle resulted in a two-year shutdown at the Davis Bessie PWR, but could have resulted in a catastrophic loss-of-coolant accident if the SCC was not identified before the remaining 3/8'' stainless steel cladding failed. [11] Fortunately, SCC is limited to as-yet experimentally-determined combinations of stress, alloy, and environment.

SCC is an outcome which can result from several different mechanisms. For active path dissolution, corrosion follows some extra-susceptible path such as a grain boundary as stress opens the crack to speed product migration. For hydrogen embrittlement, hydrogen dissolves through the alloy to sites of high triaxial stress, such as just past a crack tip, and either precipitates as hydrides or reforms as a bubble of hydrogen gas. For film-induced cleavage, a crack which starts in a brittle surface film (such as a continuously reforming

oxide film) can continue a short distance into otherwise fracture-resistant ductile bulk metal. [12]

These three known mechanisms may occur simultaneously or separately, with or without other mechanisms to produce cracks along grain boundaries (intergranular cracks), through grains (transgranular cracks) or a mix of both. Additionally, changes in the machining, pretreatment, environment, or coating of a normally-susceptible alloy may produce different kinds of SCC by different mechanisms or may stop SCC altogether. [12]

The effect of stress in SCC is represented by the critical stress intensity factor, K_{ISCC}, as a normalization of the critical stress. While all alloys will fracture above their ultimate tensile stress, stress corrosion cracks propagate at some critical stress which is often well below the ultimate tensile stress. This critical stress is the stress at which a stress corrosion crack will occur at infinite time and can be determined by many different types of tests. As infinite time is impractical for actual data gathering, this critical stress is normally extrapolated from trials performed at shorter times.

2.2 Experimentation Techniques

There are multiple common techniques for testing SCC, each with weaknesses and strengths. It would be preferable to maintain a constant stress on the tested sample as it cracks as stress intensity factor is the reported parameter for SCC, but no technique maintains a constant stress as a crack occurs. Instead, tests control a related parameter such a strain or load from which stress can be calculated.

One of the most common testing techniques is the Constant Load test, where an alloy sample and a set of springs are tightened within a fixed distance to achieve a near-constant applied load even as the sample cracks. The curvature of the C-ring, O-ring or U-bend sample causes a region of tensile stress in the otherwise compressed sample. A C-ring compressed by this method is shown below as Figure 5, where the volume of highest tensile stress occurs at the region in red.

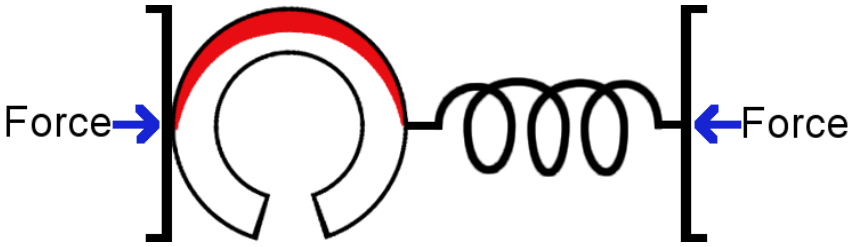

Figure 5: C-ring Constant Load (Red is Volume of Tensile Stress)

This technique is less expensive than the more common slow strain rate test, as there are no moving parts once the fixed strain is applied. As a downside, the strain must be applied with great precision, as small errors in strain cause large offsets of the final stress. As well, this technique is aggressive, as cracking reduces the cross-sectional area of the sample while force is nearly maintained which results in stress increasing as the crack progresses.

Presently, accepted practice for constant-load tests is described in ASTM G38-01, which was written in 2001 and re-approved in 2013. The recommended practice for determining

the stress of a loaded sample is to apply circumferential and transverse strain gauges at room temperature, heat to the operating temperature, adjust the tightening nut until the desired apex stress is reached, cool to room temperature, remove the strain gauges and clean all adhesive, then put the loaded sample in the environment. [13] As the CANDU-SCWR operating temperatures are above 600 ^{o}C, the requirement of precisely operating the tightening nut at operating temperature makes this technique impractical.

The alternative practice recommended by ASTM is to adjust the tightening nut at temperature while measuring the deflection of the C-ring outer diameter. For a given C-ring initial outer diameter and thickness, ASTM provides an equation which relates the deflected outer diameter to the apex stress. Unfortunately, the precision of the apex stress given by the equation is acceptable only at high target stress; that is, the technique precision worsens from 3% at a target apex stress of 345 MPa to only 30% at 34.5 MPa, where an example target stress is the yield strength of 316 stainless steel at 600 ^{o}C, 153 MPa. [13] This technique also requires tightening nut operation at operating temperature and is also impractical.

Another common testing technique is the Constant Extension Rate Test (CERT) or Slow Strain Rate Test (SSRT), where a tensile bar sample is strained at a constant, known extension rate until failure. Results can be very precise, but tests must be repeated until the rate at which SCC occurs is found, if such a rate exists for that alloy and environment combination. A CERT test setup is shown below as Figure 6, where the volume of highest tensile stress occurs at the region in red.

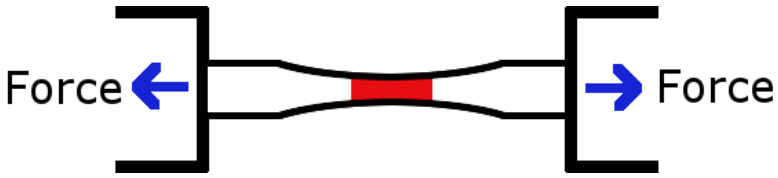

Figure 6: Constant Extension Rate Test (Red is Volume of Highest Tensile Stress)

Zheng et al. collected 33 papers of SCC test results for many alloys, temperatures, pressures, water oxygenation levels, and test durations. Among their findings was the discovery that the SCC resistance of the alloy depended on the technique used; for example, "[cracks in SSRT or CERT tests] could have initiated any where between the yield and the UTS point of the alloy on its stress-strain curve. SCC [sic] or CERT tests are commonly carried out for materials susceptibility study. However, in terms of data generation for alloy qualification or confirmation of code requirement, these tests have little value…" [14] Additionally, Zheng et al. remarked the low volume of overall research at high temperatures, or under irradiated conditions, or for SCC in particular.

As a final note, Gu, Zheng and Guzonas are developing a corrosion database for in-house use, as presented at 2nd Canada-China Joint Workshop on Supercritical Water-cooled Reactors. This database may be useful as a collection of SCC literature. [15]

2.3 Previous Modelling Work

To improve the precision and accuracy of stress measurements with a constant-load setup, Raoul developed a new constant-load C-ring technique whereby the C-ring sample is loaded at ambient conditions and then heated up to supercritical conditions. Raoul

further developed a mechanistic model for this scenario and implemented his model in MATLAB, a computer coding language commonly used for engineering applications. The implementation is used to calculate the operator-applied tightening nut initial deflection that would result in the desired stress at the point of highest tensile stress, the C-ring apex, after thermal expansion. [16]

In his setup, Raoul makes use of ceramic washers to isolate the C-ring from galvanic effects, metal backing washers to protect the fragile ceramics, and a tightening nut to apply the initial deflection. This setup was applied for four test runs where parts are loaded on a test sample tree with 12 branches giving a total of 42 tested samples, not including blanks. A full picture of the standard setup is shown below:

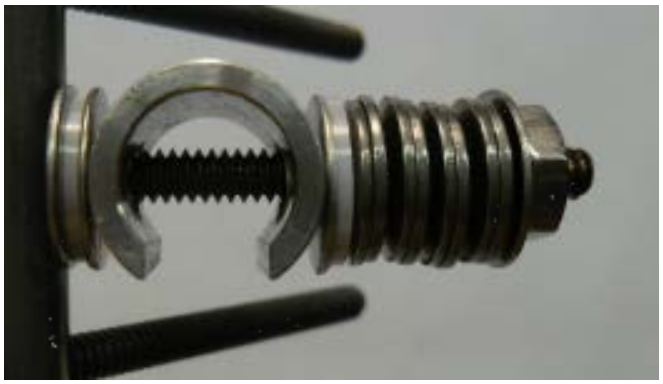

Figure 7: Tree Loaded with Sample - Raoul

As described by Raoul, the model assumes the following:

- "The geometry and expansion of the loading device (disc spring) due to temperature was negligible;
- Conditions will sustain the c-ring stress in the elastic regime;

- Linear thermal expansion of the c-ring will not be impeded as stress remains elastic;
- Thermal expansion of the bolt and support tree not considered for simplification purposes;
- Creep was neglected in the analysis;
- Stress relaxation of the disc springs and c-ring would remain under 1% and thus be ignored." [16]

In comparison to the model presented later, Raoul's model also includes the following unstated assumptions:

- Only the C-ring and metal backing washers thermally expand as heated.
- Only the Belleville washers compress due to force.
- Thermal expansion and elastic compression occur only along the axis. No radial thermal expansion.
- The tightening nut does not move with respect to the tree branch during tests.
- Disc springs are perfectly aligned.
- Steady-state conditions (No cracking/weakening/corrosion of materials over time)
- From Pilkey regarding the C-ring, "The theory of arches relies on the assumption that plane cross sections remain plane, stress is proportional to strain, rotations and translations are small, and the thickness of the bar must be small in comparison to the curvature" [17]

In his model, Raoul relates the apex stress to the force applied to either side of the C-ring by the following equation, derived by Raoul and Cook [16] from Pilkey [17]:

$$S = \frac{F}{A}\left(\frac{R}{r_{outer}}\frac{A_m\, r_{outer} - A}{A_m\, R - A} - 1\right) - P_{Operating} \tag{1}$$

where S is the Von Mises stress at the apex of the C-ring in MPa, F is the applied force in N, A is the cross-sectional area in mm^2 following Equation 2 below, r is a radius in mm, A_m is the bending moment area in mm following Equation 3 below; R is the centroidal axis radius in mm following Equation 4 below, P is the pressure in MPa, r_n is the neutral axis radius in mm following Equation 5 below, and w is the width in mm.

$$A = w\,(r_{outer} - r_{inner}) \tag{2}$$

$$A_m = \frac{A}{r_n} \tag{3}$$

$$R = \frac{r_{outer} + r_{inner}}{2} \tag{4}$$

$$r_n = \frac{r_{outer} - r_{inner}}{\ln\left(\frac{r_{outer}}{r_{inner}}\right)} \tag{5}$$

This force is used to find the deflection of one disc spring, using the following equation provided by DIN [18]:

$$F = \frac{4\,E\,t^3\,d_{OneSpring}}{(1-\mu^2)\,K\,D_{outer}}\left[\left(\frac{h-t}{t} - \frac{d_{OneSpring}}{t}\right)\left(\frac{h-t}{t} - \frac{d_{OneSpring}}{2\,t}\right) + 1\right] \tag{6}$$

where t is the thickness in mm, h is the unloaded disc spring height in mm, E is the Young's Modulus of Elasticity in MPa, d is the deflection in mm, D is the diameter in mm, μ is the dimensionless Poisson ratio, and K is a dimensionless calculation coefficient following Equation 7 below:

$$K = \frac{1}{\pi} \frac{\left(\frac{\frac{D_{out}}{D_{in}} - 1}{\frac{D_{out}}{D_{in}}} \right)^2}{\frac{\frac{D_{out}}{D_{in}} + 1}{\frac{D_{out}}{D_{in}} - 1} - \frac{2}{ln\left(\frac{D_{out}}{D_{in}}\right)}} \tag{7}$$

These equations are applied as part of Raoul's preliminary implementation. His methodology and implementation have been expanded and improved upon in this work, so his results will not be discussed.

For comparison to work presented later, the assumptions of Raoul's model should give rise to the following deflection balance, which describes how all parts deflect and expand given a consistent axial force:

$$d_{TE,C-ring} + d_{TE,washers} - \#_{springs}\, d_{OneSpring} + d_{initial} = 0 \tag{8}$$

where $\#_{Springs}$ is the number of Belleville washers used.

Raoul's model underwent partial validation at CanmetMATERIALS in Ontario. [19] For this validation, one set of test parts (C-ring, disc springs, washers) were mounted on a rod and held between the top and bottom platens of an instron machine. Then, while considering the thermal expansion of the machine itself with a calibration function, the temperature was increased from room temperature to the operating temperature, with ambient environment and pressures. The result of this method was a precise determination of the initial and final applied force for several setups, using an initial deflection and thermal expansion calculated by the MATLAB implementation of Raoul's model.

Shown below in Figure 8 are the results of the CANMET validation, presented as before-after pairs (green-red points) for each alloy of the force (vertical axis) and the deflection of each disc spring (horizontal axis), plotted against the deflection equation for a single disc spring (Equation 6, green-red lines).

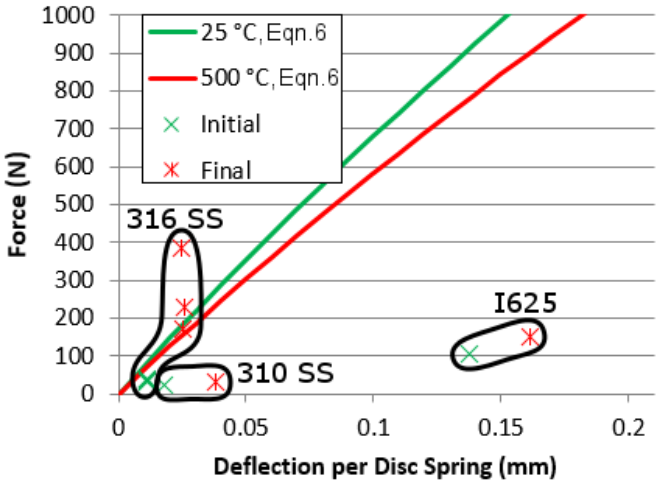

Figure 8: CANMET Validation Against Equation 6

The most noteworthy points in Figure 8 are the three final 316 SS points which share an initial point, indicating a source of inconsistency after the experiment starts, and the initial I625 point which is substantially lower than the expected curve, indicating a major problem with the force measurement at room temperature, the application of initial deflection to the setup and/or the response of the setup to the applied initial deflection. In any case, these results were not considered to have validated the model.

3 Test Methods

To test for SCC resistance of the shortlist alloys, a constant-load C-ring was chosen to achieve reproducible, conservative results with good cost effectiveness. Building on previous techniques, a modified constant-load C-ring technique was applied whereby samples are loaded onto the branches of a sample-holding tree at room temperature without the use of strain gauges and the target apex stress is reached through a combination of thermal expansion and calculated initial deflection. This is a high-temperature improvement to the techniques recommended by ASTM, which require the precise operation of a tightening nut at operating temperature. (600 °C, in this case)

This technique was developed for C-rings machined from alloy rods from the Generation IV International Forum SCWR cladding alloy shortlist. Of these alloys, UNB only received sample rods of modified 310 SS and I625 and of those, none had attached material property data spec sheets.

3.1 Sample and Autoclave Setup

Loaded Sample Tree

For this constant-load C-ring technique, samples and any peripheral parts are loaded onto the branches of an alloy sample tree, as shown below in Figure 9:

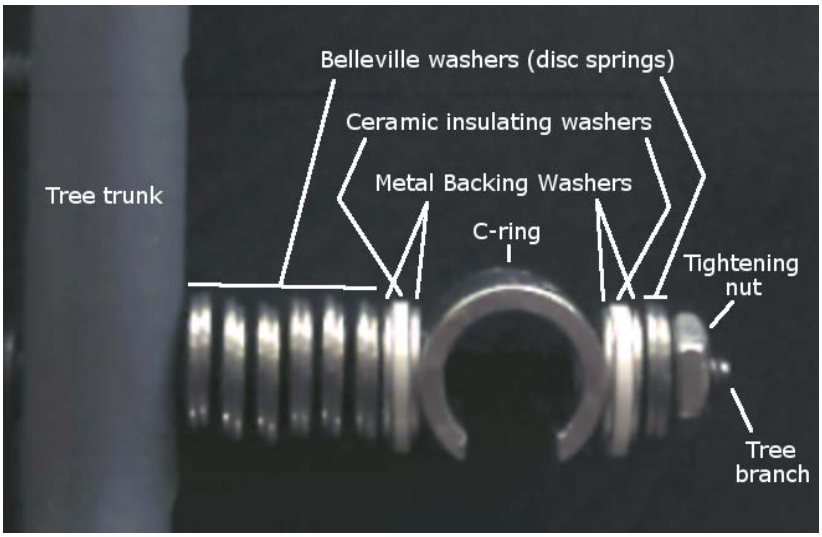

Figure 9: C-ring Loaded on Sample-holding Branch

C-rings are machined from the provided shortlist alloy rods or pipes following ASTM G38-01. [13] If deemed necessary for the sample/tree alloy combination, the C-ring can be galvanically separated from the other parts with ceramic washers. These brittle ceramic washers must themselves be mechanically protected from damage by metal backing washers. Finally, all parts are constrained by a tightening nut which is screwed on to the threaded tree branch.

The part list for one sample at UNB is as follows, with variations as needed:

- 14 disc springs (Inconel 718, 1.2192 mm unloaded height, 0.7874 mm thickness, 10.312 mm outer diameter, 4.9784 mm inner/hole diameter, no offsets, measurements from [18])
- 1 C-ring (316 stainless steel, 12.7 mm outer diameter, 12.7 mm width, 1.67 mm thickness)

- 4 backing washers (0.71 mm thickness, 9.54 mm outer diameter, 4.59 mm inner/hole diameter)
- 1 tightening nut (316 stainless steel, 1.36 mm thickness, 8.31 mm outer diameter, 2.83 mm inner diameter at tip of thread)
- 1 tree trunk (316 stainless steel, 6.4 mm diameter, 4.95 mm contact length, in contact with a 316 stainless steel washer)
- 1 tree branch (410 stainless steel, length as the sum of all other initial lengths less initial deflection, 3.31 mm diameter)

Pre-processing

Before loading, samples are pre-processed while wearing latex gloves to not contaminate the samples. All C-rings, washers, disc springs and tightening nuts are washed in a sonic bath with acetone, separated into trial number groups and weighed individually for after-trial comparison. The C-ring samples are additionally dimensioned to 0.005 mm precision with Vernier calipers and photographed for after-trial comparison. Pictures are taken along the C-ring apex, as well as at any blemishes or interesting spots. All parts are then loosely loaded onto tree branches by trial number group for later tightening.

Using a mechanistic model developed in Section 3.2 below and validated in Section 4.1 below, the initial deflection required to reach the desired apex stress at operating temperature is applied to the tightening nut of each branch, starting at the operator-determined point of zero applied force. The initial deflection of each tightening nut is calculated separately based on the dimensions and conditions of the related C-ring. The

point of zero applied force is determined to be the initial tightening nut position such that parts just barely hold do not hold each other up by friction. For each branch, the distance from the tree trunk to the tightening nut is recorded for after-trial comparison for the case of tightening nut slippage.

To produce a supercritical water environment, a calculated volume of room-temperature water is heated inside of a clean 300 mL Inconel 625 static autoclave containing the sample-holding tree. The density of both room-temperature and supercritical water is well characterized, so the required water is easily calculated from a mass balance of water:

$$V_{water,Room} = \left(V_{Autoclave} - V_{SampleTree}\right) \frac{\rho_{water,Operating}}{\rho_{water,Room}} \quad (9)$$

where V is the volume in mm^3 and ρ is the density in kg/m^3.

One goal of testing is to maintain the C-ring and environment at the desired testing conditions. It is unfortunate, then, that the C-ring experiences periods of sub-critical corrosion while the autoclave heats up at the beginning of the trial and cools down at the end of the trial. To offset this effect, care must be taken not to extend or repeat these periods.

Post-processing

Once the trial time was complete, the sample tree is removed from the autoclave and placed in a desiccator box for drying. Before samples are removed from the tree, pictures are taken of each sample in its stressed state, the water from the autoclave is collected for

environment analysis and the distance from the tree trunk to the tightening nut is recorded to determine tightening nut slippage.

Individual samples are removed from the tree one branch at a time while wearing gloves. The parts of each branch are weighed and photographed as before the trial, for comparison.

ASTM-G38 advises that stress-corrosion-resistant alloys at lower applied stresses frequently produce small cracks that are difficult to detect. For this reason, “Inasmuch as C-rings do not always fracture, it is preferable to report the first crack as the criterion of failure. It is common practice to make this inspection with the naked eye or at a low magnification.” [13] Additionally, where the suspicion of a crack cannot be confirmed with the naked eye, ASTM recommends analysis of a cross-section taken through the suspected crack to determine presence and type of cracking. [13]

At UNB, this further analysis included SEM which is performed on lightly-restressed C-ring samples set in epoxy and polished in stages while looking for cracks. The use of epoxy is necessary for cross-section oxide analysis via SEM as, without epoxy, grinding can tear off the oxide layer. Careful selection of epoxy is important as incorrect epoxy selection can result in the epoxy shrinking and pulling the oxide from the surface of the metal or the oxide floating through the epoxy. At UNB, EpoFix resin and hardener from Struers were used for 316 SS and I625 samples.

3.2 Modelling

To improve upon previous work, iterative stages of modeling, validation and improvements to technique were performed to create a mechanistic model which accurately describes the apex stress of a C-ring stressed as described in Section 3.1 above. Presented here is the final model, after all iteration.

Deflection Balance

The key statement in developing the deflection balance is that, in a static system, the forces applied to any point or part are balanced in all directions. At the operational temperature, during and after all parts have thermally expanded, all parts must have also been compressed by a shared axial force such that the total length of all parts fits precisely in the available space.

The result of this is that compression and expansion can be considered independent and additive after heating. That is, a part which is heated up to 500 ^{o}C and then given an applied force of 100 N will have the same final deflection as a part which is given the applied force before being heated; this final deflection is the thermal expansion of the part plus its negative elastic compression, considering the thermally-expanded dimensions.

The base equation of the model is a deflection balance for each loaded part and the apparatus itself, presented below as Equation 10. On the left hand side of the equation is the elastic compression of all parts, which relates to the apex stress of the C-ring through

the force. On the right hand side of the equation are all terms which increase (positive sign) or decrease (negative sign) the elastic compression.

$$\sum d_{EC}\,(\text{material}, \text{shape}(T), \mathbf{F}) = \sum d_{TE,Part}\,(\text{material}, T) + \boldsymbol{d_{Initial}} - d_{TE,Branch}(T) - d_{ET,Branch}(T, \mathbf{F}) \qquad (10)$$

where T is the temperature in °C.

The applied initial deflection and the change in length due to thermal expansions of all non-apparatus parts cause an increase in elastic compression due to the constrained space, so they are given positive signs. As a special case, the apparatus tree branch is elongated by the applied force (elastic tension, not elastic compression) and by thermal expansion, so both effects reduce the elastic compression and are represented with negative signs.

Equation 10 is suitable for any linear combination of parts as long as force to deflection equations/data are available and all assumptions are met. In the constant-load C-ring experiments performed at UNB, it is common to make use of one C-ring, multiple disc-geometry parts (backing washer, ceramic washer, tightening nut, apparatus tree branch), multiple disc springs, and a tree-like apparatus upon which parts are loaded.

Elastic Compression

The geometry of each part determines elastic compression/tension equation, which relate an applied force to the part's deflection. Since the shape of contact between parts has an impact on the force to deflection curve of each part, it is necessary to either model the contact as it exists or to use experimental techniques to reduce the effect of contact on the

equation. For example, the contact between a pair of disc springs placed symmetrically back to back will have no effect on the force to deflection equation of either disc spring; this is not the case if there is any offset between disc springs.

The C-ring force to deflection equation is given as follows: [17]

$$d_{C-ring} = \frac{-\pi\ 6\ F\ R^3}{E\ w\ t^3} \tag{11}$$

where π is the ratio of the circumference of a circle to its diameter.

The metal backing washers, insulating ceramic washers, the tightening nut, and the apparatus tree branch have similar geometry and can be approximated to share a force to deflection equation which is re-arranged from the definition of Young's modulus:

$$d_{discs} = \frac{-4\ F\ t}{\pi\ E\ (D_{outer}^2 - D_{inner}^2)} \tag{12}$$

where *t* is the thickness of the disc geometry in question in mm:

- t is the full thickness for the ceramic washers and metal backing washers
- t is half of the thickness of the tightening nut (center assumed to not move with respect to the tree branch)
- t is length from the tree trunk (inclusive) to the tightening nut (inclusive) for the tree branch.

The disc spring force to deflection equation is given as follows:

$$F = \frac{4\,E\,t^3\,d_{OneSpring}}{(1-\mu^2)\,K\,D_{Outer}^2}\left[\left(\frac{h-t}{t}-\frac{d_{OneSpring}}{t}\right)\left(\frac{h-t}{t}-\frac{d_{OneSpring}}{2\,t}\right)+1\right] \quad (13)$$

In practice, this equation is solved for deflection by putting it in the form of polynomial equation for deflection and solving using the Cardano Method. The cubic equation of deflection is as follows:

$$a_3\,d^3 + a_2\,d^2 + a_1\,d + a_0 = 0 \quad (14)$$

where *a* is a coefficient where the units depend on each case. Re-arranging Equation 13 into Equation 14 causes the coefficients to be as follows:

$$a_3 = \frac{\lambda}{2\,t^2} \quad (15)$$

$$a_2 = -\frac{3\,\lambda\,(h-t)}{2\,t^2} \quad (16)$$

$$a_1 = \frac{\lambda\,(h-t)^2}{t^2} + \lambda \quad (17)$$

$$a_0 = -F \quad (18)$$

where λ is a disc spring calculation intermediate parameter in N/mm following Equation 19 below:

$$\lambda = \frac{4\,E\,t^3}{(1\,-\,\mu^2)\,KD_{Outer}^2} \quad (19)$$

As a cubic equation has three roots, some which some may be imaginary numbers, the Cardano method is applied to give only the real root, if it exists. Equation 14 presented above has one real root for any force within the intended operational range, so the equations below are valid. The Cardano method involves a conversion from Equation 14 to a depressed cubic without a squared term, which is then solved by substitution and

taking a cubic root. [20] That work aside, the solutions are given below for the intermediate parameters p, q, s, and u with units of mm^3, mm^2, mm, and mm respectively:

$$p = \frac{9\,a_3\,a_2\,a_1 - 27\,{a_3}^2\,a_0 - 2\,{a_2}^3}{54\,{a_3}^3} \tag{20}$$

$$q = \frac{3\,a_3\,a_1 - {a_2}^2}{9\,{a_3}^2} \tag{21}$$

$$s = \sqrt[3]{p + \sqrt{q^3 + p^2}} \tag{22}$$

$$u = \sqrt[3]{p - \sqrt{q^3 + p^2}} \tag{23}$$

These equations for s and u give the single real solution to the equation. The final deflection is solved with the following equation:

$$d_{OneSpring} = -\left(s + u - \frac{a_2}{3\,a_3}\right) \tag{24}$$

Equations 13 through 24 above must be modified if there is any offset between adjacent disc springs. The observed effect of an offset on the force to deflection curve is an initial linear section, followed by an adjusted curve similar to the un-offset curve. Equations 26 and 29 below were used as a fitting function for this shape, as discussed in Section 4.1 ahead.

If the deflection is less than the transition deflection, the curve is within a linear section and Equations 13 and 24 are replaced by Equations 25 and 26, respectively:

$$F = a_{Linear}\, d_{OneSpring} \tag{25}$$

$$d_{OneSpring} = \frac{F}{a_{Linear}} \tag{26}$$

If the deflection is greater than the transition deflection, the curve is offset and modified from the original equation and Equations 13, 18 and 24 are replaced by Equations 27, 28 and 29, respectively:

$$F = a_{Linear}\, d_{Transition} + a_{Curved} \frac{4\, E\, t^3\, (d_{OneSpring} - d_{Transition})}{(1-\mu^2)\, K\, D_{Outer}^2} \cdot \left[\left(\frac{h-t}{t} - \frac{(d_{OneSpring} - d_{Transition}}{t}\right)\left(\frac{h-t}{t} - \frac{(d_{OneSpring} - d_{Transition}}{2\, t}\right) + 1\right] \tag{27}$$

$$a_0 = -\frac{F - a_{Linear}\, d_{Transition}}{a_{Curved}} \tag{28}$$

$$d_{OneSpring} = -\left(s_1 + u_1 - \frac{a_2}{3\, a_3} + d_{Transition}\right) \tag{29}$$

a_{Linear}, $d_{Transition}$ and a_{Curved} are all functions of the offset and depend on which side of the disc spring is in contact. The following equations were experimentally determined for disc springs with the same dimensions and material properties as those used at UNB:

Wide side contact:

$$d_{Transition} = -0.00301\, mm^{-1}\, Q^2 + 0.09345\, Q \tag{30}$$

$$a_{Curved} = -0.0256\, mm^{-2}\, Q^2 + 0.0891\, mm^{-1}\, Q + 1 \tag{31}$$

$$a_{Linear} = 3000 \frac{N}{mm} \tag{32}$$

where Q is the offset between adjacent disc springs in mm.

Short side contact:

$$d_{Transition} = -0.004\, mm^{-1}\, Q^2 + 0.232\, Q \tag{33}$$

$$a_{Curved} = -0.064\, mm^{-2}\, Q^3 + 0.4\, mm^{-1}\, Q^2 - 0.3\, Q + 1 \tag{34}$$

$$a_{Linear} = -313 \frac{N}{mm^2}\, Q + 5767 \frac{N}{mm} \tag{35}$$

In the same way that each part having its own force to deflection curve gives a combined force to deflection curve as the parts heat up, each disc spring having its own offset gives a combined force to deflection curve. Shown below in Figure 10 is the combined force to deflection curve for four disc springs with two wide-side offsets of 0.5 mm and 1 mm and one short-side offset of -1.5 mm, compared to the unmodified curve, Equation 13:

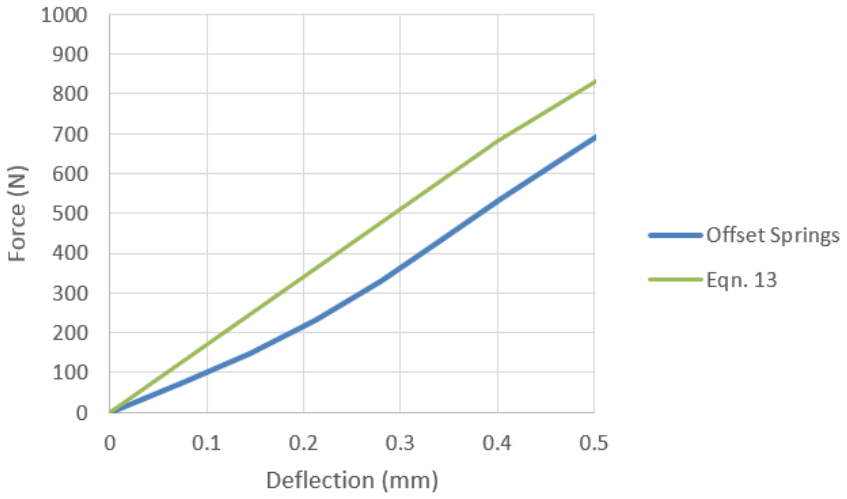

Figure 10: Combined Offset Disc Spring Force To Deflection Curve

For the tree trunk, the following equation describes the force to deflection curve based on contact between the tree trunk and the short side of a disc spring, as a slightly modified

version of the equation found by Puttock and Thwaite for use with contact between the tree trunk and an infinite bar: [21]

$$d_{trunk} = 0.35\frac{F}{c}U\left(1 + \ln\left(\frac{2\,c^3}{0.35\,U\,F\,D}\right)\right) \tag{36}$$

where U is a calculation coefficient in MPa^{-1} following Equation 37 below and c is the tree trunk contact length in mm following Equation 38 below:

$$U = \frac{1-\mu_1^2}{\pi\,E_1} + \frac{1-\mu_2^2}{\pi\,E_2} \tag{37}$$

$$c = D_{Outer,washer} - D_{Inner,washer} \tag{38}$$

Note: The parameter U is presented as V in the original source, but V is used for volume in this work.

Equation 36 above was experimentally determined (see Section 4.1 below) as a modification from Equation 39 below and has not been validated with an independent method.

$$d_{trunk} = \frac{F}{c}U\left(1 + \ln\left(\frac{2\,c^3}{U\,F\,D}\right)\right) \tag{39}$$

Thermal Expansion

The definition of linear thermal expansion is as follows:

$$\alpha = \frac{1}{L}\frac{dL}{dT} \tag{40}$$

where α is the instantaneous coefficient of thermal expansion in K^{-1}.

Equation 40 can be re-arranged and partially integrated (Equation 41 below) to give the thermal expansion equation for all parts: (Equation 42 below)

$$\ln\left(\frac{d_{TE} + L_{T_{Room}}}{L_{T_{Operating}}}\right) = \int_{T_{Room}}^{T_{Operating}} \alpha \, dT \tag{41}$$

$$d_{TE} = L_{T_{Room}}\left(\mathrm{e}^{\int_{T_{Room}}^{T_{Operating}} \alpha \, \mathrm{d}T} - 1\right) \tag{42}$$

where *L* is the part length parallel to the tree branch in mm and *e* is Euler's number, approximately 2.718.

This form of the thermal expansion equation is used because thermal expansion data is regularly given as an averaged thermal expansion coefficient, as described in the next sub-section.

Each part uses its initial part length (before any elastic compression has occurred) as L in Equation 42. For the C-ring, *L* is the outer diameter. For the ceramic washers and metal backing washers, *L* is the thickness. For the tightening nut, *L* is half of the thickness, since it is assumed the center of the nut does not move with respect to the tree branch. For the tree trunk, *L* is the radius.

In the case of the apparatus tree branch, *L* is the length from the tree trunk (exclusive) to the tightening nut (inclusive), which is the total initial length of all other components minus the initial deflection. However, since applying the initial deflection causes a force

which extends the tree branch, the initial deflection subtracted from the length of parts also includes the length of extension of the branch. This is presented as follows:

$$L_{branch} = \sum L_{part,untightened} - d_{Initial} - \frac{4\,F_{initial}\,L_{branch}}{\pi\,E\,D_{Outer}^2} \tag{43}$$

This equation can be re-arranged to group and isolate L_{branch}, giving the following:

$$L_{branch} = \frac{\sum L_{part,untightened} - d_{Initial}}{1 + \frac{4\,F_{initial}}{\pi\,E\,D_{Outer}^2}} \tag{44}$$

Since the elastic compression of the tree branch due to the applied initial deflection as a fraction of the total length at room temperature (denominator right term) should always be much less than 1 (denominator left term), the denominator is taken as 1 in the model implementation.

Material Properties

The material properties of a given alloy depend significantly on the fabricating process of the sample as well as its composition. Unfortunately, many of the alloy rods given to UNB for research purposes do not have fabrication data available and it is not UNB's intention to independently determine the necessary material property data over the large temperature range. For this reason, material property data was gathered from online alloy retailers where available. The four types of data that needed to be collected to model each alloy were Poisson ratio, the modulus of elasticity, the thermal expansion integral, and the yield strength. Data found online was typically presented as a set of data points at varying temperatures, so the data was fit to a polynomial of lower order than the number of data points.

Thermal expansion data was often presented as an averaged thermal expansion coefficient over a temperature range. To find a fit for thermal expansion data, the temperature difference of the range was multiplied by the average coefficient of thermal expansion to give an integral of thermal expansion over the range as described by the following equation:

$$\int_{T_{Room}}^{T_{Operating}} \alpha \, dT \; = \; \alpha_{Average}\left(T_{Operating} - T_{Room}\right) \tag{45}$$

Then, a fit was made of the integral with the input temperature adjusted by the shared lower bound of all temperature ranges. For example, specialmetals.com has the following coefficient of thermal expansion data for Inconel 625 (columns 1, 2 and 3 of Table 1 below): [22]

Table 1: I625 Thermal Expansion Coefficient Calculation Table

Specialmetals data			Calculated		Fit
Lower (°C)	Upper (°C)	Coefficient (1/K)	Temp Diff (K)	Integral	Integral
21	93	0.0000128	72	0.000922	0.000933
21	204	0.0000131	183	0.002397	0.002386
21	316	0.0000133	295	0.003924	0.003919
21	427	0.0000137	406	0.005562	0.005547
21	638	0.000014	517	0.007238	0.007312
21	649	0.0000148	628	0.009294	0.009228
21	760	0.0000153	739	0.011307	0.011293
21	871	0.0000158	850	0.01343	0.013492
21	927	0.0000162	906	0.014677	0.014643

Column 5 shows the integral of coefficient of thermal expansion over that temperature range (equivalent to the temperature difference times the coefficient of thermal

expansion), while column 6 shows the fit equation applied at the temperature difference, which is sufficiently close. In practice, the temperature difference is the operating temperature minus the lower bound of the data.

The following alloys have data collected and implemented in the code:

- 316 stainless steel (UNS S31600)
- Inconel 625 (UNS N06625)
- 310 stainless steel (UNS S31008)
- 347 stainless steel (UNS S34700)
- Alloy 800HT (UNS N08811)
- Haynes 214 (UNS N07214)
- Hastalloy C (UNS N10002)
- Hastalloy C-276 (UNS N10276)
- Inconel 718 (UNS N07718)
- 410 stainless steel (UNS S41000)

C-ring Stress

Once the force applied to the C-ring is known, the stress at the apex of the C-ring can be calculated. Ideal C-ring geometry is described by three measured parameters: the inside radius (r_{Inner}), the outside radius (r_{Outer}) and the width of the C-ring (w) are the root of all calculations.

For a force applied laterally to a C-ring, the stress distribution according to Pilkey [17] is given by the following equation, with F used for applied force instead of the original source's P:

$$\sigma_x = \frac{F}{A} + \frac{Mz}{Agr} \tag{46}$$

where σ is the compressive stress at the apex of the C-ring in MPa, g is the shift in location of the neutral axis in mm following Equation 47 below, z is the distance from the neutral axis to the radius of interest in mm following Equation 48 below and M is the bending moment in MPa·mm following Equation 49 below:

$$g = R - r_n \tag{47}$$

$$z = r_n - r_{Outer} \tag{48}$$

$$M = F\,R \tag{49}$$

Note: The parameter g is e in the original source, but e is used for Euler's number in this work.

The centroidal axis (R) is horizontal to the center of the cross-sectional area. The neutral axis (r_n) is the axis along which the stress is zero – neither tensile nor compressive. Due to the curved geometry of the C–ring, these two axes are not coincident, as shown in Figure 11 below which also demonstrates the conventions for F (the applied force) and M (the bending moment):

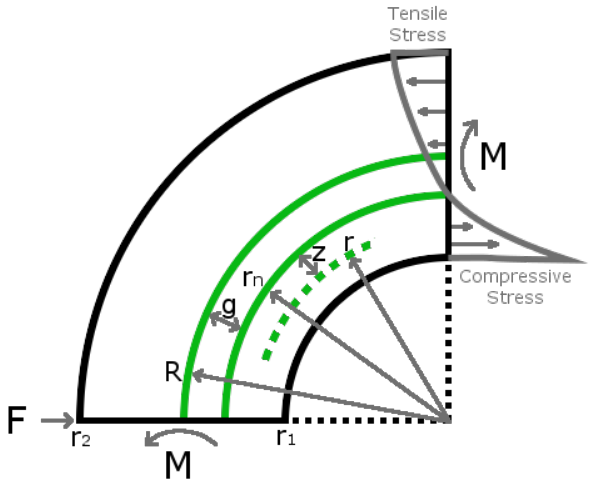

Figure 11: C-ring Deflection Diagram
After [17]

Considering that σ_x is stated to be compressive by Pilkey and the model is concerned with tensile stress, the sign must be inverted. The following equation describes the tensile stress (S) after replacing parameters with equations in Equation 46:

$$S = -\sigma_x = -\frac{F}{A} - \frac{(F\,R)(r_n - r_{Outer})}{A\,(R - r_n)\,r_{Outer}} \tag{50}$$

As the stress is linearly proportional to the force, the equation can be represented as a ratio of stress to force. Re-arranging the equation and simplifying gives the following:

$$\frac{S}{F} = \frac{-1}{A}\left(\frac{R}{r_2}\,\frac{r_n - r_{Outer}}{R - r_n} + 1\right) \tag{51}$$

This equation can be further compacted by moving the -1 to the numerator, moving r_2 from before the fraction to the numerator, moving R from before the fraction to the denominator, then replacing the hanging 1 with the denominator over itself, and finally cancelling terms. A final division of numerator and denominator by r_n gives the present model's equation as follows:

$$\frac{S}{F} = \frac{1}{A}\left(\frac{\frac{1}{R} - \frac{1}{r_{Outer}}}{\frac{1}{r_n} - \frac{1}{R}}\right) \tag{52}$$

The final step is to consider that the operating pressure of the autoclave acts as a compressive stress (subtracted from S) evenly over the entire C-ring sample. This means that the complete force to stress equation is approximated by the following equation:

$$S = \frac{1}{A}\left(\frac{\frac{1}{R} - \frac{1}{r_{Outer}}}{\frac{1}{r_n} - \frac{1}{R}}\right)F - P_{Operating} \tag{53}$$

Assumptions

This model was created for constant-load or constant-strain C-ring experiments for SCC where all parts are loaded along an axis and constrained by an operator-tightened tightening nut. This axis is the sample tree branch, which goes through all other parts to retain symmetry where possible. In all calculations, steady state operating conditions (No cracking/weakening/corrosion of materials over time) are assumed.

From the deflection balance and setup, the model assumes the following:

- Axial thermal expansion and elastic compression occur in the direction of the axis. (e.g. Disc springs don't compress at an angle) The model does not assume no radial thermal expansion.
- Each part is loaded in a straight line and is only in contact with the two adjacent parts.

- Tightening nut center does not move with respect to the tree branch after tightening has been performed.
- The tree branch remains parallel to all parts and perpendicular to the tree trunk.
- The tree branch is not in contact with any part except the tightening nut.

From the material properties, the model assumes the following:

- Material properties are a function of only alloy composition and the temperature. That is, material properties do not change because of corrosion, creep, stress relaxation, or plastic strain.
- No residual stresses from casting, machining, transport or processing of samples.
- The tensile young's modulus is the same as the compressive young's modulus for all alloys.
- All alloys are perfectly homogenous. Material properties are determined from alloys with imperfections and grains, then assumed to apply evenly to the entire alloy.

From the elastic compression equations, the model assumes the following:

- Except where otherwise determined through validation, contact with other parts does not change the deflection equation for any part.
- The geometry of each part does not change outside of thermal expansion and elastic compression. That is, no cracking, corrosion or other geometry-modifying damage occurs.

- Complex shapes may be approximated as simpler shapes. That is, the C-ring hole, the tree branch threading and the tightening nut edges do not alter their respective deflection equations.
- For the C-ring, all assumptions related Pilkey's theory of deformations for curved beams: Plane cross-sections remain plane, rotations and translations are small, stress is directly proportional to strain, and the thickness of the C-ring is much less than the radius of curvature of the C-ring. [17]
- For the disc springs, there are no deviations from the geometrically ideal form and there are no residual stresses from fabrication. [18]
- For the tree trunk, "the surfaces in contact are perfectly smooth, the elastic limits of the materials are not exceeded, the materials are homogeneous, and there are no frictional forces within the contact area." [21]

From the C-ring force to stress equation, the model retains all assumptions related to Pilkey's theory of deformations for curved beams: Plane cross-sections remain plane, rotations and translations are small, stress is directly proportional to strain, and the thickness of the C-ring is much less than the radius of curvature of the C-ring. [17]

4 Results

4.1 Finite Element Analysis Validation – Abaqus

Validation for the model was performed through the finite-element modeling software Abaqus CAE with Static General step calculations. The purpose of this software for this work was to validate the relationships between stress, strain and applied force for the geometry of each part at operating conditions. For an equation to be considered validated, validation must demonstrate that (1) the equation describes its intended situation and (2) the intended situation matches the actual situation experienced by the physical part.

In Abaqus, each part was sketched using CAD and extruded/swept into three dimensions. Extruded parts were then given constraining boundary conditions and symmetry was used to improve calculation speed and quality. Parts were partitioned into calculation elements (meshed) sufficiently small for no change in results to occur with smaller elements. Finally, the software attempted to iteratively find the state of each element such that all boundary conditions were fulfilled.

As an example of boundary conditions, shown below is the tightening nut symmetry boundary conditions (left, Figure 12) and the shape those boundary conditions would produce. (right, Figure 13)

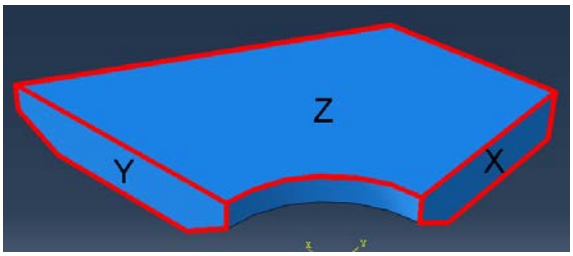

Figure 12: Symmetry Boundary Conditions

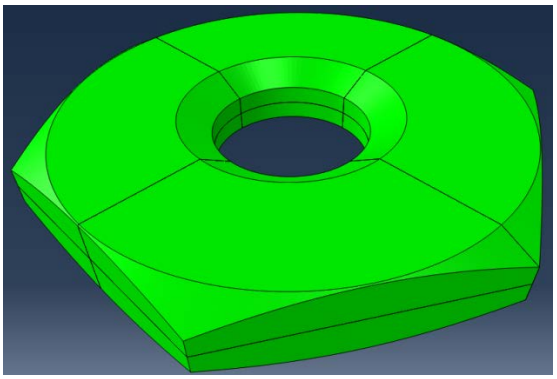

Figure 13: Complete Abaqus Part

To measure the relationship between force and deflection for each part, a reference point was set to behave as the load-bearing surface of the part using an Equation constraint. A deflection was applied to the reference point, which moved the load-bearing surface, and the load-bearing surface had a reaction force, which was copied by the reference point. This allowed analysis of the deflection and force by querying only one point – the reference point.

As Abaqus does not have an internal set of units, the following consistent units were used:

mm, N, tonne (1000 kg), s, MPa, mJ, tonne/mm^3

Similarly, as Abaqus does not have pre-established material properties, this modeling used a Young's modulus of elasticity of 198925 MPa, a poisson ratio of 0, a mass density of 7.95×10^{-5} tonnes/mm^3, and frictionless, hard contact with Penalty (Standard) constraint enforcement for contact where applicable.

The force to deflection curve was validated for each part individually, then specific cases of contact between parts were considered. Thermal expansion was not considered in this application of Abaqus, but Abaqus can consider thermal expansion if Coupled Temp-displacement is used instead of Static General at additional computational complexity.

The C-ring was modeled both with (Figure 14 below) and without (Figure 15 below) the mounting hole which exists in the actual part:

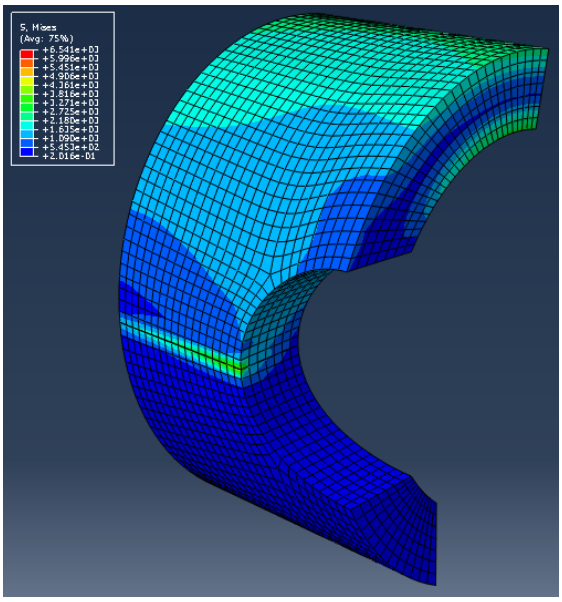

Figure 14: Von Mises Stress, C-ring with Mounting Hole

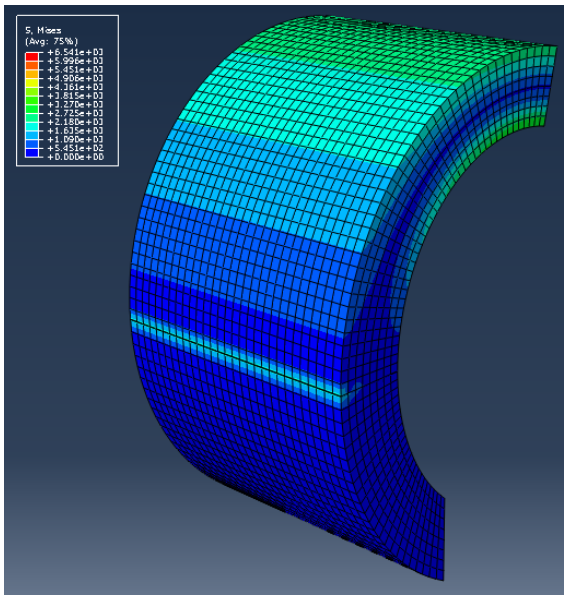

Figure 15: Von Mises Stress, C-ring without Mounting Hole

These Abaqus models were used to validate Equation 11 (Figure 16 below) and Equation 53 (Figure 17 below) for the C-ring. In Figure 17 below, the C-ring with hole model had a range of apex stress values at each applied force due to the mounting hole.

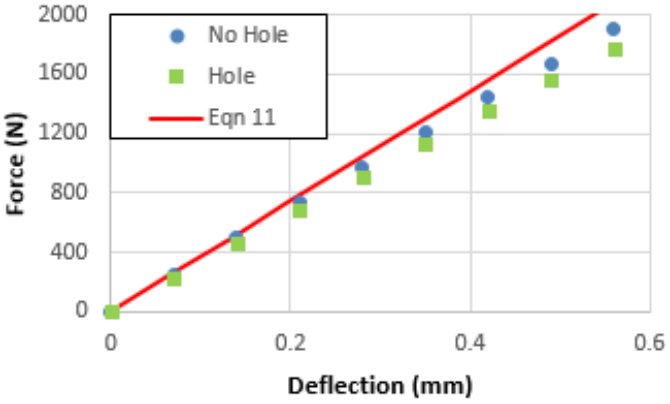

Figure 16: C-ring Force to Deflection

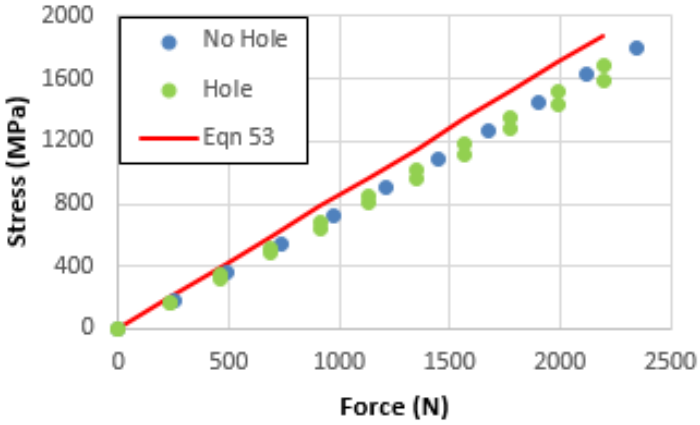

Figure 17: C-ring Force to Stress

Below 800 N applied force, the force to deflection Abaqus results are within 12% of Equation 11 while the force to stress Abaqus results are within 18% of Equation 53.

Additionally, Abaqus was used to validate the geometry of all other parts: (Equations 12, 12, and 13 for the backing washer, tightening nut, and disc spring respectively)

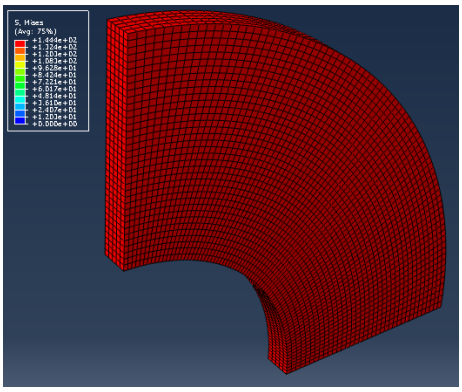

Figure 18: Washer Geometry

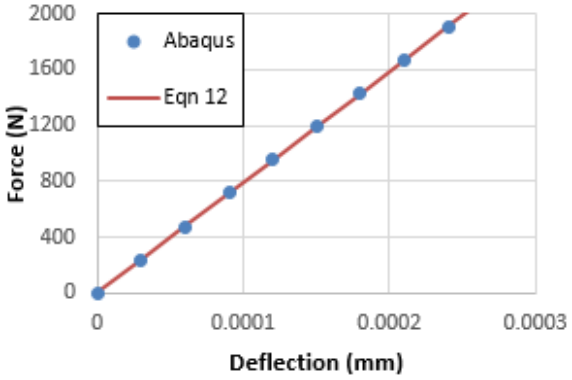

Figure 19: Washer and Tree Branch Abaqus Validation

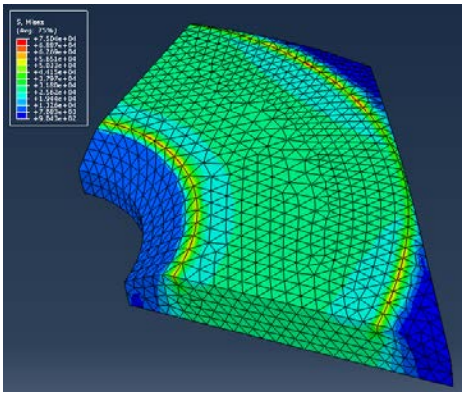

Figure 20: Nut Geometry

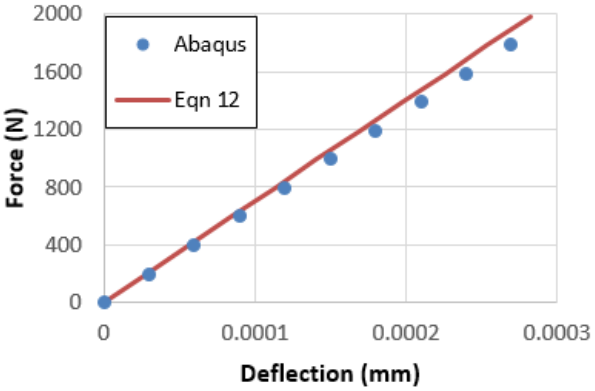

Figure 21: Nut Abaqus Validation

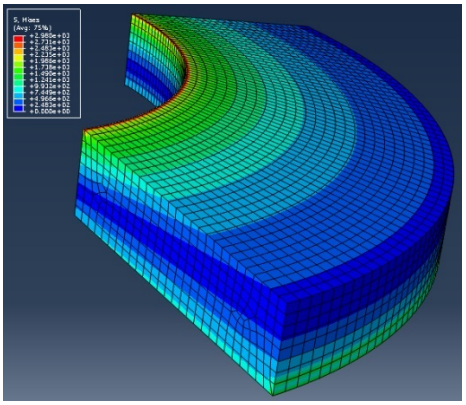

Figure 22: Disc Spring Geometry

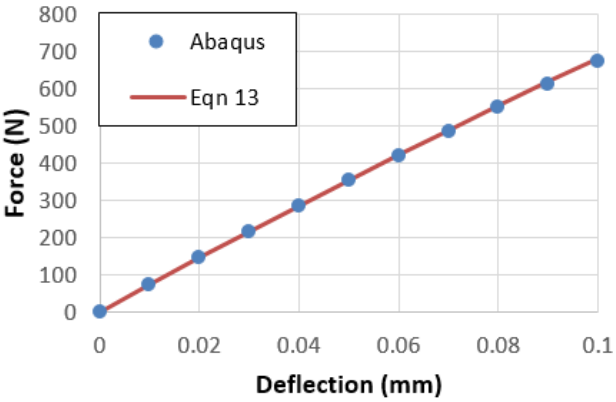

Figure 23: Disc Spring Abaqus Validation

For the backing washer, tree branch, and disc spring, the Abaqus data points were within 1% of the predicted mechanistic equation over the entire displayed range. The Abaqus

data from the tightening nut model was almost exactly 6% from the mechanistic equation at all points, likely because the mechanistic equation models a disc with a larger contact area than the Abaqus and real-life tightening nuts.

For the tree trunk, Abaqus validation showed that the original mechanistic equation (Equation 39) and the Abaqus data points agree at high force, (Def - Bar in Figure 25 below), but not at the operation forces. (Def - Bar in Figure 24 below) This agreement is only experienced for the deflection of an infinite rod applied to the tree trunk; the trunk itself (Def – Rod) is significantly offset from the mechanistic equation.

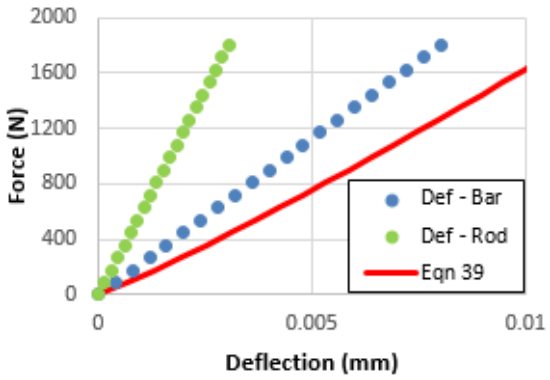

Figure 24: Tree Trunk Validation with Infinite Bar (Low Force)

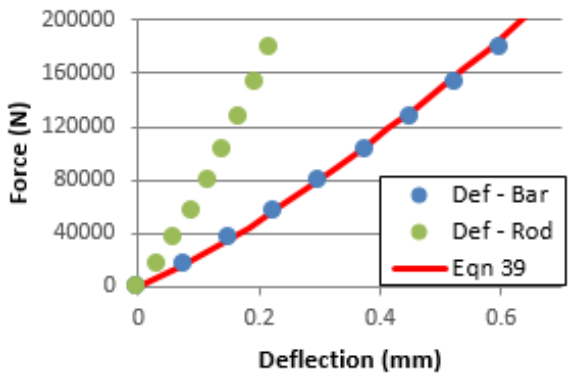

Figure 25: Tree Trunk Validation with Infinite Bar (High Force)

This was resolved through analysis of the equation's source: the mechanistic equation was derived to describe the distance that an infinite bar presses past the surface of an impinging cylinder, not the distance that the cylinder deflects due to the infinite bar. To properly model the deflection of the cylinder, contact with a backing washer was

modeled to be more realistic and the deflection of the cylinder was recorded, as shown in Figure 26 below.

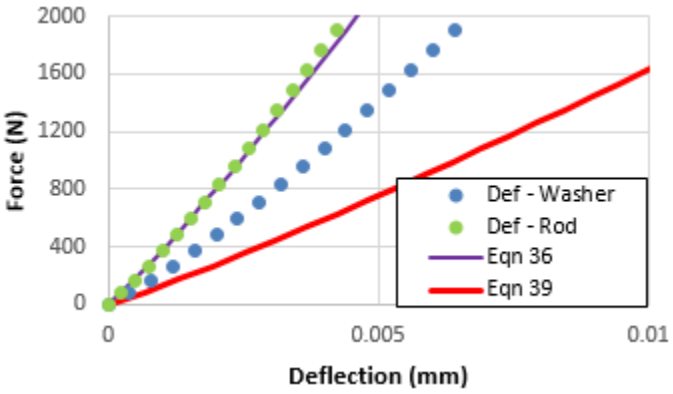

Figure 26: Tree Trunk Validation with Washer Geometry

Finally, Abaqus was used to experimentally determine unknown disc spring offset curves for both wide side contact (Figure 27 below) and short side contact: (Figure 28 below)

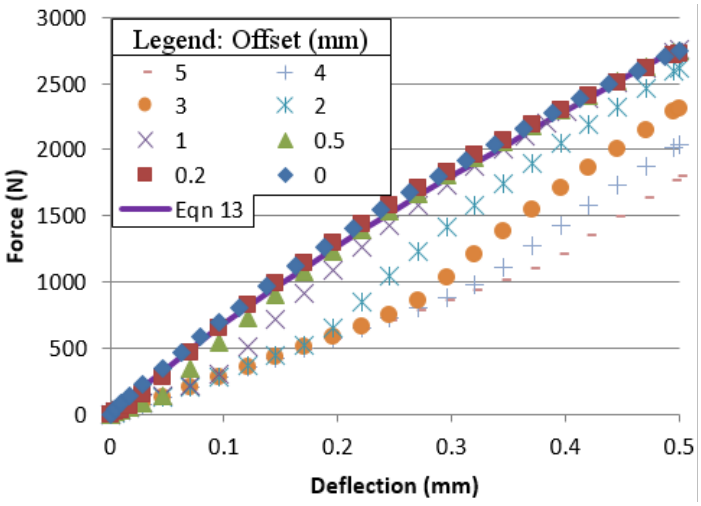

Figure 27: Disc Spring Wide Side Offset – Force to Deflection

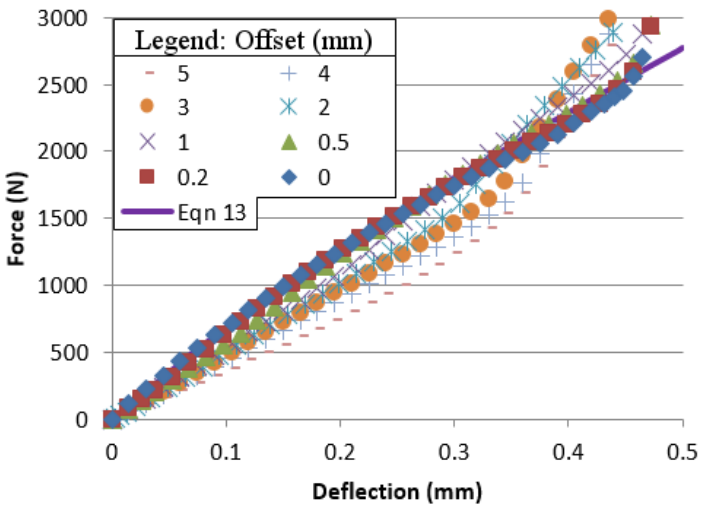

Figure 28: Disc Spring Short Side Offset – Force to Deflection

Note that the equations generated from these curves are only applicable to disc springs with the same dimensions and material properties as those used at UNB.

4.2 Model and Implementation

With each equation of the model individually validated, the model was implemented in Visual Basic for Microsoft Excel. The primary goal of the implementation is to accurately characterize the relationship between stress, initial deflection and sample setup geometry with less computational strain than a full Abaqus model. For example, shown below in Tables 2 to 4 are deflection data for each part at three stages of an experimental test at 600 °C and 25 MPa:

Table 2: I625 Example Test Part Lengths Before Loading (mm)
(Force: 0 N, Apex Stress: 0 MPa, Yield Strength: 312.5 MPa)

	C-ring	Springs	Washer	Nut	Trunk	Branch
Base Length	12.70	17.07	2.84	1.36	6.40	39.24

Table 3: I625 Example Test Part Lengths Before Heating (mm)
(Force: 492.6 N, Apex Stress: 369.2MPa, Yield Strength: 420.8 MPa)

	C-ring	**Springs**	**Washer**	**Nut**	**Trunk**	**Branch**
Thermal Expansion	0	0	0	0	0	0
Elastic Compression	-0.12685	-0.99104	-0.00013	-0.00007	-0.00130	-0.01092
Total Deflection	-0.12685	-0.99104	-0.00013	-0.00007	-0.00130	-0.01092

Table 4: I625 Example Test Part Lengths After Heating (mm)
(Force: 444.2 N, Apex Stress: 324.8 MPa, Yield Strength: 324.8 MPa)

	C-ring	**Springs**	**Washer**	**Nut**	**Trunk**	**Branch**
Thermal Expansion	0.10158	0.14625	0.02962	0.01418	0.06674	-0.26408
Elastic Compression	-0.13521	-1.07499	-0.00015	-0.00008	-0.00143	-0.01273
Total Deflection	-0.03363	-0.92874	0.02947	0.01410	0.06531	-0.27681

This information is useful to visualize how loading and heating takes place in the autoclave. As well, it would be useful to compare with validation from sources such as the Advanced Photon Source at Argonne National Laboratory, which can show the strain of each part as the experiment proceeds.

Another function of the implementation is to evaluate the apex stress resulting from an initial deflection applied to a known setup. For example, shown below in Table 5 is a collection of experiments performed by Raoul (316 SS C-ring samples with 4 washers at varying conditions) with apex stresses calculated by both Raoul's implementation and by this work's implementation for comparison. Samples labeled A#.BB were part of a sub-critical test at 288 ºC and 1.73 MPa for 500 hours, while samples labeled B#.SC were part of a sub-critical test at 500 ºC and 16.5 MPa for 502 hours.

Table 5: Previous Work Samples Re-calculated

	C-ring Dimensions			Parts			Stress	
	t (mm)	D_{Outer} (mm)	w (mm)	$\#_{Discs}$	$\#_{Ceramics}$	$d_{Initial}$ (mm)	Raoul (MPa)	This Work (MPa)
A1.BB	1.58	12.63	12.39	7	2	0.1084	145.45	88.83
A2.BB	1.57	12.62	12.39	9	2	0.0491	72.72	46.61
A3.BB	1.57	12.64	12.37	7	2	0.1053	145.45	87.81
A4.BB	1.58	12.64	12.39	7	2	0.1081	145.45	88.71
A5.BB	1.57	12.62	12.28	9	2	0.0481	72.72	46.40
A6.BB	1.6	12.61	12.32	7	2	0.1130	145.45	90.43
A7.BB	1.58	12.65	12.04	9	2	0.047	72.72	46.13
A8.BB	1.63	12.65	12.38	7	2	0.1208	145.45	92.55
A9.BB	1.58	12.6	12.36	7	2	0.1076	145.45	88.41
A10.BB	1.59	12.64	12.33	7	2	0.1098	145.45	89.31
A11.BB	1.57	12.69	12.23	9	2	0.0465	74.14	45.84
A12.BB	1.59	12.61	12.35	1	1	0	0 - Blank	0
B1.SC	1.6	12.7	11.84	9	0	0.1071	121.26	75.17
B2.SC	1.63	12.68	11.89	10	0	0.09	90.95	61.16
B3.SC	1.62	12.64	11.89	9	0	0.1167	121.26	77.54
B4.SC	1.67	12.66	11.96	9	0	0.1350	121.26	81.05
B5.SC	1.6	12.69	11.99	10	0	0.0826	90.95	59.69
B6.SC	1.66	12.69	12.1	9	0	0.1333	121.26	80.50
B7.SC	1.64	12.66	11.89	10	0	0.0937	90.95	61.90
B8.SC	1.62	12.7	11.94	9	0	0.1157	121.26	77.01
B9.SC	1.7	12.67	12.02	9	0	0.1173	121.26	69.95
B10.SC	1.64	12.73	11.96	9	0	0.122	121.26	78.20
B11.SC	1.66	12.7	11.95	10	0	0.0997	90.95	62.74
B12.SC	1.59	12.66	11.91	0	0	0	0 - Blank	0

In every case, including those presented above, the old model under-calculated the required stress. This may explain why none of Raoul's completed trials underwent SCC.

4.3 Autoclave Results

Four separate tests in the static autoclave were conducted on the zirconium modified 310s SS (Fe-25.9Cr-20.5Ni-0.9Mn-0.5Mo-0.6Zr) material fabricated at CANMET at the conditions shown in Table 6 below to develop and improve the testing technique. As no validation was performed on the loading technique, these trials are unsuitable for precise determination of SCC resistance.

Table 6: Test Conditions

Test	**FX.SC**	**GX.SC**	**HX.SC**	**IX.SC**
Temperature (ºC)	600	600	600	600
Pressure (MPa)	27.6 decreasing to 11.6	26.89	25	22.06
Time (hrs)	600	858	500	845
Materials	310 SS mod Zr	Hast C-276, 310 SS, I625	310 SS mod Zr	310 SS mod Zr
Number of Samples	12	3 of each	6	11
Number of Blanks	0	1 of each	0	0
Low Stress (MPa)	184.2	66.88	127.92	123.94
High Stress (MPa)	unknown*	105.01	392.56	404.95

* Some samples in FX.SC were stressed past the elastic region intentionally.

Each completed trial produced samples for analysis.

Optical Microscope Pictures

Samples undergo general surface corrosion during trials, so optical microscope pictures taken after the trial can differ significantly from pictures taken before the trial. For example, shown below as Figure 29 and Figure 30 are the trial samples I1.SC I2.SC before and after Trial I:

Figure 29: I1.SC Before (Left) and After (Right) Trial

Figure 30: I2.SC Before (Left) and After (Right) Trial

Samples are very reflective in pictures taken before the trial, so all manner of imperfections are visible. After the trial, however, samples have been oxidized and are significantly less reflective. The difference between pictures is so great that the orientation of samples is difficult to determine by picture alone.

To ensure that all samples are compared before/after with the right orientations, each sample should be marked in a consistent place before cleaning. For example, an

indentation can be made on the open cross-section at the tip of either side of the C-ring; this mark identifies that side of the C-ring and all pictures can be taken with the marked side to the left, ensuring the correct orientation. This marking can be in addition to the markings advised by ASTM G38-01 for specimen numbers. [13]

Scanning Electron Microscope (SEM) Pictures

SEM pictures of a cross-section can be used to determine the presence and characteristics of a crack which does not fully fracture a sample. Additionally, energy-dispersive X-ray spectroscopy can be performed to characterize the base metal, oxide layers and corrosion products. Unfortunately, applying an epoxy to mount a sample for SEM crack analysis will cover any corrosion products. For this reason, an operator must choose what type of analysis will be performed for each sample.

Completed C-ring samples from trial FX.SC were viewed with an optical microscope between stages of incremental polishing to find cracks for further analysis. Select samples were incrementally polished further, ending with a 1 micron diamond polish.

As no validation was performed for the loading technique, only preliminary analysis has been completed on these samples to improve the technique and sample preparation. For example, sample F11.SC was stressed far past the yield point with the intention of inducing a mechanical fracture for analysis. Shown below in Figure 31 is a cross-section of the fractured sample:

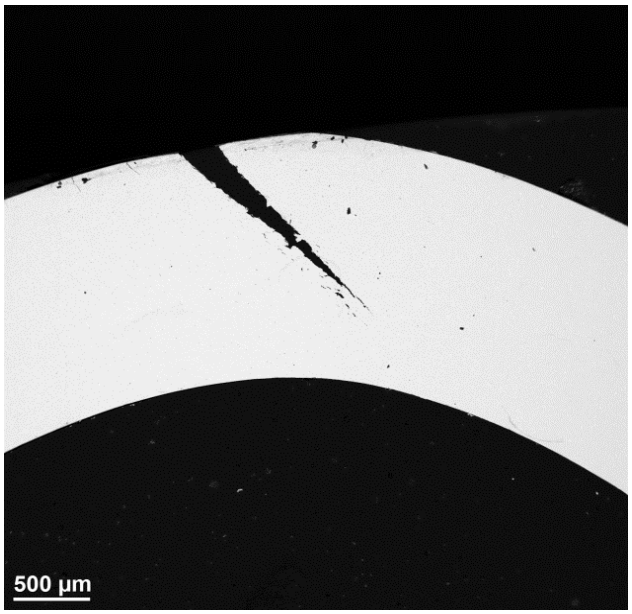

Figure 31: F11.SC Cross-section with Scanning Electron Microscope

It is impossible to try and estimate the actual magnitude of the stress applied before cracking since the equations developed here assume that the material is still in the elastic region. The mode of failure is obviously brittle fracture but there is evidence of oxidation along the crack surfaces. Cracking of this magnitude has not yet been observed with any other samples, although other samples were stressed more aggressively.

Analysis of the crack shows other fractures passing through the sample which look like void spaces, as shown in Figure 32 below. At a higher magnification, a picture was taken along an inside edge of the internal fracture and labeled for use with oxide analysis through EDX, as shown in Figure 33 below:

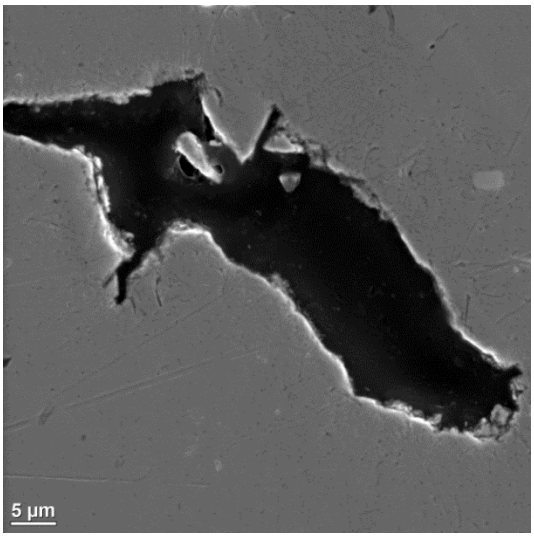

Figure 32: F11.SC Void Near Crack Tip

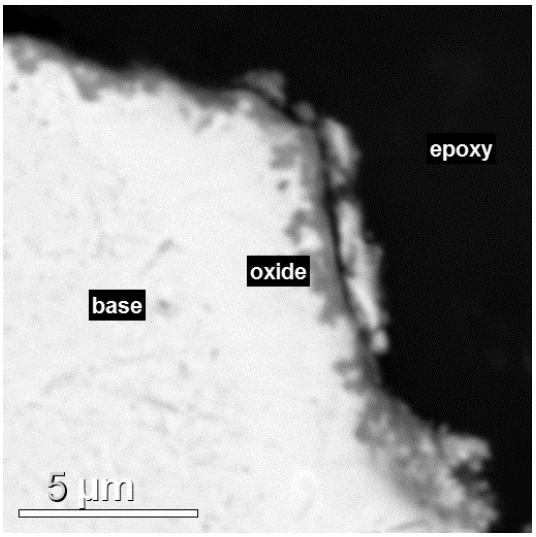

Figure 33: F11.SC magnification of Void

Figures 34 to 36 below show the EDX analysis performed at each of the labeled spots in Figure 33:

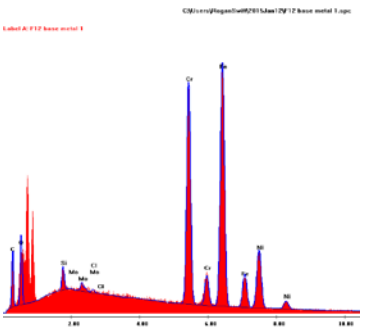

Figure 34: F11.SC Base Metal

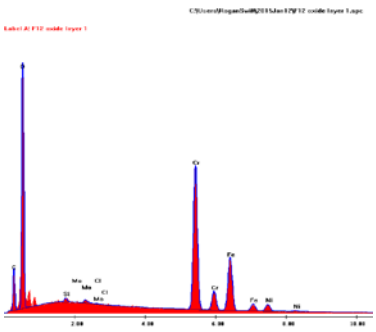

Figure 35: F11.SC Oxide Coating

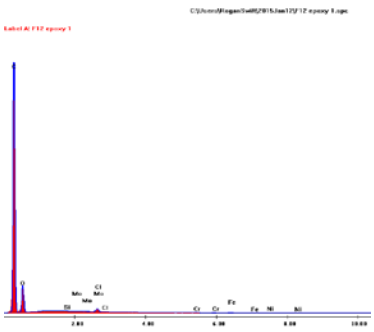

Figure 36: F11.SC Epoxy

A quick glace over Figures 34 to 36 above shows that the oxide coating (Figure 35) is rich in chromium and oxygen compared to the base metal, (Figure 34) suggesting a chromium oxide layer as is standard for stainless steel, while the epoxy (Figure 36) is

almost exclusively carbon as expected. No further analysis has been performed using these figures.

Additionally, it was determined that retaining a tested blank and an untested blank for SEM comparison would be useful for a full characterization of the tested alloy samples.

4.4 Stress While Heating Up

The intent for this technique was to apply a base force onto the C-ring with the initial deflection, then allow thermal expansion to increase the applied force such that the desired final force and stress are reached precisely at the final operating temperature. However, it was discovered that the stress at the apex of the C-ring at room temperature due to the initial deflection alone could exceed the desired final stress. That is, the sample may de-stress during heating as shown in Figure 37 below where the stress of an Inconel 625 sample is compared to its yield strength:

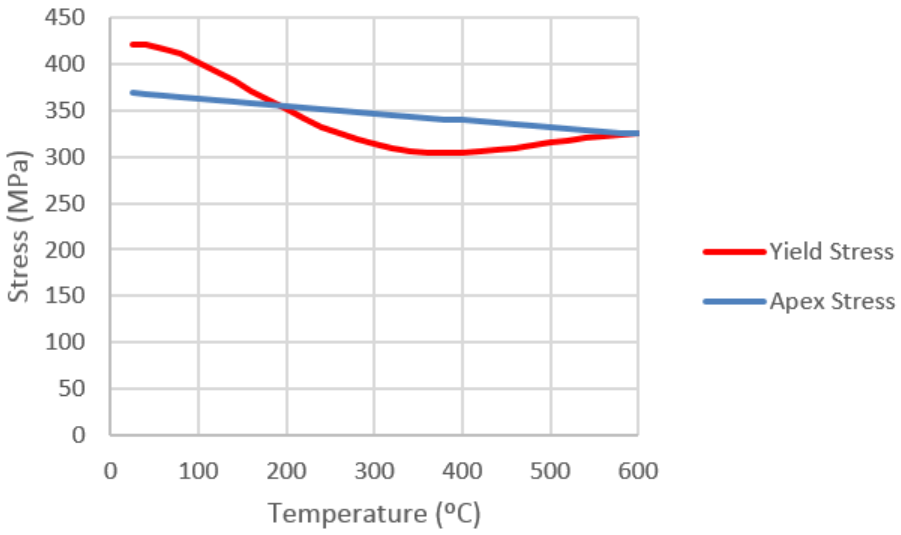

Figure 37: I625 Apex Stress during Heating

Surpassing the yield strength on the way to the final apex stress causes plastic deformation, so care must be made to fully understand this effect and how it can be reduced or completely mitigated with changes to the experimental setup.

Two mechanisms contribute to the shape of the stress curve while heating up. First, the deflection balance applied at room temperature is set for the final temperature, so the change of thermal expansion between temperatures is balanced by an opposing change in elastic compression according to the deflection balance. Second, the force to deflection curve for each part depends significantly on temperature, so the combined force to deflection curve of the setup changes significantly between temperatures.

These two mechanisms are displayed together in Figure 38 below, which shows the combined force to deflection curves at each temperature for the default setup using an Inconel 625 C-ring, as well as the actual deflection/force points. Note that the upper left point is at room temperature, while the lower right point is at operating temperature.

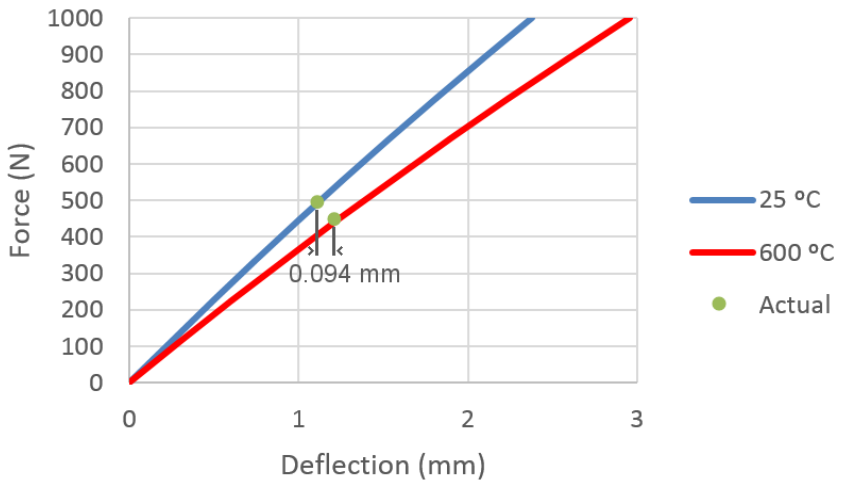

Figure 38: Setup Force to Deflection Curves with Operating Positions

Effect 1: Working backwards, the setup loses 0.094 mm of thermal expansion from the operating temperature point to the room-temperature point. (0.358 mm from non-branch parts, 0.264 mm of which is counteracted by the branch) The deflection balance is always maintained, so the elastic compression decreases by the same amount; this is reflected by a decrease of 0.094 mm in deflection along the x-axis.

Effect 2: If both temperatures had the same force to deflection curve, the room-temperature force would be lower than the operating-temperature force as desired; instead, the room-temperature force to deflection curve is higher and the resulting final room-temperature force is higher.

Result: The applied force at room temperature is higher than at operating temperature, so the resulting apex stress is also higher at room temperature than at operating temperature.

On a related note, as the thermal expansion of the tree branch significantly counteracts the thermal expansion of the rest of the parts, reducing the thermal expansion of the tree branch would increase the amount of net thermal expansion lost and decrease the room-temperature force. Similarly, a lower target stress would have experienced less offset between curves and an improved room-temperature force.

Finally, some alloys (I625 above included) experience a yield strength anomaly where the yield strength increases over a range of temperature, leading to a bump in the yield strength curve. Roy and Marthandam [23] attribute the yield strength anomaly of Inconel 617 around 900 ºC to the formation and accumulation of other-phase precipitates, as well as other dislocation and subgrain effects, although they recognize that a unified mechanism for all alloys has not yet been accepted.

For cases like I625 where the target temperature is within the yield strength anomaly range, the technique is limited to a maximum target stress. This effect is demonstrated in Figure 39 below where the line aiming for 100% of the final stress (Case 1) exceeds the yield strength, while the line aiming for 89% of the final stress (Case 2) does not exceed the yield strength:

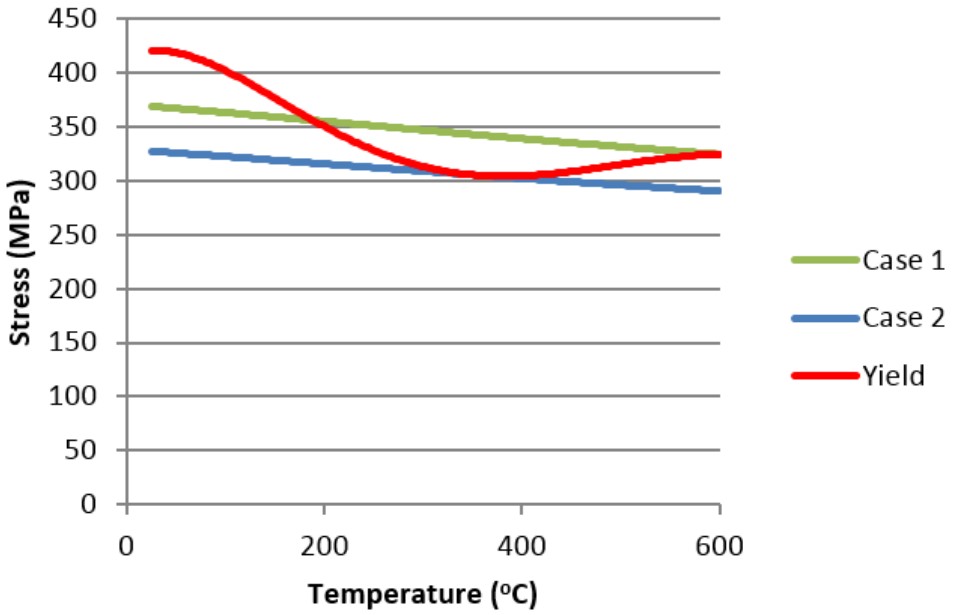

Figure 39: I625 Apex Stress during Heating (Alternate)

Heating-up effects do not constrain this technique for 347 SS and Alloy 800 HT, for example, as they experience an increase in force while heating. Similarly, this technique is not limited by this phenomenon for 316 SS, 310 SS, Hast-C, Hast C-276, and 410 SS, as they experience a decrease in heating but remain below the target stress at all points due to a greater drop in yield strength between temperatures. However, operators should always ensure that this technique does not cross the yield strength line for their own conditions.

4.5 Variation of Parameters Analysis

To characterize the variability of constant-load experiments at the University of New Brunswick, Monte-Carlo analysis was performed with the model implementation. Each measurable parameter was varied with an even distribution over a range of the average minus and plus 0.005 mm. (half the precision of a pair of Vernier calipers) Additionally,

initial deflection was varied over plus/minus 0.01 mm to account for the zero-force determination, temperature was varied over plus/minus 5 K, operating pressure was varied over plus/minus 1 MPa, yield strength was varied over plus/minus 84.66 MPa, modulus of elasticity was varied over plus/minus 2.554 GPa, the integral of thermal expansion coefficient was varied over plus/minus 0.00013938, and the Poisson ratio was varied over plus/minus 0.005896.

This analysis assumes that the relevant dimensions of each part are measured before each trial and that each dimension of the 15 disc springs is independently measured. If each part is not measured before each trial, the variance of each measurement should instead be the variance between parts, not between measurement instances. For example, if the C-ring thickness is not measured before every trial, the variance of that measurement should be the range containing all C-ring thicknesses, not the smaller range of Vernier caliper precision.

Shown below is the distribution of final stress with all parameters varying (left, Figure 40) and with all parameters except the yield strength varying (right, Figure 41). Note that the vertical axis scale for the two figures is very different.

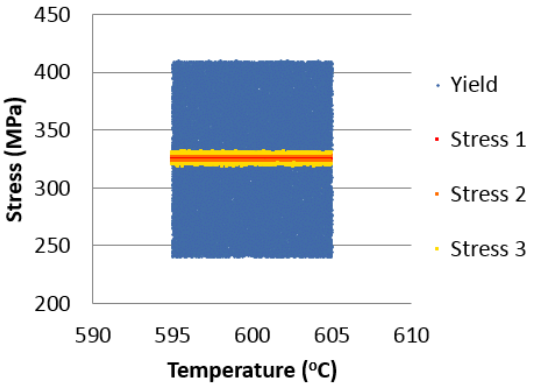

Figure 40: Monte Carlo (All Parameters Varying)

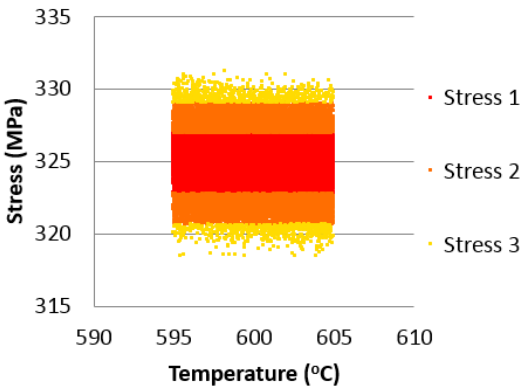

Figure 41: Monte Carlo (All Parameters Except Yield Strength)

Figure 40 represents the current experiment conditions, comparing the final apex stress (warm colors) to the varied 0.2% offset yield strength (blue) while aiming for the expected 0.2% offset yield strength of I625 at 600 °C, 324.8 MPa. Sources for the yield strength of Inconel 625 vary significantly based on alloy processing, such as extrusion or rolling, annealing and chemical treatments. Given the wide range of possible processing techniques, the yield strength of I625 varies evenly over plus/minus 84.66 MPa. Such a large variation in target stress is unacceptable; if the yield strength is not known with precision, all samples together (as they presumably share processing) have a significant chance of being well above what should have been the target stress (all samples risk cracking due to purely mechanical causes) or being well below what should have been the target stress (if SCC would have occurred, it instead forms no cracks and is not detected).

Figure 41 represents a case where the yield strength is known. In 30000 repetitions of the Monte Carlo simulation, the stress was within 4.16 MPa of the desired final stress 28883 times or 96.3% of the time with a nearly normal distribution.

The Monte Carlo simulation was modified to determine the most significant parameters for later optimization. Shown below in Table 7 is a list of scenarios and the variation of their final stress presented as two standard deviations for normal distributions or the variation of their half-range for even distributions.

Table 7: Sensitivities of Measured Model Parameters

Scenario	**Variation (MPa)**	**Distribution**
Including Yield Strength	**84.66**	Even
All but Yield Strength	**4.16**	Normal
Initial Deflection (mm)	2.56	Even
C-ring Thickness (mm)	2.09	Even
Disc Spring Thickness (mm)	1.10	Normal
Operating Pressure (MPa)	1.00	Even
Disc Spring Unloaded Height (mm)	0.466	Normal
Temperature (C^o)	0.335	Even

All measurements not shown in this list are below 0.1 MPa apex stress standard deviation, which is negligible in comparison to the scenarios listed above.

4.6 Ways to Reduce Stress Variation

First, yield strength must be determined accurately by measurement or spec sheet from the supplier.

The stress variation due to the various measured parameters can be reduced in other ways if desired, as shown in the following cases. In each case, the actual stress precision is calculated with less accuracy than the Monte Carlo method by using an approximation to speed calculations: all even-distribution measurements are approximated to be normal distribution, with two times the normal-distribution standard deviation equal to the even-distribution half-range. This changes readings for the total stress variability from 4.16 MPa to 5.64 MPa.

This approximation enables the use of Equation 54 below, which requires the instantaneous derivative of the stress with respect to each measurement (dS/dm) and two times the standard deviation of the measurement for each measurement. (v) This equation also assumes that derivatives higher than the first are small and random errors in measurements of each parameter are independent: [24]

$$v_S = \sqrt{\sum_m \left(\frac{dS}{dm}\right)^2 v_m^2} \tag{54}$$

where m is a measurement of a setup parameter using the units of that measurement and v is two times the standard deviation of some measurement in the units of that measurement.

Note: The parameter v here is one standard deviation in the original source, but quick replacement demonstrates that the equation is equally applicable for one standard deviation or two.

In all scenarios that follow, the following constraints are maintained so that the model's assumptions remain met:

1. The C-rings must have a D_{Outer}/t ratio of more than 2.2. [17]
2. The C-rings must have a D_{Outer}/t ratio of less than 17. [17]
3. The C-rings may not deflect more than 75% of their outer diameter, or 22 kN with current dimensions. As C-ring dimensions change, this limit will also change.
4. The disc springs may not deflect more than 75% of their unloaded height, or 1716 N with current dimensions. [18]
5. The number of disc springs must be a whole number.
6. The C-ring width must be between 5 mm, to still have space for a loading hole, and 20 mm, so that the model equation is not disturbed by the contact area.
7. If a secondary C-ring is used, the secondary C-ring must not have a higher apex stress than the primary C-ring, as that would cause undesired cracking in the secondary C-ring before cracking was expected in the primary C-ring.

A straightforward modification that can be made is the addition of more available space for part loading. With more space, any offsets in the initial deflection are distributed over more parts, leading to less error in the C-ring deflection and finally in the C-ring stress.

Depending on how the added space is used, this modification can improve the sensitivity of different measurements. For example, adding additional disc springs in the available space reduces the stress variation from 5.6365 MPa at 40 mm available space (14 disc springs) to 5.4265 MPa at 80 mm available space. (46 disc springs)

As the C-ring apex stress is the primary consideration, the C-ring parameters are important considerations to improve sensitivity. The three modifiable dimensions for the C-ring are the outer diameter (D_{Outer}, 12.7 mm), the thickness (t, 1.67 mm) and the width (w, 12.7 mm). For example, optimizing the C-ring parameters at 40 mm available space reduces the stress variation from 5.6365 MPa to 4.9521 MPa at 23.7 mm outer diameter, 20 mm width, 1.39 mm thickness, and 5 disc springs.

Non-C-ring parts contribute to the C-ring apex stress only through the sum of their thermal expansion and elastic compression/tension. As well, since the C-ring is not changed with these modifications, the target apex stress is reached with the same force, no matter the changes. With these things in mind, sensitivity can be improved by any change with a shallower deflection to force curve at the target force. Four examples below demonstrate proper and improper ways to make changes:

1) Using a material with a lower modulus of elasticity for any non-C-ring part will flatten that part's force to deflection curve and improve sensitivity. This is only a small improvement at best.

2) Replacing of some disc springs with an equivalent-length C-ring is not an improvement of sensitivity, as the optimal secondary C-ring given the constraints above always has a higher variation in stress than the existing case.
3) Removing all disc springs and using a much larger C-ring is a small improvement in stress variation as all disc spring-related variations are removed. However, the experiment is then constant-strain instead of constant-load, so the stress during cracking is no longer a conservative engineering estimate.

It is important to note that the premise of this section – sensitivity can be improved by flattening the force to deflection curve of non-C-ring parts – can be at odds with the heating up effect discussed in Section 4.4 above. An ideal selection of non-C-ring parts would combine a low local force to deflection curve tangent with an otherwise desirable high total deflection.

5 Conclusions

To improve the experimental setup for conducting SCC testing in supercritical water, the UNB Supercritical Water Group have been developing a technique using constant load C-ring samples. The technique, which relies upon thermal expansion to induce the force on the samples, has been validated through modelling but not tested with in-situ experimentation. Monte-Carlo simulations indicate that the final stress is within 4.16 MPa of the target stress 96.3% of the time, if the yield strength is well-known. Results of the revised modelling indicate that certain alloys experience a yield strength anomaly and have a limited maximum target stress using this technique; suitable materials include 316SS, 310 SS and A800. Preliminary in-situ experimentation found no SCC in 310 SS samples after 500 hours at 600 ºC and 25 MPa over a wide range of apex stress.

6 Recommendations

6.1 Sample and Autoclave Setup

Two identified weaknesses of the technique have not yet been resolved:

- Slippage of the tightening nut during a trial is possible. If the tightening nut slips after initial tightening, the entire setup will experience less applied force and the C-ring apex will experience less tensile stress. This can be checked before/after an experiment, but it should be mitigated somehow.
- Considering that even small offsets from the intended initial deflection have a significant effect on the final stress, it was identified that a consistent way to measure initial deflection was required. For example, measuring from the outer side of the nut to the outer side of the tree trunk is inconsistent, as the threading of the tree branch puts the nut at enough of an angle for measurements to differ depending on the radial side of the nut.

Additionally, four improvements to the technique were recognized after the experiments presented here were performed:

- The zero-force point definition is far too subjective. The presented technique requires that an operator identify the initial deflection at which parts just barely do not hold each other up by friction, but if necessary, strain gauges can be used at room temperature to check the room-temperature stress and thus verify the initial deflection.
- Take pictures of the loaded tree before and after trial. General pictures would have given a small insight into disc spring offsets for earlier trials.

- If sensitivity becomes low enough, put multiple C-rings per tree branch. Validation must be performed to determine the number and dimensions of optimally-set disc springs.
- The amount of available space for a given setup can be slightly increased by calculating the part setup and initial deflection such that the unloaded parts to not fit on the tree branch, but the initial deflection brings them to just barely fitting, perhaps by loading the tightening nut on a loose screw and transferring during loading. This is risky, as even slight slippage of the tightening nut will undo all loading.

6.2 Modelling

The following three effects are estimated to be on or below the scale of 0.01 mm impact, but can be added for improved model accuracy:

- Operating pressure applies a deflection balance compression to all parts in addition to the implemented applied compressive stress.
- The branch length depends on the force before heating, but after loading. Note that this effect is estimated to be negligible.
- All part contacts cause equations which are different from their individual mechanistic equations.

6.3 Validation

To validate the technique, the following two tests are recommended:

- Perform a purely-mechanical test with strain gauges at a low temperature to show that the loaded sample experiences the expected stress.

- Perform a stress corrosion cracking test with an alloy that is known to consistently crack at the testing conditions.

Either test can be performed at a Synchrotron facility for significantly improved data.

Validation of individual disc springs showed that the mechanistic equation is valid only if the contact area between adjacent disc springs is very small. Further validation can be performed on the exact shape and size of the disc spring contact area.

6.4 Future Work

The existing disc spring can be replaced with some as-yet undiscovered disc spring equivalent that has a high EC at the target force to reduce heating up problem and a low Force-deflection tangent at that EC to improve sensitivity.

A major consideration in stress corrosion cracking tests is change in stress at apex/crack tip while cracking. Abaqus modeling can approximate cracking through at least two methods, so this can be further researched: Abaqus has in-built crack analysis and an operator can perform pseudo-steady-state crack analysis with the Static General mode.

7 Bibliography

[1] Generation IV International Forum, "Framework Agreement for International Collaboration on Research and Development of Generation IV Nuclear Energy Systems," February 2005. [Online]. Available: https://www.gen-4.org/gif/upload/docs/application/pdf/2014-01/framework_agreement.pdf. [Accessed May 2016].

[2] Generation IV International Forum, "A Technology Roadmap for Generation IV Nuclear Energy Systems," December 2002. [Online]. Available: https://www.gen-4.org/gif/upload/docs/application/pdf/2013-09/genivroadmap2002.pdf. [Accessed May 2016].

[3] Generation IV International Forum, "Technology Roadmap Update for Generation IV Nuclear Energy Systems," 2013. [Online]. Available: https://www.gen-4.org/gif/upload/docs/application/pdf/2014-03/gif-tru2014.pdf. [Accessed May 2016].

[4] Generation IV International Forum, "Generation IV Goals," 2002. [Online]. Available: https://www.gen-4.org/gif/jcms/c_9502/generation-iv-goals. [Accessed May 2016].

[5] M. Yetisir, "Generation IV Supercritical Water-Cooled Reactor," in *2012 Deep River Science Academy Summer Lecture*, Deep River, 2012.

[6] I. L. Pioro, H. F. Khartabil and R. B. Duffey, "Heat transfer to supercritical fluids flowing in channels - empirical correlations (survey)," *Nuclear Engineering and Design 230,* pp. 69-91, 2003.

[7] GIF Experts' Group, "Use of Thorium in the Nuclear Fuel Cycle," Generation IV International Forum, 2010.

[8] B. Sur, "Canadian Nuclear Laboratories' Thoria Roadmap Project," in *Thorium Energy Conference*, 2015.

[9] D. Santoianni, "Setting the Benchmark: The World’s Most Efficient Coal-Fired Power Plants," 16 March 2015. [Online]. Available: http:cornerstonemag.net/setting-the-benchmark-the-worlds-most-efficient-coal-fired-power-plants/.

[10] D. Guzonas, M. Edwards and W. Zheng, "Assessment of Candidate Fuel Cladding Alloys for the Canadian Supercritical Water-cooled Reactor Concept," in *The 7th International Symposium on Supercritical Water-cooled Reactors*, Helsinki, 2015.

[11] NRC, "Davis-Besse Reactor Pressure Vessel Head Degradation: Overview, Lessons Learned, and NRC Actions Based on Lessons Learned," August 2008. [Online]. Available: http://www.nrc.gov/docs/ML0824/ML082490129.pdf.

[12] National Physical Laboratory, "Stress Corrosion Cracking," 2000. [Online]. Available: www.npl.co.uk/upload/pdf/stress.pdf. [Accessed June 2016].

[13] ASTM International, "Standard Practice for Making and Using C-Ring Stress-Corrosion Test Specimens (G38-01)," *ASTM*, 2013.

[14] W. Zheng, G. Gu, D. Guzonas and J. Luo, "Assessment of corrosion and stress corrosion cracking results for SCWR development: Gaps and Needs," in *The 2nd Canada-China Joint Workshop on Supercritical Water-Cooled Reactors (CCSC-2010)*, Toronto, Ontario, 2010.

[15] G. Gu, W. Zheng and D. Guzonas, "Corrosion Database for SCWR Development," in *2nd Canada-China Joint Workshop on Supercritical Water-cooled Reactors*, Toronto, 2010.

[16] B. Raoul, Evaluation of stress-corrosion cracking of materials in supercritical water using a novel spring-loaded c-ring technique, Fredericton: University of New Brunswick, 2014.

[17] Pilkey, Formulas for Stress, Strain and Structural Matrices, NY: John Wiley & Sons, 1994.

[18] DIN, DIN 2092: Disc Springs - Calculation, Berlin: DIN Deutsches Institut für Normung, 1992.

[19] R. Swift, W. Cook, C. Bradley, R. C. Newman and W. Zheng, "Validation of

Constant Load C-ring Apex Stresses for SCC Testing in Supercritical Water," in *The 7th International Symposium on Supercritical Water-cooled Reactors*, Helsinki, 2015.

[20] C.-S. Cheong, A. Salazar, S. Rufus and J. Khim, "Cardano's Method," [Online]. Available: https://brilliant.org/wiki/cardano-method/.

[21] M. Puttock and E. Thwaite, Elastic Compression of Spheres and Cylinders at Point and Line Contact, Melbourne: Commonwealth Scientific and Industrial Research Organization, 1969.

[22] Specialmetals, "Inconcel alloy 625," 13 August 2013. [Online]. Available: http://www.specialmetals.com/assets/documents/alloys/inconel/inconel-alloy-625.pdf.

[23] A. K. Roy and V. Marthandam, "Mechanism of yield strength anomaly of Alloy 617," *Materials Science and Engineering: A (Volume 517, Issues 1-2)*, pp. 276-280, 2009.

[24] H. H. Ku, "Notes on the Use of Propagation of Error Formulas," *Jorunal of Research of the National Bureau of Standards,* vol. 70C, no. 4, pp. 263-273 (Eqn. 2.10), 1966.

[25] K. Sorensen, "What's the Difference Between a "Thermal Spectrum Reactor" and a "Fast Spectrum Reactor"?," 28 April 2006. [Online]. Available: http://energyfromthorium.com/2006/04/28/whats-the-difference-between-a-thermal-spectrum-reactor-and-a-fast-spectrum-reactor/. [Accessed May 2016].

[26] Generation IV International Forum, "Supercritical Water Cooled Reactor (SCWR)," 2013. [Online]. Available: https://www.gen-4.org/gif/jcms/c_42151/supercritical-water-cooled-reactor-scwr. [Accessed May 2016].

[27] Simulia, "Abaqus 6.10 Analysis User's manual," Simulia.

8 Appendices

8.1 Raw Data

Each Table below is matched with its processed data in the thesis, as shown in Table 8 below:

Table 8: Master List of Raw Data Sources

Thesis Source	Table Below
Figure 10: Combined Offset Disc Spring Force To Deflection Curve	Table 9
Figure 16: C-ring Force to Deflection Figure 17: C-ring Force to Stress	Table 10 and Table 11
Figure 19: Washer and Tree Branch Abaqus Validation	Table 12
Figure 21: Nut Abaqus Validation	Table 13
Figure 23: Disc Spring Abaqus Validation	Table 14
Figure 24: Tree Trunk Validation with Infinite Bar (Low Force) Figure 25: Tree Trunk Validation with Infinite Bar (High Force)	Table 15
Figure 26: Tree Trunk Validation with Washer Geometry	Table 16
Figure 27: Disc Spring Wide Side Offset – Force to Deflection	Table 17
Figure 28: Disc Spring Short Side Offset – Force to Deflection	Table 18
Figure 37: I625 Apex Stress during Heating Figure 39: I625 Apex Stress during Heating (Alternate)	Table 19
Figure 40: Monte Carlo (All Parameters Varying) Figure 41: Monte Carlo (All Parameters Except Yield Strength)	Too much data to present. These plots together used 90 000 data points.

Note: All deflections (X) are in millimeters and all forces (Y) are in Newtons.

Table 9: Offset Springs Calculated Parameters

Offsets of 0.5, 1, -1.5, 0		Eqn. 13	
SpringDefl	Force	SpringDefl	Force
0.001706777	0.003596	0	0
0.073544155	72.45139	0.4	680.9163
0.145086356	146.1183	0.8	1271.06
0.213199471	231.86	1.2	1797.788
0.278389154	327.9111	1.6	2288.458
0.341241247	432.2248	2	2770.429
0.404420722	535.471		
0.467925048	637.6491		
0.531751675	738.7625		
0.59589656	838.8169		
0.660356269	937.8239		
0.725125663	1035.797		
0.790198692	1132.756		
0.855568293	1228.721		
0.920983986	1323.373		

Table 10: Raw Numerical Results – C-ring (No Hole)

Deflection	Force	Stress
0	0	0
0.035	124.553	183.114
0.07	247.306	365.521
0.105	368.337	547.223
0.14	487.697	728.237
0.175	605.445	908.578
0.21	721.634	1088.26
0.245	836.317	1267.3
0.28	949.544	1445.7
0.315	1061.36	1623.48
0.35	1171.82	1800.66

Table 11: Raw Numerical Results – C-ring (Hole)

Hole		innermost	6th	11th	16th	outermost
Deflection	Force	S 2256	S 2571	S 4947	S 4632	S4317
0	0	0	0	0	0	0
0.035	116.428	170.842	166.342	163.069	161.521	161.891
0.07	231.214	340.984	332.037	325.556	322.513	323.283
0.105	344.429	510.43	497.085	487.461	482.974	484.173
0.14	456.122	679.196	661.505	648.8	642.917	644.573
0.175	566.343	847.298	825.309	809.584	802.354	804.494
0.21	675.143	1014.75	988.51	969.824	961.296	963.946
0.245	782.569	1181.56	1151.12	1129.53	1119.75	1122.94
0.28	888.666	1347.76	1313.16	1288.72	1277.73	1281.48
0.315	993.479	1513.34	1474.63	1447.4	1435.25	1439.58
0.35	1097.05	1678.33	1635.54	1605.59	1592.31	1597.25

C-ring: Before inverting both deflection and force (both occurred in the negative X direction), multiplying force by 2 (Z symmetry) and multiplying deflection by 2 (X Symmetry)

Table 12: Raw Numerical Results – Washer

X	0	-0.000015	-0.00003	-0.000045	-0.00006	-0.000075	-0.00009	-0.000105	-0.00012	-0.000135	-0.00015
Y	0	-59.543	-119.089	-178.637	-238.187	-297.741	-357.296	-416.855	-476.415	-535.979	-595.545

Washer: Before inverting both deflection and force (both occurred in the negative Z direction), multiplying deflection by 2 (Z symmetry), and multiplying force by 4 (X and Y symmetry).

Table 13: Raw Numerical Results - Nut

X	0	-0.000015	-0.00003	-0.000045	-0.00006	-0.000075	-0.00009	-0.000105	-0.00012	-0.000135	-0.00015
Y	0	-49.6218	-99.2437	-148.866	-198.487	-248.109	-297.731	-347.353	-396.975	-446.597	-496.218

Nut: Before inverting both deflection and force (both occurred in the negative Z direction), multiplying deflection by 2 (Z symmetry), and multiplying force by 4 (X and Y symmetry)

Table 14: Raw Numerical Results – Disc Spring

X	0	-0.01	-0.02	-0.03	-0.04	-0.05	-0.06	-0.07	-0.08	-0.09	-0.1
Y	0	-18.3711	-36.3708	-54.0085	-71.2931	-88.2335	-104.838	-121.116	-137.075	-152.724	-168.071

Disc spring: Before inverting both deflection and force (both occurred in the negative Z direction) and multiplying force by 4 (X and Z symmetry)

Table 15: Raw Numerical Results - Tree Trunk Contact With Infinite Bar

Def - Bar	Def - Rod	Force
0	0	0
-0.0004	-0.000157632	-21.0046
-0.0008	-0.000309901	-43.5943
-0.0012	-0.000462185	-66.1752
-0.0016	-0.000614455	-88.7605
-0.002	-0.000766722	-111.346
-0.0024	-0.000918985	-133.931
-0.0028	-0.00107124	-156.516
-0.0032	-0.0012235	-179.101
-0.0036	-0.00137575	-201.685
-0.004	-0.001528	-224.27
-0.0044	-0.00168024	-246.855
-0.0048	-0.00183248	-269.439
-0.0052	-0.00198471	-292.024
-0.0056	-0.00213694	-314.608
-0.006	-0.00228917	-337.193
-0.0064	-0.00244139	-359.777
-0.0068	-0.00259361	-382.361
-0.0072	-0.00274583	-404.946
-0.0076	-0.00289804	-427.53
-0.008	-0.00305025	-450.114

Table 16: Raw Numerical Results - Tree Trunk Contact With Washer

Def - Wash	Def - Rod	Force
0	0	0
-0.0004	-0.000232833	-19.2782
-0.0008	-0.000487669	-41.1204
-0.0012	-0.000746889	-65.4203
-0.0016	-0.00100841	-91.74
-0.002	-0.00127154	-119.556
-0.0024	-0.00153639	-148.015
-0.0028	-0.00180242	-177.231
-0.0032	-0.00206861	-207.38
-0.0036	-0.00233292	-238.566
-0.004	-0.00259928	-270.756
-0.0044	-0.00286646	-303.373
-0.0048	-0.00313536	-336.536
-0.0052	-0.0034054	-370.366
-0.0056	-0.0036766	-404.965
-0.006	-0.00395092	-440.192
-0.0064	-0.00422648	-475.669
-0.0068	-0.00450497	-511.927
-0.0072	-0.00478478	-548.609
-0.0076	-0.00506525	-585.579
-0.008	-0.00534623	-623.367

Tree trunk: Before inverting both deflection and force (both occurred in the negative X direction) and multiplying force by 4 (Y and Z symmetry)

Table 17: Raw Numerical Results - Disc Spring Offset Wide Side

X	Y 0	X	Y 0.2	X	Y 0.5	X	Y 1	X	Y 2	X	Y 3	X	Y 4	X	Y 5
0	0	0	0	0	0	0	0	0	0	0	0	0	0	0	0
-0.01	-20.0174	-0.01	-7.73751	-0.01	-7.19697	-0.01	-6.85456	-0.01	-6.14056	-0.01	-5.89851	-0.01	-0.80309	-0.01	-0.0342
-0.02	-39.8261	-0.02	-15.4487	-0.02	-14.3729	-0.02	-13.6923	-0.02	-12.7866	-0.02	-11.8055	-0.02	-8.82033	-0.02	-7.16802
-0.035	-69.1391	-0.035	-29.4501	-0.035	-25.9732	-0.035	-24.8148	-0.035	-24.1257	-0.035	-21.8974	-0.035	-20.7646	-0.035	-19.1016
-0.0575	-112.096	-0.0575	-74.1281	-0.0575	-43.9603	-0.0575	-42.3774	-0.0575	-41.0195	-0.0575	-39.4222	-0.0575	-38.5089	-0.0575	-36.8375
-0.09125	-173.665	-0.09125	-140.482	-0.09125	-71.3303	-0.09125	-68.5708	-0.09125	-66.1893	-0.09125	-65.4142	-0.09125	-64.6426	-0.09125	-63.0684
-0.125	-233.097	-0.14125	-235.412	-0.14125	-171.708	-0.14125	-107.539	-0.14125	-104.827	-0.14125	-103.367	-0.14125	-102.301	-0.14125	-101.162
-0.15875	-291.56	-0.19125	-325.972	-0.19125	-270.662	-0.19125	-153.347	-0.19125	-142.902	-0.19125	-140.685	-0.19125	-139.023	-0.19125	-138.432
-0.1925	-348.531	-0.24125	-412.29	-0.24125	-364.088	-0.24125	-257.514	-0.24125	-181.651	-0.24125	-178.75	-0.24125	-176.515	-0.24125	-174.912
-0.22625	-403.799	-0.29125	-494.307	-0.29125	-452.874	-0.29125	-358.305	-0.29125	-220.255	-0.29125	-216.586	-0.29125	-213.54	-0.29125	-210.576
-0.27625	-482.42	-0.34125	-572.512	-0.34125	-537.181	-0.34125	-454.268	-0.34125	-260.052	-0.34125	-254.922	-0.34125	-251.264	-0.34125	-245.815
-0.32625	-558.718	-0.39125	-647.528	-0.39125	-617.488	-0.39125	-545.467	-0.39125	-323.163	-0.39125	-293.478	-0.39125	-288.89	-0.39125	-281.552
-0.37625	-632.271	-0.44125	-719.433	-0.44125	-694.12	-0.44125	-631.736	-0.44125	-423.366	-0.44125	-332.501	-0.44125	-325.616	-0.44125	-318.542
-0.42625	-703.017	-0.49125	-788.237	-0.49125	-766.698	-0.49125	-713.365	-0.49125	-522.162	-0.49125	-372.993	-0.49125	-364.188	-0.49125	-354.562
-0.47625	-770.939	-0.54125	-854.185	-0.54125	-834.932	-0.54125	-791.138	-0.54125	-616.805	-0.54125	-430.962	-0.54125	-402.345	-0.54125	-390.835
-0.52625	-836.279	-0.59125	-917.372	-0.59125	-902.646	-0.59125	-865.169	-0.59125	-706.535	-0.59125	-517.445	-0.59125	-442.733	-0.59125	-427.084
-0.57625	-899.127	-0.64125	-978.027	-0.64125	-967.189	-0.64125	-935.643	-0.64125	-791.561	-0.64125	-605.15	-0.64125	-489	-0.64125	-465.001
-0.62625	-960.457	-0.69125	-1036.65	-0.69125	-1029.29	-0.69125	-1002.62	-0.69125	-872.396	-0.69125	-690.788	-0.69125	-556.769	-0.69125	-504.084
-0.67625	-1020.99	-0.74125	-1093.67	-0.74125	-1089.41	-0.72875	-1051.16	-0.74125	-949.445	-0.74125	-773.352	-0.74125	-633.997	-0.74125	-549.29
-0.72625	-1079.65	-0.79125	-1148.98	-0.79125	-1147.66	-0.76625	-1099.41	-0.79125	-1023.19	-0.79125	-852.935	-0.79125	-712.194	-0.79125	-606.238
-0.77625	-1136.47	-0.84125	-1202.82	-0.84125	-1204.4	-0.80375	-1146.34	-0.84125	-1094.16	-0.84125	-929.588	-0.84125	-788.784	-0.84125	-674.218
-0.82625	-1191.61	-0.89125	-1255.24	-0.89125	-1259.65	-0.84125	-1192.16	-0.89125	-1162.68	-0.89125	-1003.37	-0.89125	-863.634	-0.89125	-745.286
-0.87625	-1245.27	-0.94125	-1306.35	-0.94125	-1313.55	-0.89125	-1251.63	-0.94125	-1229.21	-0.94125	-1074.64	-0.94125	-936.199	-0.94125	-815.818
-0.92625	-1297.7	-0.99125	-1356.32	-0.99125	-1366.31	-0.94125	-1309.65	-0.99125	-1294.05	-0.99125	-1144.11	-0.99125	-1006.45	-0.99125	-884.314
-0.97625	-1349.1	-1	-1364.95	-1	-1375.4	-0.99125	-1366.58	-1	-1305.23	-1	-1156.05	-1	-1018.57	-1	-896.055
-1	-1373.22					-1	-1376.47								

Table 18: Raw Numerical Results - Disc Spring Offset Short Side

X	Y 0	X	Y 0.2	X	Y 0.5	X	Y 1	X	Y 2	X	Y 3	X	Y 4	X	Y 5
0	0	0	0	0	0	0	0	0	0	0	0	0	0	0	0
-0.03	-56.2445	-0.03	-41.9452	-0.03	-38.472	-0.03	-35.4179	-0.0075	-6.55236	-0.03	-29.4111	-0.03	-28.5182	-0.03	-24.6689
-0.06	-110.778	-0.0525	-75.3808	-0.0525	-69.8649	-0.06	-75.3211	-0.015	-13.3868	-0.06	-65.4254	-0.06	-60.3745	-0.06	-50.9959
-0.09	-163.711	-0.075	-109.537	-0.075	-101.95	-0.09	-116.374	-0.02625	-27.4927	-0.09	-101.109	-0.09	-93.5643	-0.09	-78.1039
-0.12	-215.095	-0.105	-157.034	-0.105	-145.081	-0.12	-157.877	-0.04313	-48.9503	-0.12	-136.435	-0.12	-127.707	-0.12	-106.126
-0.15	-264.989	-0.135	-210.156	-0.135	-188.425	-0.15	-199.368	-0.06844	-80.7785	-0.15	-174.245	-0.15	-161.663	-0.15	-134.222
-0.18	-313.451	-0.165	-262.935	-0.165	-231.933	-0.18	-240.872	-0.09844	-118.726	-0.18	-212.824	-0.18	-195.089	-0.18	-162.546
-0.21	-360.538	-0.195	-314.152	-0.195	-275.789	-0.21	-282.228	-0.12844	-158.079	-0.21	-250.898	-0.21	-229.036	-0.21	-191.222
-0.24	-406.303	-0.225	-363.889	-0.225	-320.616	-0.24	-323.379	-0.15844	-197.179	-0.24	-288.286	-0.24	-263.078	-0.24	-219.916
-0.27	-450.797	-0.255	-412.307	-0.255	-368.189	-0.27	-364.563	-0.18844	-236.877	-0.27	-325.077	-0.27	-297.481	-0.27	-249.399
-0.3	-494.074	-0.285	-459.374	-0.285	-420.395	-0.3	-405.66	-0.21844	-275.969	-0.3	-361.361	-0.3	-332.714	-0.3	-278.992
-0.33	-536.185	-0.315	-505.11	-0.315	-471.9	-0.33	-446.923	-0.24844	-315.595	-0.33	-398.529	-0.33	-367.693	-0.33	-308.858
-0.36	-577.193	-0.345	-549.575	-0.345	-521.963	-0.36	-488.794	-0.27844	-354.391	-0.36	-435.005	-0.36	-402.091	-0.36	-339.214
-0.39	-617.142	-0.375	-592.825	-0.375	-570.683	-0.39	-532.136	-0.30844	-393.251	-0.39	-470.759	-0.39	-435.98	-0.39	-370.112
-0.42	-656.074	-0.405	-634.918	-0.405	-618.016	-0.42	-578.616	-0.33844	-431.581	-0.42	-506.705	-0.42	-469.859	-0.42	-401.45
-0.45	-694.031	-0.435	-675.908	-0.435	-664.029	-0.45	-631.588	-0.36844	-469.99	-0.45	-543.773	-0.45	-503.826	-0.45	-434.283
-0.48	-731.06	-0.465	-715.848	-0.465	-708.786	-0.48	-686.999	-0.39844	-508.241	-0.48	-580.238	-0.48	-537.781	-0.48	-467.482
-0.51	-767.213	-0.495	-754.79	-0.495	-752.352	-0.51	-740.961	-0.42844	-546.482	-0.51	-617.043	-0.51	-572.278	-0.51	-502.322
-0.54	-802.543	-0.525	-792.785	-0.525	-794.792	-0.54	-793.385	-0.45844	-584.997	-0.54	-653.947	-0.54	-607.21	-0.54	-538.926
-0.57	-837.068	-0.555	-829.882	-0.555	-836.176	-0.57	-844.36	-0.48844	-623.865	-0.57	-691.537	-0.57	-642.095	-0.57	-577.079
-0.6	-870.856	-0.585	-866.15	-0.585	-876.549	-0.6	-893.964	-0.51844	-663.647	-0.6	-730.996	-0.6	-679.003	-0.6	-618.252
-0.63	-903.932	-0.615	-901.616	-0.615	-915.969	-0.63	-942.298	-0.54844	-705.31	-0.63	-773.021	-0.63	-718.659	-0.63	-662.999
-0.66	-936.355	-0.645	-936.324	-0.645	-954.492	-0.66	-989.451	-0.57844	-750.609	-0.66	-820.942	-0.66	-761.515	-0.66	-712.349
-0.69	-968.192	-0.675	-970.331	-0.675	-992.192	-0.69	-1035.49	-0.60844	-804.571	-0.69	-885.66	-0.69	-812.621	-0.69	-770.245
-0.72	-999.433	-0.705	-1003.7	-0.705	-1029.1	-0.72	-1080.48	-0.63844	-875.03	-0.72	-983.551	-0.72	-883.212	-0.72	-843.188
-0.75	-1030.13	-0.735	-1036.47	-0.735	-1065.31	-0.75	-1124.55	-0.66844	-952.901	-0.75	-1091.18	-0.75	-991.297	-0.75	-940.084
-0.78	-1060.3	-0.765	-1068.85	-0.765	-1100.97	-0.78	-1167.79	-0.69844	-1028.64	-0.78	-1195.84	-0.78	-1104.49	-0.78	-1051.02
-0.81	-1104.7	-0.795	-1101.14	-0.795	-1136.35	-0.81	-1210.71	-0.72844	-1102.12	-0.81	-1297.53	-0.81	-1215.11	-0.81	-1162.51
-0.84	-1149.08	-0.825	-1136.7	-0.825	-1172.62	-0.84	-1254.27	-0.75844	-1173.51	-0.84	-1396.42	-0.84	-1326.72	-0.84	-1278.45
-0.8625	-1176.19	-0.855	-1178.84	-0.855	-1215.58	-0.87	-1303.06	-0.78844	-1243.13	-0.87	-1493.48	-0.87	-1439.09	-0.87	-1392.88
-0.87938	-1201.77	-0.885	-1229.65	-0.885	-1266.76	-0.9	-1362.01	-0.81844	-1311.24	-0.9	-1594.65	-0.9	-1554.81	-0.9	-1527.65
-0.89625	-1227.77	-0.915	-1296.7	-0.915	-1327.1	-0.93	-1437.86	-0.84844	-1378.4	-0.93	-1703.03	-0.93	-1690.18	-0.93	-1696.26
-0.91313	-1279.76	-0.945	-1463.82	-0.945	-1471.04	-0.96	-1643.36	-0.87844	-1446.67	-0.96	-1853.78	-0.96	-1891.21	-0.96	-1934.17
-0.93	-1348.89	-0.975	-1920.54	-0.975	-1913.28	-0.99	-2842.45	-0.90844	-1522.77	-0.99	-2488.34	-0.99	-2472.76	-0.99	-2481.02
-0.95531	-1571.72	-1	-6147.95	-1	-5215.14	-1	-4153.1	-0.93844	-1619.19	-1	-3028.23	-1	-2890.22	-1	-2826.83
-0.98531	-2631.73							-0.96844	-1828.22						
-1	-6519.3							-0.99844	-3196.93						
								-1	-3318.33						

Offset disc springs: After inverting both deflection and force (both occurred in the negative Y direction), multiplying force by 2 (Z symmetry) and dividing deflection by 2 (two disc springs)

Table 19: I625 Apex Stress during Heating

Temp (°C)	Case 1 (MPa)	Case 2 (MPa)	Yield (MPa)	Temp (°C)	Case 1 (MPa)	Case 2 (MPa)	Yield (MPa)
25.00	369.19	327.58	420.83	318.95	345.54	307.67	309.53
32.74	368.60	327.08	420.86	326.68	344.93	307.15	308.30
40.47	368.00	326.58	420.32	334.42	344.31	306.63	307.24
48.21	367.40	326.07	419.26	342.15	343.70	306.12	306.36
55.94	366.79	325.56	417.73	349.89	343.08	305.61	305.65
63.68	366.19	325.05	415.77	357.62	342.47	305.10	305.11
71.41	365.58	324.53	413.42	365.36	341.86	304.59	304.72
79.15	364.96	324.02	410.74	373.09	341.26	304.09	304.48
86.88	364.35	323.50	407.76	380.83	340.65	303.59	304.39
94.62	363.73	322.98	404.52	388.57	340.05	303.09	304.43
102.35	363.11	322.45	401.06	396.30	339.45	302.59	304.61
110.09	362.49	321.93	397.40	404.04	338.86	302.09	304.91
117.83	361.87	321.41	393.60	411.77	338.26	301.60	305.33
125.56	361.25	320.88	389.66	419.51	337.67	301.11	305.85
133.30	360.62	320.35	385.63	427.24	337.08	300.62	306.46
141.03	359.99	319.82	381.53	434.98	336.49	300.14	307.17
148.77	359.37	319.29	377.39	442.71	335.91	299.66	307.95
156.50	358.74	318.76	373.24	450.45	335.33	299.18	308.80
164.24	358.11	318.23	369.08	458.18	334.75	298.70	309.70
171.97	357.48	317.70	364.96	465.92	334.18	298.23	310.66
179.71	356.85	317.17	360.88	473.65	333.61	297.76	311.65
187.44	356.22	316.63	356.86	481.39	333.04	297.30	312.67
195.18	355.58	316.10	352.93	489.13	332.48	296.83	313.71
202.91	354.95	315.57	349.09	496.86	331.92	296.37	314.75
210.65	354.32	315.04	345.36	504.60	331.36	295.92	315.80
218.39	353.69	314.51	341.75	512.33	330.81	295.47	316.83
226.12	353.06	313.97	338.28	520.07	330.26	295.02	317.83
233.86	352.43	313.44	334.95	527.80	329.71	294.57	318.81
241.59	351.80	312.91	331.77	535.54	329.17	294.13	319.74
249.33	351.17	312.38	328.75	543.27	328.63	293.70	320.63
257.06	350.54	311.85	325.90	551.01	328.10	293.26	321.46
264.80	349.91	311.33	323.23	558.74	327.57	292.84	322.21
272.53	349.28	310.80	320.72	566.48	327.04	292.41	322.90
280.27	348.66	310.27	318.40	574.22	326.52	291.99	323.50
288.00	348.03	309.75	316.26	581.95	326.00	291.57	324.01
295.74	347.41	309.23	314.30	589.69	325.49	291.16	324.42
303.48	346.79	308.70	312.53	600.00	324.81	290.62	324.81
311.21	346.16	308.18	310.94	326.68	344.93	307.15	308.30

8.2 Full VBA Code with Comments

```
Option Explicit

Function FLegacy(mat As String, _
    Optional percentYS As Double = 100, Optional th As Double = 1.67, Optional
Dia As Double = 12.7, _
    Optional Wd As Double = 12.7, Optional T As Double = 600, Optional Pop As
Double = 25, _
    Optional initialDeflection As Double = -1000, Optional numSprings As
Integer = 14, Optional Excess As String = "", _
    Optional Modifiers As String = "", Optional SpringOffsets As String = "")
As Variant

On Error GoTo ErrHandler:
' Room temperature is assumed to be 25 oC. Using temperatures below this gives
negative thermal expansion.

' Author:  R Swift
' Id:      3319317
' Date:    2014-07-03
'
' Description: The following program will calculate the necessary deflection
'              to obtain a particular stress in the operating environment by
'              iterating through a constructed list of parameters, the
'              compstring.
'
' Inputs:          mat, the material of the C-ring sample
'         Optional percentYS, the target percentage of the yield strength
'         Optional th, C-ring thickness in mm (t in thesis)
'         Optional Dia, C-ring outer diameter in mm (Douter in thesis)
'         Optional Wd, C-ring wideth in mm (w in thesis)
'         Optional T, operating temperature in degrees Celsius (T in thesis)
'         Optional Pop, operating pressure in MPa (POperating in thesis)
'         Optional initialDeflection, desired initial deflection in mm
(dInitial in thesis)
'         Optional numSprings, number of disc springs (#springs in thesis)
'         Optional Excess, non-default part definitions.
'                   "Empty" removes all before; "Exit" removes all after.
'                   "Empty" is used to scrap all defaults and make something
new.
'                   "Exit" is used to ignore the branch in calculations.
'         Optional Modifiers, material property or output changes. See section
3 below.
'         Optional SpringOffsets, a string representing disc springs offsets in
mm.
'
'   If initialDeflection is given, the code solves the deflection balance (Eqn
10 in thesis)
'   for the missing Force, (x in loop is guessed Force) then calculates the
resulting Stress.
'   If initialDeflection is not given, the code solves the deflection balance
for the missing
'   initialDeflection. (x in loop is guessed initialDeflection)
'
' Outputs: If output = 1 (default) Then Array(Stress, initialDeflection, Force,
Trim(Join(lengths)))
'               Stress, the tensile apex stress in MPa
'               initialDeflection, the required initial deflection in mm
'               Force, the force applied by each part to each adjacent part in
N
```

```
'                lengths, the base length, thermal expansion and elastci
compression of each part
'          If output = 2 (modifiers includes "initDef") Then initialDeflection
'          If output = 3 (modifiers includes "lengths") Then
Trim(Join(lengths))
'          If output = 4 (modifiers includes "force") Then Force
'          If output = 5 (modifiers includes "springDef") Then springDeflection
'                springDeflection, the deflection of all springs in mm
'          If output = 6 (modifiers includes "totalLn") Then totalLn
'                totalLn, the total length of all non-branch parts before
loading
'

' ------------------ '
'  1 - Input Parsing  '
' ------------------ '

Const pi As Double = 3.14159265358979
Const sf As Integer = 5 ' Number of significant figures for outputs
Dim FindingStress As Boolean

FindingStress = initialDeflection > -1000
' If desired deflection is defined (-1000), find stress not deflection

Dim j As Integer ' General-purpose loop index

' --------------------- '
'  2 - Compstring Setup  '
' --------------------- '

Dim Compstring As String
' String representing components and parameters
'    Cring Material Do wd th
'    (Washer|Nut|Ceramic) Material Do Di L
'    Trunk Material1 Material2 D L
'    Branch Material Dou
'
'    DCring, DWasher, DNut, DCeramic, DTrunk, DBranch are replaced with default
values.
'    Empty resets calculations up to that point in compstring. deflection =
totalLn = 0
'    Exit stops calculations at that point in compstring - no further sections
are considered.
'    initDef, numSprings, lengths, force, springDef cause function to give
different outputs.
'
'    Branch (or DBranch) will always be the last definition, as it requires the
total length of all other components.
'    If you need it gone, put Exit as the last item in Excess. Otherwise, omit
it and it'll add itself.
'    The length of disc springs is automatically tacked on to the back of
branch as its final argument.
'
'    Everything should be case-insensitive.

Compstring = "DCring DWasher DNut DTrunk DCeramic " & Excess & " DBranch "
Compstring = Replace(Compstring, "DCring", "Cring " & CStr(mat) & " " &
CStr(Dia) & " " & CStr(Wd) & " " & CStr(th), , , vbTextCompare)
Compstring = Replace(Compstring, "DWasher", "Washer 316 9.54 4.59 2.84", , ,
vbTextCompare)
```

```
Compstring = Replace(Compstring, "DNut", "Nut 316 8.31 2.83 1.36", , ,
vbTextCompare)
Compstring = Replace(Compstring, "DTrunk", "Trunk 316 316 6.4 4.95", , ,
vbTextCompare)
'Compstring = Replace(Compstring, "DCeramic", "Ceramic ZrO 10.26 5.11
2.04",,,vbTextCompare)
Compstring = Replace(Compstring, "DBranch", "Branch 410 3.31", , ,
vbTextCompare)

' -------------------- '
'  3 - Modifiers Check  '
' -------------------- '

' Applies any requested output changes or material property modifiers.

'Material property modifiers for the C-ring
Dim m_C_poi As Double: m_C_poi = 1 ' Not actually used, C-ring does not need
poi
Dim m_C_E As Double: m_C_E = 1
Dim m_C_TEInt As Double: m_C_TEInt = 1
Dim m_C_yieldSt As Double: m_C_yieldSt = 1

'Material property modifiers for other parts
Dim m_O_poi As Double: m_O_poi = 1
Dim m_O_E As Double: m_O_E = 1
Dim m_O_TEInt As Double: m_O_TEInt = 1
Dim m_O_yieldSt As Double: m_O_yieldSt = 1 'Not actually used, Other does not
need yieldSt

Dim output As Integer: output = 1

Dim Mods() As String ' Array of strings representing modifiers and parameters
Mods = Split(Modifiers)

For j = LBound(Mods) To UBound(Mods) ' For all components
    ' Modifications to output style
    If UCase(Mods(j)) = UCase("initDef") Then
        output = 2
    End If
    If UCase(Mods(j)) = UCase("lengths") Then
        output = 3
    End If
    If UCase(Mods(j)) = UCase("force") Then
        output = 4
    End If
    If UCase(Mods(j)) = UCase("springDef") Then
        output = 5
    End If
    If UCase(Mods(j)) = UCase("totalLn") Then
        output = 6
    End If

    ' Material property modifications below
    ' Modification is applied as a factor to the parameter
    ' Example: "CE 1.45" causes all equations for the C-ring to use
    '                    a Modulus of Elasticity (E) 45% higher.
    ' Example: "OTEInt 0.65" causes all equations for other parts (not C-ring)
    '                    to use a thermal expansion coefficient 35% lower.

    ' Scaling for C-ring material properties. Sensitivity analysis only
    If UCase(Mods(j)) = UCase("Cpoi") Then
```

```
        m_C_poi = Mods(j + 1)
    End If
    If UCase(Mods(j)) = UCase("CE") Then
        m_C_E = Mods(j + 1)
    End If
    If UCase(Mods(j)) = UCase("CTEInt") Then
        m_C_TEInt = Mods(j + 1)
    End If
    If UCase(Mods(j)) = UCase("CyieldSt") Then
        m_C_yieldSt = Mods(j + 1)
    End If

    ' Scaling for Other material properties. Sensitivity analysis only
    If UCase(Mods(j)) = UCase("Opoi") Then
        m_O_poi = Mods(j + 1)
    End If
    If UCase(Mods(j)) = UCase("OE") Then
        m_O_E = Mods(j + 1)
    End If
    If UCase(Mods(j)) = UCase("OTEInt") Then
        m_O_TEInt = Mods(j + 1)
    End If
    If UCase(Mods(j)) = UCase("OyieldSt") Then
        m_O_yieldSt = Mods(j + 1)
    End If
Next j

' ------------------------------------------------------ '
'  4 - Moment Calculation Definitions (Force to Stress)  '
' ------------------------------------------------------ '

Dim r2 As Double: r2 = Dia * Exp(TEInt(mat, T, m_C_TEInt)) / 2 ' Outer radius
Dim r1 As Double: r1 = r2 - th * Exp(TEInt(mat, T, m_C_TEInt)) ' Inner radius

' Centroidal Axis, the axis in the center of the cross-sectional area (Called R
in textbook)
Dim CA As Double: CA = (r1 + r2) / 2
' Neutral Axis, the axis in terms of neutral stress (Called rn in textbook)
Dim NA As Double: NA = (r2 - r1) / Log(r2 / r1) 'Log is the natural logarithm
in VBA
' The cross-sectional area
Dim Area As Double: Area = (r2 - r1) * Wd * Exp(TEInt(mat, T, m_C_TEInt))

' Tensile Stress is linear with force by "Stress = Force * StressMult -
OperatingPressure"
' Formulas for Stress and Strain in Structural Matrices by Pilkey
Dim StressMult As Double: StressMult = (1 / Area) * (1 / CA - 1 / r2) / (1 / NA
- 1 / CA)

' ----------------- '
'  5 - Definitions  '
' ----------------- '

' General
Dim deflection As Double: deflection = 0 ' mm (Starting value; will be built
along the way)

Dim lengths() As Variant ' Records, for each component, Name OriginalLength
ThermalExp ElastComp
Dim totalLn As Double: totalLn = 0 ' mm (Starting value; will be built along
the way)
```

```
Dim okay As Boolean: okay = True ' Signals success in combining arrays

Dim springDeflection As Double
Dim Force, Stress As Double

Dim x, y, xl, yl, xi As Double
'Looping parameters
'x and y are for current iteration, xl and yl are from last iteration, xi is an
intermediate

' Parts
Dim al, EE, Dou, Di, R, L, E1, E2, poi1, poi2, V As Double
Dim thermalExpansion, elasticCompression As Double

Dim Comp() As String ' Array of strings representing components and parameters
Comp = Split(Compstring)

' Disc Spring
Dim alSpring As Double: alSpring = TEInt("718", T, m_O_TEInt)

Dim h As Double: h = 1.2192 * Exp(alSpring) ' Unloaded spring height (Height of
individual washer) (mm)
Dim thbell As Double: thbell = 0.7874 * Exp(alSpring) ' Thickness of the spring
material (mm)
Dim Dbellout As Double: Dbellout = 10.312 * Exp(alSpring) ' Outside spring
diameter (total washer) (mm)
Dim Dbellin As Double: Dbellin = 4.9784 * Exp(alSpring) ' Inside spring
diameter (inside hole) (mm)

Dim springTE, springEC As Double ' Thermal Expansion and Elastic Compression of
all springs, respectively
Dim a, b, c, d, q, p, sPart, uPart, s, u As Double ' Cardano variables

Dim SpringIter As Integer
Dim Offsets() As String ' Array of Doubles representing disc spring offsets
Offsets = Split(SpringOffsets)
Dim Offset As Double ' Offset holder while passing through Offsets()

Dim Trans As Double ' Transition deflection for an offset spring
Dim ForceFac As Double ' F2D Coefficient for an offset spring
Dim PreMult As Double ' Pre-transition slope for an offset spring
Dim ForceTrans As Double ' Force at the deflection Trans

Dim hh As Double: hh = h - thbell ' (mm) Unloaded height of truncated cone of
free spring
Dim delta As Double: delta = Dbellout / Dbellin ' Ratio of Diameters
Dim K1 As Double: K1 = (1 / pi) * ((((delta - 1) / delta) ^ 2) / (((delta + 1)
/ (delta - 1)) - (2 / Log(delta)))) 'Log is the natural logarithm in VBA
Dim lamda As Double: lamda = (4 * E("718", T, m_O_E) * (thbell ^ 3)) / ((1 -
(poi("718", T, m_O_poi) ^ 2)) * K1 * (Dbellout ^ 2))

' ------------------------------ '
'  6 - Calculations and The Loop  '
' ------------------------------ '

If FindingStress Then
    'x (force) and y (sum of deflections)
    x = 1: y = -0.22825: xl = 116.71487: yl = -0.22 ' Decent guesses
Else
    'x (initialDeflection) and y (sum of deflections)
    x = 1.2258: y = 0.438499: xl = 0.79193: yl = -5.5511E-17 ' Decent guesses
```

```
    Stress = percentYS / 100 * yieldSt(mat, T, m_C_yieldSt) ' MPa
    Force = (Stress + Pop) / StressMult ' N
End If

Do While Abs(y) > 0.000001 ' Tolerance. Given y is set above, it will always
run at least once.
    ' Guessing function
    xi = x
    x = x - y * (xl - x) / (yl - y) ' Newton method

    xl = xi
    yl = y

    If FindingStress Then
        If (x <= 0) Then
            If xi > 0.01 Then
                x = 0.01
            Else
                x = 0
            End If
        End If

        Force = x
        ' When finding stress, we need to solve for Force
    Else
        initialDeflection = x
        ' When finding initial deflection, we need to solve for
initialDeflection
    End If

    totalLn = 0
    ReDim lengths(0)

' ---------------------------------------- '
'  6.1 - Force to Deflection - Disc Springs  '
' ---------------------------------------- '

springEC = 0

' Cubic solver: ax^3+bx^2+cx+d = 0
' Based on Cardano's Formula -> Reduce to x^3+Q+R = 0
a = lamda / (2 * thbell ^ 2)
b = -3 * lamda * hh / (2 * thbell ^ 2)
c = lamda * hh ^ 2 / thbell ^ 2 + lamda

q = (3 * a * c - b ^ 2) / (9 * a ^ 2)

SpringIter = 0 ' Used as an incrementing counter

Do While SpringIter < numSprings
  If SpringIter <= UBound(Offsets) Then
    Offset = Offsets(SpringIter)

    If Offset > 0 Then
      Trans = -0.00301 * Offset ^ 2 + 0.09345 * Offset
      ForceFac = -0.0256 * Offset ^ 2 + 0.0891 * Offset + 1
      PreMult = 3000
    Else
      Offset = -Offset
```

```
      Trans = -0.004 * Offset ^ 2 + 0.232 * Offset
      ForceFac = -0.064 * Offset ^ 3 + 0.4 * Offset ^ 2 - 0.3 * Offset + 1
      PreMult = -313 * Offset + 5767
    End If

    ForceTrans = PreMult * Trans

    If Force < ForceTrans Then
      springEC = springEC - Force / PreMult
    Else
      d = -(Force - PreMult * Trans) / ForceFac
      p = (9 * a * b * c - 27 * a ^ 2 * d - 2 * b ^ 3) / (54 * a ^ 3)

      s = Application.WorksheetFunction.Power(p + (q ^ 3 + p ^ 2) ^ 0.5, 1 / 3)
      u = Application.WorksheetFunction.Power(p - (q ^ 3 + p ^ 2) ^ 0.5, 1 / 3)

      springEC = springEC - (s + u - b / (3 * a) + Trans)
    End If
  Else ' All remaining offsets are 0
    d = -Force
    p = (9 * a * b * c - 27 * a ^ 2 * d - 2 * b ^ 3) / (54 * a ^ 3)

    s = Application.WorksheetFunction.Power(p + (q ^ 3 + p ^ 2) ^ 0.5, 1 / 3)
    u = Application.WorksheetFunction.Power(p - (q ^ 3 + p ^ 2) ^ 0.5, 1 / 3)

    springEC = springEC - (numSprings - SpringIter) * (s + u - b / (3 * a))

    GoTo springsBreakout
  End If

  SpringIter = SpringIter + 1
Loop
springsBreakout:

springTE = numSprings * h * (Exp(alSpring) - 1) / Exp(alSpring) ' Thermal
expansion
springDeflection = springEC + springTE

okay = ConcatenateArrays(lengths, Array("Springs", Round(1.2192 * numSprings,
sf), Round(springTE, sf), Round(springEC, sf)))

totalLn = totalLn + numSprings * h / Exp(alSpring) 'Add original length for
branch

' ---------------------------------- '
'  6.2 - Force to Deflection - Parts  '
' ---------------------------------- '

deflection = 0

'http://www.ewp.rpi.edu/hartford/~ernesto/F2008/MEF2/Z-
Links/Papers/Intro_Termoelast.pdf
For j = LBound(Comp) To UBound(Comp) ' For all components
    If UCase(Comp(j)) = UCase("Cring") Then
        ' Cring Material Do wd th
        al = TEInt(Comp(j + 1), T, m_C_TEInt)
        EE = E(Comp(j + 1), T, m_C_E)

        Dou = Comp(j + 2) * Exp(al) 'Accounting for thermal expansion
        Wd = Comp(j + 3) * Exp(al) 'Accounting for thermal expansion
        th = Comp(j + 4) * Exp(al) 'Accounting for thermal expansion
```

```
        R = 0.5 * Dou - 0.5 * th

        thermalExpansion = Dou * (Exp(al) - 1) / Exp(al)
        elasticCompression = -6 * pi * Force * R ^ 3 / (EE * Wd * th ^ 3)

        deflection = deflection + thermalExpansion + elasticCompression

        okay = ConcatenateArrays(lengths, Array(Comp(j), Round(Dou / Exp(al),
sf), Round(thermalExpansion, sf), Round(elasticCompression, sf)))

        totalLn = totalLn + Dou / Exp(al) 'Add original length for Branch
    End If
    If UCase(Comp(j)) = UCase("Washer") Then
        ' Disc Material Do Di L
        al = TEInt(Comp(j + 1), T, m_O_TEInt)
        EE = E(Comp(j + 1), T, m_O_E)

        th = Comp(j + 4) * Exp(al) 'Accounting for thermal expansion
        Dou = Comp(j + 2) * Exp(al) 'Accounting for thermal expansion
        Di = Comp(j + 3) * Exp(al) 'Accounting for thermal expansion

        thermalExpansion = th * (Exp(al) - 1) / Exp(al)
        elasticCompression = -4 * Force * th / (pi * EE * (Dou ^ 2 - Di ^ 2))

        deflection = deflection + thermalExpansion + elasticCompression

        okay = ConcatenateArrays(lengths, Array(Comp(j), Round(th / Exp(al),
sf), Round(thermalExpansion, sf), Round(elasticCompression, sf)))

        totalLn = totalLn + th / Exp(al) 'Add original length for Branch
    End If
    If (UCase(Comp(j)) = UCase("Nut") Or UCase(Comp(j)) = UCase("Ceramic"))
Then
        ' Disc Material Do Di L
        al = TEInt(Comp(j + 1), T, m_O_TEInt)
        EE = E(Comp(j + 1), T, m_O_E)

        Dou = Comp(j + 2) * Exp(al) 'Accounting for thermal expansion
        Di = Comp(j + 3) * Exp(al) 'Accounting for thermal expansion
        th = Comp(j + 4) * Exp(al) 'Accounting for thermal expansion

        thermalExpansion = th * (Exp(al) - 1) / Exp(al)
        elasticCompression = -4 * Force * th / (pi * EE * (Dou ^ 2 - Di ^ 2))
        deflection = deflection + thermalExpansion + elasticCompression

        okay = ConcatenateArrays(lengths, Array(Comp(j), Round(th / Exp(al),
sf), Round(thermalExpansion, sf), Round(elasticCompression, sf)))

        totalLn = totalLn + th / Exp(al) 'Add original length for Branch
    End If
    If UCase(Comp(j)) = UCase("Trunk") Then
        ' Trunk Material1 Material2 D L
        al = TEInt(Comp(j + 1), T, m_O_TEInt)
        E1 = E(Comp(j + 1), T, m_O_E)
        E2 = E(Comp(j + 2), T, m_O_E)
        poi1 = poi(Comp(j + 1), T, m_O_poi)
        poi2 = poi(Comp(j + 2), T, m_O_poi)

        Dou = Comp(j + 3) * Exp(al) 'Accounting for thermal expansion
        L = Comp(j + 4) * Exp(al) 'Accounting for thermal expansion
```

```
        V = (1 - poi1 ^ 2) / (pi * E1) + (1 - poi2 ^ 2) / (pi * E2)

        thermalExpansion = Dou * (Exp(al) - 1) / Exp(al)
        If Force > 0 Then
            elasticCompression = -0.35 * (Force / L) * V * (1 + Log((2 * L ^ 3)
/ (0.35 * V * Force * Dou))) 'Log is the natural logarithm in VBA
            '0.35 multiplier overall and 0.35 multiplier on denominator from
validation for washer contact
        Else
            elasticCompression = 0
        End If
        '
http://emtoolbox.nist.gov/publications/nationalstandardslaboratorytechnicalpape
rno25.pdf for elastic compression
        deflection = deflection + thermalExpansion + elasticCompression

        okay = ConcatenateArrays(lengths, Array(Comp(j), Round(Dou / Exp(al),
sf), Round(thermalExpansion, sf), Round(elasticCompression, sf)))

        totalLn = totalLn + Dou / Exp(al) 'Add original length for Branch
    End If
    If UCase(Comp(j)) = UCase("Branch") Then
        ' Branch Material Dou
        ' Branch must be done last, since its length requires totalLn.
        al = TEInt(Comp(j + 1), T, m_O_TEInt)
        EE = E(Comp(j + 1), T, m_O_E)

        Dou = Comp(j + 2) * Exp(al) 'Accounting for thermal expansion
        L = (totalLn - initialDeflection) * Exp(al)
        'SpringLength is set right after CompString
        '-ID because that length of branch does not contribute to the nut
        'Effect is actually -ID - [ 4 * initialForce * L / (pi * EE * Dou ^ 2)
]
        ' as application of force changes branch frame of reference

        thermalExpansion = -L * (Exp(al) - 1) / Exp(al)
        ' Sign negative because expansion adds space
        elasticCompression = -4 * Force * L / (pi * EE * Dou ^ 2)
        ' Sign negative because branch is under tension, which adds space.
        deflection = deflection + thermalExpansion + elasticCompression

        okay = ConcatenateArrays(lengths, Array(Comp(j), Round(L / Exp(al),
sf), Round(thermalExpansion, sf), Round(elasticCompression, sf)))
    End If
    If UCase(Comp(j)) = UCase("Empty") Then
        deflection = 0
        totalLn = 0
        ReDim lengths(0)
    End If
    If UCase(Comp(j)) = UCase("Exit") Then
        GoTo partsBreakout
    End If
Next j

'After the above loop, "deflection" is now complete

partsBreakout:

' ---------------------------------- '
'  6.3 - End of Force to Deflection  '
```

```
' --------------------------------- '

    y = initialDeflection + deflection + springDeflection

    If Force = 0 Then ' This is only the case if the parts aren't actually
compressed
        GoTo OutputTime
    End If
Loop

OutputTime:

If FindingStress Then
    Stress = Force * StressMult - Pop
End If

If output = 1 Then
    FLegacy = Array(Stress, initialDeflection, Force, Trim(Join(lengths)))
ElseIf output = 2 Then
    FLegacy = initialDeflection
ElseIf output = 3 Then
    FLegacy = Trim(Join(lengths))
ElseIf output = 4 Then
    FLegacy = Force
ElseIf output = 5 Then
    FLegacy = springDeflection
ElseIf output = 6 Then
    FLegacy = totalLn
End If

'Note that output strings longer than 255 will cause #VALUE errors in Excel,
but not bother vba.

Exit Function

' ----------------------------- '
'  A1 - Stuff to Fix and Notes  '
' ----------------------------- '

' 1) Implement properties for ZrO2, the ceramics.
' 2) Single space added to front of lengths if initialDeflection is defined
' 3) To reduce load at high looping, compstring could be run once to build
'    a metastring which compacts all parameters. Example: Cring Material Do wd
th
'    becomes Cring TE EC_coefficient for cost-effective looping without
'    re-calculating the TE, EC and calling the material properties again.
' 4) To reduce load at low looping, the two pre-set guesses can be actually
'    run instead of guessed. This would remove the first two awful loops.

ErrHandler:
If Err.Number <> 0 Then
FLegacy = "Error " & Err.Number & ": " & Err.Description
End If

End Function

' -------------------------- '
'  A2 - MATERIAL PROPERTIES  '
' -------------------------- '
'
' T is in degrees Celsius. T+273.15 is used if the equation requires Kelvin.
```

```
'

Function Polyval(ByVal Coefficients As Variant, ByVal Index As Variant)
    ' Gives the evaluation of a polynomial of the form below at x value Index:
    ' a*x^2 + b*x^1 + c*x^0 for the array coefficients = (a, b, c), but any
size.

    Dim i As Integer: i = UBound(Coefficients)
    Do While i >= 0
        Polyval = Polyval + Coefficients(UBound(Coefficients) - i) * Index ^
(i)
        i = i - 1
    Loop
End Function

Public Function poi(ByVal mat As String, ByVal T As Double, Optional ByVal Mult
As Double = 1)
' Returns Poisson's ratio. (unitless)

If UCase(mat) = UCase("718") Then 'Found in BLegacy (Inconel 718)
    poi = Polyval(Array(0, 0, 1.97081956402585E-10, -3.49734337819423E-08, -
7.81486842518733E-05, 0.294624818653242), T) ' (unitless)
ElseIf UCase(mat) = UCase("316") Then 'UNS S31600
    poi = Polyval(Array(0, 0, 0, -6.51538213861499E-07, 6.16588593855505E-04,
0.180608355680713), T) ' (unitless)
ElseIf UCase(mat) = UCase("625") Then 'UNS N06625
    poi = Polyval(Array(0, 0, -1.45658036148705E-10, 2.49632382174811E-07, -
3.87018316948589E-05, 0.28078146190786), T) ' (unitless)
ElseIf UCase(mat) = UCase("magic") Then
    poi = 0
ElseIf UCase(mat) = UCase("magicB") Then
    poi = 0
Else
    poi = "Error: Incorrect material. The only working materials are 718 and
316."
    MsgBox "poi broke @ mat = " & mat
End If

poi = poi * Mult
' Mult = 1 by default. Can be changed for sensitivity analysis
End Function

Public Function E(ByVal mat As String, ByVal T As Double, Optional ByVal Mult
As Double = 1)
' Returns the Young's Modulus (Elastic modulus of tension), with units of MPa.

If UCase(mat) = UCase("316") Then 'UNS S31600
    E = Polyval(Array(0, 0, -1.89897030481575E-05, 9.95532071191233E-03, -
83.7213703860691, 201841.651595075), T) ' (MPa)
ElseIf UCase(mat) = UCase("625") Then 'UNS N06625
    E = Polyval(Array(0, 0, -5.88729338962222E-05, 0.041191041422617, -
61.6822786464262, 209103.985273616), T) ' (MPa)
ElseIf UCase(mat) = UCase("310") Then 'UNS S31008
    E = Polyval(Array(0, 0, -1.61926606838124E-05, -3.84791081708521E-02, -
36.5738459059422, 194381.153675081), T) ' (MPa)
ElseIf UCase(mat) = UCase("347") Then 'UNS S34700
    E = Polyval(Array(0, 0, -2.89899061392674E-04, 0.420603158969883, -
232.179262621369, 199722.240084696), T) ' (MPa)
ElseIf UCase(mat) = UCase("800") Then 'UNS N08811
    E = Polyval(Array(0, 0, 2.49575111721045E-05, -4.00417324671658E-02, -
49.8416525080946, 198158.833495469), T) ' (MPa)
```

```
ElseIf UCase(mat) = UCase("214") Then 'UNS N07214
    E = Polyval(Array(0, 0, -1.89701312412866E-04, 0.15997189728984, -
105.546779976668, 220093.345482517), T) ' (MPa)
ElseIf UCase(mat) = UCase("HastC") Then 'UNS N10002
    E = Polyval(Array(0, 0, 5.29721219294895E-05, -4.28196638793587E-02, -
47.9607231052128, 205992.46616535), T) ' (MPa)
ElseIf UCase(mat) = UCase("276") Then 'UNS N10276
    E = Polyval(Array(0, 0, -1.89501323221787E-05, -1.94391865550155E-03, -
45.2715881553291, 206721.388427404), T) ' (MPa)
ElseIf UCase(mat) = UCase("718") Then 'Found in BLegacy (Inconel 718)
    E = Polyval(Array(0, 0, 0, -1.81962003403374E-02, -45.7269823314408,
200413.485692858), T) ' (MPa)
ElseIf UCase(mat) = UCase("410") Then 'UNS S41000
    E = Polyval(Array(0, 0, -1.19097994015584E-05, 8.07848376779429E-03, -
83.6412046931095, 207846.83363265), T) ' (MPa)
ElseIf UCase(mat) = UCase("magic") Then
    E = 1000
ElseIf UCase(mat) = UCase("magicB") Then
    E = 0.01
Else
    E = "Error: Incorrect material. The only working materials are 316, 625,
310, 347, 800, 214, HastC, 276, and 718."
    MsgBox "E broke @ mat = " & mat
    Exit Function
End If

E = E * Mult
' Mult = 1 by default. Can be changed for sensitivity analysis
End Function

Public Function TEInt(ByVal mat As String, ByVal T As Double, Optional ByVal
Mult As Double = 1)
' Returns the linear coefficient of thermal expansion, integrated from room
temperature to the given temperature. (unitless)

Dim RoomT: RoomT = 25
' Some of these were calculated with respect to a non-zero starting
temperature.
' Those have been adjusted to account for that temperature by subtracting the
original from the given.

If UCase(mat) = UCase("316") Then 'UNS S31600
    TEInt = Polyval(Array(0, 0, 0, 5.72226143393056E-09, 1.44653356205755E-05,
0), T) _
        - Polyval(Array(0, 0, 0, 5.72226143393056E-09, 1.44653356205755E-05,
0), RoomT) ' (Unitless)
ElseIf UCase(mat) = UCase("625") Then 'UNS N06625
    TEInt = Polyval(Array(0, 0, -2.30491255144034E-12, 8.00768518518519E-09,
9.96417258230453E-06, 0), T - 21) _
        - Polyval(Array(0, 0, -2.30491255144034E-12, 8.00768518518519E-09,
9.96417258230453E-06, 0), RoomT - 21) ' (Unitless)
ElseIf UCase(mat) = UCase("310") Then 'UNS S31008
    TEInt = Polyval(Array(3.14292243395954E-11, -2.04868194860622E-08,
1.90457530099737E-05, 0), T) _
        - Polyval(Array(3.14292243395954E-11, -2.04868194860622E-08,
1.90457530099737E-05, 0), RoomT) ' (Unitless)
ElseIf UCase(mat) = UCase("347") Then 'UNS S34700
    TEInt = Polyval(Array(0, 0, 0, 2.39398094087245E-09, 1.7132230111509E-05,
0), T) _
        - Polyval(Array(0, 0, 0, 2.39398094087245E-09, 1.7132230111509E-05, 0),
RoomT)  ' (Unitless)
```

```
ElseIf UCase(mat) = UCase("800") Then 'UNS N08811
    TEInt = Polyval(Array(0, 0, 1.4484720513894E-12, 2.16961274257399E-09,
1.54018306001163E-05, 0), T - 21) _
        - Polyval(Array(0, 0, 1.4484720513894E-12, 2.16961274257399E-09,
1.54018306001163E-05, 0), RoomT - 21) ' (Unitless)
ElseIf UCase(mat) = UCase("214") Then 'UNS N07214
    TEInt = Polyval(Array(0, 0, 5.41221952364153E-12, 2.5541714504038E-10,
1.32041379710923E-05, 0), T - 25) _
        - Polyval(Array(0, 0, 5.41221952364153E-12, 2.5541714504038E-10,
1.32041379710923E-05, 0), RoomT - 25) ' (Unitless)
ElseIf UCase(mat) = UCase("HastC") Then 'UNS N10002
    TEInt = Polyval(Array(0, 0, -1.04343277724292E-11, 1.12527706701269E-08,
1.03710762781793E-05, 0), T - 24) _
        - Polyval(Array(0, 0, -1.04343277724292E-11, 1.12527706701269E-08,
1.03710762781793E-05, 0), RoomT - 24) ' (Unitless)
ElseIf UCase(mat) = UCase("276") Then 'UNS N10276
    TEInt = Polyval(Array(-1.04343277724292E-11, 1.12527706701269E-08,
1.03710762781793E-05, 0), T) _
        - Polyval(Array(-1.04343277724292E-11, 1.12527706701269E-08,
1.03710762781793E-05, 0), RoomT) ' (Unitless)
ElseIf UCase(mat) = UCase("718") Then 'UNS N07718 (Inconel 718)
    TEInt = Polyval(Array(0, 0, 7.41455028357607E-12, -2.63578205147425E-09,
1.39018518713836E-05, 0), T - 25) _
        - Polyval(Array(0, 0, 7.41455028357607E-12, -2.63578205147425E-09,
1.39018518713836E-05, 0), RoomT - 25) ' (Unitless)
ElseIf UCase(mat) = UCase("410") Then 'UNS S41000
    TEInt = Polyval(Array(0, 0, 0, 2.33189024441575E-09, 1.02077839443027E-05,
0), T) _
        - Polyval(Array(0, 0, 0, 2.33189024441575E-09, 1.02077839443027E-05,
0), RoomT) ' (Unitless)
ElseIf UCase(mat) = UCase("magic") Then
    TEInt = 0.000001 * (T - RoomT)
ElseIf UCase(mat) = UCase("magicB") Then
    TEInt = 0
Else
    TEInt = "Error: Incorrect material. The only working materials are 316,
625, 310, 347, 800, 214, HastC, 276, and 718."
    MsgBox "TEInt broke @ mat = " & mat
    Exit Function
End If

TEInt = TEInt * Mult
' Mult = 1 by default. Can be changed for sensitivity analysis.
' I considered using + Log(Mult) instead, but found that I wanted
'   exp(TEInt)-1 to be multiplied by Mult, not exp(TEInt).
End Function

Public Function yieldSt(ByVal mat As String, ByVal T As Double, Optional ByVal
Mult As Double = 1)
' Returns the yield strength or 2% offset yield strength, in units of N/mm^2 or
MPa.

If UCase(mat) = UCase("316") Then 'UNS S31600
    yieldSt = Polyval(Array(0, 0, 8.58745610825783E-08, -5.27640046050734E-05,
-0.223815848735083, 287.905897830171), T) ' (N/mm^2)
ElseIf UCase(mat) = UCase("625") Then 'UNS N06625
    yieldSt = Polyval(Array(1.14877148090439E-11, -2.72001490580215E-08,
2.21106664853876E-05, -6.78063275725426E-03, 0.342711555159302,
416.163752794117), T) ' (N/mm^2)
ElseIf UCase(mat) = UCase("310") Then 'UNS S31008
```

```
    yieldSt = Polyval(Array(0, 0, 0, 0.00024, -0.37, 321.589847011948), T) '
(N/mm^2)
ElseIf UCase(mat) = UCase("347") Then 'UNS S34700
    yieldSt = Polyval(Array(-2.5231682196618E-07, 5.97101387231545E-04, -
0.424438384798524, 223.377241495202), T) ' (N/mm^2)
ElseIf UCase(mat) = UCase("800") Then 'UNS N08811
    yieldSt = Polyval(Array(0, 0, -1.79578632947168E-07, 5.13147778115104E-04,
-0.412717050351184, 176.998432080756), T) ' (N/mm^2)
ElseIf UCase(mat) = UCase("214") Then 'UNS N07214
    yieldSt = Polyval(Array(0, 0, 0, 1.13795535345037E-04, -0.165869908610768,
607.932127185973), T) ' (N/mm^2)
ElseIf UCase(mat) = UCase("HastC") Then 'UNS N10002
    yieldSt = Polyval(Array(0, 0, 0, 2.53360332557831E-04, -0.438974333838084,
365.187126911462), T) ' (N/mm^2)
ElseIf UCase(mat) = UCase("276") Then 'UNS N10276
    yieldSt = Polyval(Array(0, 0, 0, 2.79487796758438E-04, -0.455864867251205,
367.699135754255), T) ' (N/mm^2)
ElseIf UCase(mat) = UCase("410") Then 'UNS S41000
    yieldSt = Polyval(Array(0, 0, -3.80667752929198E-07, 3.94852732496838E-05,
-0.224648845570676, 696.817303253182), T) ' (N/mm^2)
ElseIf UCase(mat) = UCase("718") Then 'UNS N07718
    yieldSt = Polyval(Array(0, 0, 0, 0, -0.301706714574444, 1178.85788606932),
T) ' (N/mm^2)
ElseIf UCase(mat) = UCase("magic") Then
    yieldSt = 300
ElseIf UCase(mat) = UCase("magicB") Then
    yieldSt = 300
Else
    yieldSt = "Error: Incorrect material. The only working materials are 316,
625, 310, 347, 800, 214, HastC, and 276."
    MsgBox "yieldSt broke @ mat = " & mat
    Exit Function
End If

yieldSt = yieldSt * Mult
' Mult = 1 by default. Can be changed for sensitivity analysis
End Function

Public Function SplitEx(section As String)
' Implemented to make VBA's Split function accessible in Excel
    SplitEx = Split(section)
End Function

Function JoinAll(ByRef rng As Range, ByVal delim As String)
Dim i As Long
JoinAll = rng(1)
For i = 2 To rng.Count
    JoinAll = JoinAll & delim & rng(i)
Next
End Function
```

8.3 Sample Calculations

Parameters

These sample calculations are performed for the following hypothetical setup:

4 disc springs (Inconel 718, 1.2192 mm height, 0.7874 mm thickness, 10.312 mm outer diameter, 4.9784 mm inner diameter, offsets of [1mm, 0.5mm, -0.5 mm, 0 mm])

1 C-ring (316 stainless steel, 12.7 mm outer diameter, 12.7 mm width, 1.67 mm thickness)

4 backing washers (0.71 mm thickness, 9.54 mm outer diameter, 4.59 mm inner diameter)

1 tightening nut (316 stainless steel, 1.36 mm thickness, 8.31 mm outer diameter, 2.83 mm inner diameter)

1 tree trunk (316 stainless steel, 6.4 mm outer diameter, 4.95 mm contact length, in contact with a 316 stainless steel washer)

1 tree branch (410 stainless steel, length as the sum of all other initial lengths less initial deflection, 3.31 mm outer diameter)

Operating temperature: 600 ^{o}C

Operating pressure: 25 MPa

These sample calculations assume access to material property data for any required materials in the form of temperature-dependent functions for Poisson ratio (μ), Young's modulus (E), integrated thermal expansion coefficient (TEInt), and 0.2% offset yield strength.

Part dimensions are included in a table at the beginning of each part section, before and after thermal expansion to 600 ^{o}C. Thermal expansion was applied with the following equation:

$$L_{part,AfterTE} = L_{part,beforeTE} * e^{\mathrm{TEInt}}$$

Deflection Balance and Newton Method

For both determining stress and determining initial deflection, the following is true:

$$y = d_{Initial} + d_{NotSprings} + d_{Springs} = 0$$

This equation is a function of many static parameters as well as the force and the initial deflection, one of which is determined by applying this equation. To determine one parameter while the other is known, the unknown parameter (called x) is guessed iteratively until the function is satisfied. (y=0) To reduce the required number of guesses, the newton method of root finding is applied to the two most recent guesses to determine the next guess.

Assuming that the root (y=0) and both past guesses ($<x_{i-2}, y_{i-2}>$ and $<x_{i-1}, y_{i-1}>$) lie on a straight line gives the following equation:

$$\frac{y_{i-1} - y_{i-2}}{x_{i-1} - x_{i-2}} = slope = \frac{y_{i-1} - 0}{x_{i-1} - x}$$

$$x = \frac{x_{i-1} - x_{i-2}}{y_{i-1} - y_{i-2}} y_{i-1} + x_{i-1}$$

In practice, the function y is not a straight line and this method must be applied iteratively to get closer to the root value with each step, up to a defined closeness tolerance.

The method requires two points to start with, so <1.2258 mm, 0.43850 mm> and <0.79193 mm, -5.5511*10^{-17} mm> are used as the calculation below will solve for the unknown initial deflection. Note that these two y values are pre-set and not calculated from their respective x values using the code.

$$x_i = \frac{x_{i-1} - x_{i-2}}{y_{i-1} - y_{i-2}} y_{i-1} + x_{i-1}$$

$$x_1 = \frac{1.2258 \text{ mm} - 0.79193 \text{ mm}}{0.43850 \text{ mm} - (-5.5511 * 10^{-17}\, mm)} 0.43850 \text{ mm} + 1.2258 \text{ mm}$$

$$x_1 = 0.79193\, mm$$

$$y_1 = code(x_1) = code(0.79193\, mm) = 0.59196\, mm$$

These two equations are repeated until y is within a defined tolerance of 0. The remaining iterations are shown below in Table 20:

Table 20: Newton Method Root Finding

i	Unknown Parameter (x value) (mm)	Deflection Balance (y value) (mm)
-1	0.79193	-5.5511*10^{-17}
0	1.2258	0.43850
1	0.79193	0.59196
2	2.4656	2.2771
3	0.20403	-1.7347*10^{-16}

y_3 is within the tolerance of $1*10^{-6}$ of zero, so the method has converged on a solution to the deflection balance. The solution initial deflection is x_3, 0.20403 mm.

The usage of an iterative method to determine the unknown parameter means that the rest of the code needs only determine (multiple times) the value y given both initial deflection and force instead of determining the unknown between the two.

Deflection Balance Terms

Using F = 250 N and $d_{Initial}$ = 1.25 mm find the following:

$$y = d_{Initial} + d_{NotSprings} + d_{Springs}$$

Spring Deflection ($d_{Springs}$)

$d_{Springs}$ = sum of thermal expansion and four elastic compressions

Quantity: 4, Material: Inconel 718 (TEInt = 0.008532, E = 166430 MPa, poi = 0.27777)

Table 21: Disc Spring Dimensions

Parameter	Before Thermal Expansion	After Thermal Expansion
h (mm)	1.2192	1.2296
t (mm)	0.7874	0.79415
D_{Outer} (mm)	10.312	10.400
D_{Inner} (mm)	4.9784	5.0211

$$d_{TE,Springs} = \#_{Springs} * \left(D_{Outer,afterTE} - D_{Outer,beforeTE}\right)$$

$$d_{TE,Springs} = 4 * (1.2296\ mm - 1.2192\ mm)$$

$$d_{TE,Springs} = 0.041785\ mm$$

$$\Delta = \frac{Do}{Di} = \frac{10.400\ mm}{5.0211\ mm} = 2.0713$$

$$K = \frac{1}{\pi} * \frac{\left[\frac{\Delta - 1}{\Delta}\right]^2}{\left[\frac{\Delta + 1}{\Delta - 1} - \frac{2}{\ln(\Delta)}\right]} = \frac{1}{\pi} * \frac{\left[\frac{2.0713 - 1}{2.0713}\right]^2}{\left[\frac{2.0713 + 1}{2.0713 - 1} - \frac{2}{\ln(2.0713)}\right]} = 0.70780$$

$$\lambda = \frac{4\ *\ E\ *\ t^3}{(1\ -\ \mu^2) *\ K\ *\ D_{Outer}^2}$$

$$\lambda = \frac{4\ *\ 166430\ MPa\ *\ (0.79415\ mm)^3}{(1\ -\ 0.27777^2) *\ 0.70780\ *\ (10.400\ mm)^2}$$

$$\lambda = 4718.8 \frac{N}{mm}$$

With these initial parameters, the force to deflection equation for the disc springs is as follows, which is equivalent to a cubic equation for deflection:

$$F = \lambda * d_{EC,Springs} * \left[\left(\frac{h - t}{t} - \frac{d_{EC,Springs}}{t}\right) * \left(\frac{h - t}{t} - \frac{d_{EC,Springs}}{2t}\right) + 1\right]$$

The above cubic equation for deflection is solved with the following steps using the Cardano method:

$$a_3 = \frac{\lambda}{2\ t^2} = \frac{4718.8 \frac{N}{mm}}{2 * (0.79415\ mm)^2} = 3741.1 \frac{N}{mm^3}$$

$$a_2 = -\frac{3\,\lambda\,(h-t)}{2\,t^2} = -\frac{3 * 4718.8\frac{N}{mm} * (1.2296\,mm - 0.79415\,mm)}{2 * (0.79415\,mm)^2}$$

$$a_2 = -4887.8\frac{N}{mm^2}$$

$$a_1 = \frac{\lambda\,(h-t)^2}{t^2} + \lambda = \frac{4718.8\frac{N}{mm} * (1.2296\,mm - 0.79415\,mm)^2}{(0.79415\,mm)^2} + 4718.8\frac{N}{mm}$$

$$a_1 = 6137.9\frac{N}{mm}$$

$$q = \frac{3 * a_3 * a_1 - {a_2}^2}{9 * a_3^2} = \frac{3 * 3741.1\frac{N}{mm^3} * 6137.9\frac{N}{mm} - \left(-4887.8\frac{N}{mm^2}\right)^2}{9 * \left(3741.1\frac{N}{mm^3}\right)^2}$$

$$q = 0.35700\,mm^2$$

Elastic compression 1: *Offset* = Q = 1 mm

Q > 0, so the following equations are used for a_{Linear}, $d_{Transition}$ and a_{Curved}:

$$d_{Transition} = -0.00301\ \text{mm}^{-1} * \text{Q}^2 + 0.09345 * \text{Q}$$

$$d_{Transition} = -0.00301\ \text{mm}^{-1} * (1\ \text{mm})^2 + 0.09345 * 1\ \text{mm}$$

$$d_{Transition} = 0.09044\ \text{mm}$$

$$a_{Curved} = -0.0256\ \text{mm}^{-2} * \text{Q}^2 + 0.0891\ \text{mm}^{-1} * \text{Q} + 1$$

$$a_{Curved} = -0.0256\ \text{mm}^{-2} * (1\ \text{mm})^2 + 0.0891\ \text{mm}^{-1} * 1\ \text{mm} + 1$$

$$a_{Curved} = 1.0635$$

$$a_{Linear} = 3000 \frac{N}{mm}$$

$$a_{Linear} * d_{Transition} = 3000 \frac{N}{mm} * 0.09044 \text{ mm} = 271.32\ N$$

F < a_{Linear} * $d_{Transition}$, so the curve is within the linear region.

$$d_{EC,Springs,1} = -\frac{F}{a_{Linear}} = -\frac{250\ N}{3000 \frac{N}{mm}} = -0.083333\ mm$$

Elastic compression 2: *Offset* = Q = 0.5 mm

Q > 0, so the following equations are used for a_{Linear}, $d_{Transition}$ and a_{Curved}:

$$d_{Transition} = -0.00301 \text{ mm}^{-1} * \text{Q}^2 + 0.09345 * \text{Q}$$

$$d_{Transition} = -0.00301 \text{ mm}^{-1} * (0.5 \text{ mm})^2 + 0.09345 * 0.5 \text{ mm}$$

$$d_{Transition} = 0.045973 \text{ mm}$$

$$a_{Curved} = -0.0256 \text{ mm}^{-2} * \text{Q}^2 + 0.0891 \text{ mm}^{-1} * \text{Q} + 1$$

$$a_{Curved} = -0.0256 \text{ mm}^{-2} * (0.5 \text{ mm})^2 + 0.0891 \text{ mm}^{-1} * 0.5 \text{ mm} + 1$$

$$a_{Curved} = 1.0382$$

$$a_{Linear} = 3000 \frac{N}{mm}$$

$$a_{Linear} * d_{Transition} = 3000\frac{N}{mm} * 0.045973 \text{ mm } = 137.92\ N$$

F < a_{Linear} * $d_{Transition}$, so the curve is not within the linear region.

$$a_0 = -\frac{F - a_{Linear} * d_{Transition}}{a_{Curved}} = -\frac{250N - 3000\frac{N}{mm} * 0.045973 \text{ mm}}{1.0382}$$

$$a_0 = -107.96\ N$$

$$p = \frac{9 * a_3 * a_2 * a_1 - 27 * a_3^2 * a_0 - 2 * {a_2}^3}{54 * a_3^3}$$

$$p = \frac{9 * 3741.1\frac{N}{mm^3} * \left(-4887.8\frac{N}{mm^2}\right) * 6137.9\frac{N}{mm}}{54 * \left(3741.1\frac{N}{mm^3}\right)^3}$$

$$- \frac{27 * \left(3741.1\frac{N}{mm^3}\right)^2 * (-107.96\ N) - 2 * \left(-4887.8\frac{N}{mm^2}\right)^3}{54 * \left(3741.1\frac{N}{mm^3}\right)^3}$$

$$p = -0.26023\ mm^3$$

$$s = \sqrt[3]{p + \sqrt{q^3 + p^2}}$$

$$s = \sqrt[3]{-0.26023\ mm^3 + \sqrt{(0.35700\ mm^2)^3 + (-0.26023\ mm^3)^2}}$$

$$s = 0.42429\ mm$$

$$u = \sqrt[3]{p - \sqrt{q^3 + p^2}}$$

$$u = \sqrt[3]{-0.26023\ mm^3 - \sqrt{(0.35700\ mm^2)^3 + (-0.26023\ mm^3)^2}}$$

$$u = -0.84195\ mm$$

$$d_{EC,Springs,2} = -\left(s + u - \frac{a_2}{3 * a_3} + d_{Transition}\right)$$

$$d_{EC,Springs,2} = -\left(0.42429\ mm - 0.84195\ mm - \frac{-4887.8\frac{N}{mm^2}}{3 * 3741.1\frac{N}{mm^3}} + 0.045973\ \text{mm}\right)$$

$$d_{EC,Springs,2} = -0.063812\ mm$$

Elastic compression 3: *Offset* = -Q = -0.5 mm

Q < 0, so the following equations are used for a_{Linear}, $d_{Transition}$ and a_{Curved}:

$$d_{Transition} = -0.004\ mm^{-1} * Q^2 + 0.232 * Q$$

$$d_{Transition} = -0.004\ mm^{-1} * (0.5\ mm)^2 + 0.232 * 0.5\ mm$$

$$d_{Transition} = 0.115\ mm$$

$$a_{Curved} = -0.064 * Q^3 + 0.4 * Q^2 - 0.3 * Q + 1$$

$$a_{Curved} = -0.064 * (0.5\ mm)^3 + 0.4 * (0.5\ mm)^2 - 0.3 * 0.5\ mm + 1$$

$$a_{Curved} = 0.942$$

$$a_{Linear} = -313\frac{N}{mm^2} * Q + 5767\frac{N}{mm}$$

$$a_{Linear} = -313\frac{N}{mm^2} * (0.5\ mm) + 5767\frac{N}{mm}$$

$$a_{Linear} = 5610.5 \frac{N}{mm}$$

$$a_{Linear} * d_{Transition} = 5610.5 \frac{N}{mm} * 0.115\ mm = 645.21\ N$$

F < a_{Linear} * $d_{Transition}$, so the curve is within the linear region.

$$d_{EC,Springs,3} = -\frac{F}{a_{Linear}} = -\frac{250\ N}{5610.5 \frac{N}{mm}} = -0.044559\ mm$$

Elastic compression 4: *Offset* = Q = 0 mm

Q = 0, so a_{Linear}, $d_{Transition}$ and a_{Curved} are not needed

$$a_0 = -F = -250\ N$$

$$p = \frac{9 * 3741.1 \frac{N}{mm^3} * \left(-4887.8 \frac{N}{mm^2}\right) * 6137.9 \frac{N}{mm}}{54 * \left(3741.1 \frac{N}{mm^3}\right)^3} - \frac{\left(3741.1 \frac{N}{mm^3}\right)^2 * (-250\ N) - 2 * \left(-4887.8 \frac{N}{mm^2}\right)^3}{54 * \left(3741.1 \frac{N}{mm^3}\right)^3}$$

$$p = -0.24124\ mm^3$$

$$s = \sqrt[3]{-0.24124\ mm^3 + \sqrt{(0.35701\ mm^2)^3 + (-0.24124\ mm^3)^2}}$$

$$s = 0.43252\ mm$$

$$u = \sqrt[3]{-0.24124\ mm^3 - \sqrt{(0.35701\ mm^2)^3 + (-0.24124\ mm^3)^2}}$$

$$u = -0.82592\ mm$$

$$d_{EC,Springs,4} = -\left(s + u - \frac{a_2}{3 * a_3}\right)$$

$$d_{EC,Springs,4} = -\left(0.43252\ mm + (-0.82592\ mm) - \frac{-4887.8\frac{N}{mm^2}}{3 * 3741.1\frac{N}{mm^3}}\right)$$

$$d_{EC,Springs,4} = -0.042096\ mm$$

$$d_{Springs} = d_{TE,Springs} + d_{EC,Springs,1} + d_{EC,Springs,2} + d_{EC,Springs,3} + d_{EC,Springs,4}$$

$$d_{Springs} = 0.041785\ mm + (-0.083333\ mm) + (-0.063812\ mm) + (-0.044559\ mm) + (-0.042096\ mm)$$

$$\boldsymbol{d_{Springs} = -0.19202\ mm}$$

Part Deflection

$d_{NotSprings}$ = sum of thermal expansion and elastic compression/tension for each part

C-ring

Quantity: 1, Material: 316 Stainless Steel (TEInt = $1.0374*10^{-2}$, E = 1510900 MPa)

Table 22: C-ring Dimensions

Parameter	Before Thermal Expansion	After Thermal Expansion
D_{Outer} (mm)	12.7	12.832

w (mm)	12.7	12.832
t (mm)	1.67	1.6874

$$R = \frac{1}{2}D_{Outer} - \frac{1}{2}t = \frac{1}{2} * 12.832\ mm - \frac{1}{2} * 1.6874\ mm = 5.5725\ mm$$

$$d_{EC,Cring} = \frac{-\pi * 6 * F * R^3}{E * w * t^3}$$

$$d_{EC,Cring} = \frac{-\pi * 6 * 250\ N * (5.5725\ mm)^3}{1510900\ MPa * 12.832\ mm * (1.6874\ mm)^3} = -0.08753\ mm$$

$$d_{TE,Cring} = D_{Outer,afterTE} - D_{Outer,beforeTE} = 12.832\ mm - 12.7\ mm$$

$$d_{TE,Cring} = 0.13244\ mm$$

Backing Washers

Quantity: 4, Material: 316 Stainless Steel (TEInt = $1.0374*10^{-2}$, E = 1510900 MPa)

Table 23: Backing Washer Dimensions

Parameter	Before Thermal Expansion	After Thermal Expansion
t (mm)	0.71	0.71740
D_{Outer} (mm)	9.54	9.6395
D_{Inner} (mm)	4.59	4.6379

$$d_{EC,Washers} = \#_{washers} * \frac{-4 * F * t}{\pi * E * (D_{outer}^2 - D_{inner}^2)}$$

$$d_{EC,Washers} = 4 * \frac{-4 * 250\ N * 0.71\ mm}{\pi * 1510900\ MPa * ((9.6395\ mm)^2 - (4.6379\ mm)^2)}$$

$$d_{EC,Washers} = -8.4660 * 10^{-5} mm$$

$$d_{TE,Washers} = \#_{washers} * \left(t_{afterTE} - t_{beforeTE}\right)$$

$$d_{TE,Washers} = 4 * (0.71740\ mm - 0.71\ mm) = 0.029615\ mm$$

Tightening Nut

Quantity: 1, Material: 316 Stainless Steel (TEInt = $1.0374*10^{-2}$, E = 1510900 MPa)

Table 24: Tightening Nut Dimensions

Parameter	Before Thermal Expansion	After Thermal Expansion
t (mm)	1.36	1.3742
D_{Outer} (mm)	8.31	8.3967
D_{Inner} (mm)	2.83	2.8595

$$d_{EC,Nut} = \frac{-4 * F * t}{\pi * E * (D_{outer}^2 - D_{inner}^2)}$$

$$d_{EC,Nut} = \frac{-4 * 250\ N * 1.3742\ mm}{\pi * 1510900\ MPa * ((8.3967\ mm)^2 - (2.8595\ mm)^2)}$$

$$d_{EC,Nut} = -4.6449 * 10^{-5}$$

$$d_{TE,Nut} = D_{Outer,afterTE} - D_{Outer,beforeTE} = 1.3742\ mm - 1.36\ mm = 0.014182\ mm$$

Tree Trunk

Quantity: 1, Material: 316 Stainless Steel (TEInt = $1.037400*10^{-2}$, E = 1510901 MPa, poi = 0.31601)

Table 25: Tree Trunk Dimensions

Parameter	Before Thermal Expansion	After Thermal Expansion
D (mm)	6.4	6.4667
c (mm)	4.95	5.0016

$$U = \frac{1-\mu_1^2}{\pi * E_1} + \frac{1-\mu_2^2}{\pi * E_2}$$
$$U = \frac{1-(0.31601)^2}{\pi * 1510900\ MPa} + \frac{1-(0.31601)^2}{\pi * 1510900\ MPa}$$
$$U = 3.7927 * 10^{-6}\ MPa^{-1}$$

$$d_{EC,Trunk} = 0.35 * \frac{F}{c} * U * (1 + \ln\left(\frac{2 * c^3}{0.35 * U * F * D}\right))$$

$$d_{EC,Trunk} = 0.35 * \frac{250\ N}{5.0016\ mm} * 3.7927 * 10^{-6}\ MPa^{-1}$$
$$* \left(1 + \ln\left(\frac{2 * (5.0016\ mm)^3}{0.35 * 3.7927 * 10^{-6}\ MPa^{-1} * 250\ N * 6.4667\ mm}\right)\right)$$

$$d_{EC,Trunk} = -8.4044 * 10^{-4}\ mm$$

$$d_{TE,Trunk} = D_{afterTE} - D_{beforeTE} = 6.4667\ mm - 6.4\ mm$$

$$d_{TE,Trunk} = 0.066739\ mm$$

Tree Branch

Quantity: 1, Material: 410 Stainless Steel (TEInt = $6.7075*10^{-3}$, E = 158000 MPa)

Table 26: Tree Branch Dimensions

Parameter	Before Thermal Expansion	After Thermal Expansion
L (mm)	26.927	27.108
D (mm)	3.31	3.3323

$$L_{BeforeTE,Branch}$$

$$= D_{BeforeTE,C-ring,Outer} + 4 * t_{BeforeTE,Washer} + t_{BeforeTE,Nut}$$

$$+ D_{BeforeTE,Trunk} + 4 * h_{BeforeTE,Spring} - d_{Initial}$$

$$L_{BeforeTE,Branch}$$

$$= 12.7\ mm + 4 * 0.71\ mm + 1.36\ mm + 6.4mm + 4 * 1.2192\ mm$$

$$- 1.25\ mm$$

$$L_{BeforeTE,Branch} = 26.927\ mm$$

$$d_{ET,Branch} = \frac{-4 * F * L}{\pi * E * D^2}$$

$$d_{ET,Branch} = \frac{-4 * 250\ N * 27.108\ mm}{\pi * 158000\ MPa * (3.3323\ mm)^2} = -4.9183 * 10^{-3} mm$$

$$d_{TE,Branch} = -(L_{afterTE} - L_{beforeTE}) = -(27.108\ mm - 26.927\ mm)$$

$$= -0.18122\ mm$$

$$d_{NotSprings} = \sum d_{EC,i} + d_{TE,i}$$

$$d_{NotSprings} = (-0.08753\ mm + 0.13244\ mm)$$

$$+ (-8.466 * 10^{-5}\ mm\ + 0.029616mm)$$

$$+ (-4.6449 * 10^{-5}\ mm + 0.014182\ mm)$$

$$+ (-8.4044 * 10^{-4}\ mm + 0.066739mm)$$

$$+ (-4.9183 * 10^{-3}\ mm - 0.18122\ mm)$$

$$d_{NotSprings} = \mathbf{-3.2523 * 10^{-2}\ mm}$$

Final Balance

$$y = d_{Initial} + d_{NotSprings} + d_{Springs}$$

$$y = -3.2523 * 10^{-2}\ mm - 0.19106\ mm + 1.25\ mm$$

$$\boldsymbol{y = 1.02546\ mm}$$

y is further than the tolerance of $1*10^{-6}$ from zero, so it would be used to calculate the next value of the unknown parameter for another calculation loop.

Force to Stress

Functionality is included in the code for both force to stress and stress to force calculations for an applied force to the C-ring.

Material: 316 Stainless Steel (TEInt = $1.0374*10^{-2}$, E = 1510900 MPa)

Table 27: C-ring Dimensions

Parameter	Before Thermal Expansion	After Thermal Expansion
D_{Outer} (mm)	12.7	12.832
w (mm)	12.7	12.832
t (mm)	1.67	1.6874

$$A = w * t = 12.832\ mm * 1.6874\ mm = 21.654\ mm^2$$

$$r_{Outer} = \frac{D_{Outer}}{2} = \frac{12.832\ mm}{2} = 6.4162\ mm$$

$$r_{Inner} = r_{Outer} - t = 6.4162\ mm - 1.6874\ mm = 4.7288\ mm$$

$$R = \frac{r_{Outer} + r_{Inner}}{2} = \frac{6.4162\ mm + 4.7288\ mm}{2} = 5.5725\ mm$$

$$r_n = \frac{(r_{Outer} - r_{Inner})}{ln\left(\frac{r_{Outer}}{r_{Inner}}\right)} = \frac{(6.4162\ mm_2 - 4.7288\ mm_1)}{ln\left(\frac{6.4162\ mm}{4.7288\ mm}\right)} = 5.5297\ mm$$

$$\left[\frac{S}{F}\right] = \frac{1}{A}\left(\frac{\frac{1}{R} - \frac{1}{r_2}}{\frac{1}{r_n} - \frac{1}{R}}\right) = \frac{1}{21.654\ mm^2}\left(\frac{\frac{1}{5.5725\ mm} - \frac{1}{6.4162\ mm}}{\frac{1}{5.5297\ mm} - \frac{1}{5.5725\ mm}}\right)$$

$$\left[\frac{S}{F}\right] = 0.78377\ mm^{-2} = 0.78377\frac{MPa}{N}$$

With a known force of 250 N, stress is calculated as follows:

$$S = \left[\frac{S}{F}\right] * F - P_{Operating}$$

$$S = 0.78377\frac{MPa}{N} * 250\ N - 25\ MPa$$

$$S = 170.94\ MPa$$

With a known stress of 150 MPa, force is calculated as follows:

$$F = \frac{S + P_{Operating}}{\left[\frac{S}{F}\right]}$$

$$F = \frac{150\ MPa + 25\ MPa}{0.78377\frac{MPa}{N}}$$

$$F = 223.28\ N$$

Variation of Parameters

Given the sensitivities $dS/dd_{Initial}$ = 302.11 MPa/mm and dS/dt = 139.87 MPa/mm as well as the precisions $v_{dInitial}$ = 0.02 mm and v_t = 0.01 mm, the precision of a stress calculated from these values is as follows:

$$v_S = \sqrt{\sum_m (\frac{dS}{dm})^2\ v_m^2}$$

$$v_S = \sqrt{(302.11\frac{MPa}{mm})^2 * (0.02\ mm)^2 + (139.87\frac{MPa}{mm})^2 * (0.01\ mm)^2}$$

$$v_S = 6.202\ MPa$$

Curriculum Vitae

Candidate's full name: Rogan Connagher Joshua Swift

Universities attended (with dates and degrees obtained):

- University of New Brunswick, BScE (Chemical), 2009-2013

Publications:

- "Validation of Constant Load C-Ring Apex Stresses for SCC Testing in Supercritical Water" in the ASME Journal of Nuclear Radiation Science, 2016, doi: 10.1115/1.4034567

Conference Presentations:

- "Validation of Constant Load C-Ring Apex Stresses for SCC Testing in Supercritical Water" at the Graduate Chemical Engineering Conference, September 3, 2015
- "Validation of Constant Load C-Ring Apex Stresses for SCC Testing in Supercritical Water" at the 7th International Symposium on Supercritical Water-Cooled Reactors, March 15-18, 2015